1/*f* noise: Implications for solid-state quantum information

E. Paladino[*]

Dipartimento di Fisica e Astronomia, Università di Catania, Via Santa Sofia 64, I-95123, Catania, Italy and CNR-IMM-UOS Catania (Universitá), Via Santa Sofia 64, I-95123, Catania, Italy

Y. M. Galperin[†]

Department of Physics, University of Oslo, PO Box 1048 Blindern, 0316 Oslo, Norway, Centre for Advanced Study, Drammensveien 78, 0271 Oslo, Norway, and Ioffe Physical Technical Institute, 26 Polytekhnicheskaya, St. Petersburg 194021, Russian Federation

G. Falci[‡]

Dipartimento di Fisica e Astronomia, Università di Catania, Via Santa Sofia 64, I-95123, Catania, Italy and CNR-IMM-UOS Catania (Universitá), Via Santa Sofia 64, I-95123, Catania, Italy

B. L. Altshuler[§]

Physics Department, Columbia University, New York, New York 10027, USA

(published 3 April 2014)

The efficiency of the future devices for quantum information processing is limited mostly by the finite decoherence rates of the individual qubits and quantum gates. Recently, substantial progress was achieved in enhancing the time within which a solid-state qubit demonstrates coherent dynamics. This progress is based mostly on a successful isolation of the qubits from external decoherence sources obtained by engineering. Under these conditions, the material-inherent sources of noise start to play a crucial role. In most cases, quantum devices are affected by noise decreasing with frequency f approximately as $1/f$. According to the present point of view, such noise is due to material- and device-specific microscopic degrees of freedom interacting with quantum variables of the nanodevice. The simplest picture is that the environment that destroys the phase coherence of the device can be thought of as a system of two-state fluctuators, which experience random hops between their states. If the hopping times are distributed in an exponentially broad domain, the resulting fluctuations have a spectrum close to $1/f$ in a large frequency range. This paper reviews the current state of the theory of decoherence due to degrees of freedom producing $1/f$ noise. Basic mechanisms of such noises in various nanodevices are discussed and several models describing the interaction of the noise sources with quantum devices are reviewed. The main focus of the review is to analyze how the $1/f$ noise destroys their coherent operation. The start is from individual qubits concentrating mostly on the devices based on superconductor circuits and then some special issues related to more complicated architectures are discussed. Finally, several strategies for minimizing the noise-induced decoherence are considered.

DOI: 10.1103/RevModPhys.86.361 PACS numbers: 03.65.Yz, 05.40.Ca, 03.67.Lx

CONTENTS

[*]epaladino@dmfci.unict.it
[†]iouri.galperine@fys.uio.no
[‡]gfalci@dmfci.unict.it
[§]bla@phys.columbia.edu

I. INTRODUCTION

Evidence of properties that fluctuate with spectral densities varying approximately as $1/f$ over a large range of frequencies f has been reported in an astonishing variety of systems. In condensed matter physics, the difficulties in reasonably explaining the shape of the spectrum and in ascribing a physical origin to the noise in the diversity of system where it has been observed have kept $1/f$ noise in the forefront of unsolved problems for a long time. The large theoretical and experimental effort in this direction up to the late 1980s, with emphasis on $1/f$ conductance fluctuations in conducting materials, has been reported by Dutta and Horn (1981) Weissman (1988), Kogan (1996), and others cited therein.

With the progressive reduction of systems size, fluctuations having $1/f$-like spectra have been frequently observed in various mesoscopic systems. The importance of magnetic flux noise in superconducting quantum interference devices (SQUIDs) was recognized already in the 1980s (Koch *et al.*, 1983; Weissman, 1988) thus opening the debate about its physical origin—noise from the substrate or mount or noise from trapped flux in the SQUID—and temperature dependence (Savo, Wellstood, and Clarke, 1987; Wellstood, Urbina, and Clarke, 1987b). Single-electron and other tunneling devices have provided compelling evidence that fluctuating background charges, either within the junctions or in the insulating substrate, are responsible for low-frequency polarization fluctuations (Zorin *et al.*, 1996; Wolf *et al.*, 1997; Krupenin *et al.*, 1998, 2001).

Nanodevices are the subject of intense research at present because of their long-term potential for quantum information. Similarly to atomic systems, the quantum nature of nanocircuits, despite being hundreds of nanometers wide and containing large numbers of electrons, is observable. Because of these characteristics solid-state quantum bits (qubits) can be relatively easily addressed to perform desired quantum operations. The drawback of tunability is sensitivity to fluctuations of control parameters. Fluctuations are partly extrinsic, such as those due to the local electromagnetic environment. This source of noise has been greatly reduced via clever engineering. In almost all quantum computing nanodevices fluctuations with $1/f$ spectral density of different variables and physical origin have been observed. There is clear evidence that $1/f$ noise is detrimental to the required maintenance of quantum coherent dynamics and represents the main source of decoherence. This fact has stimulated a large effort of both the experimental and theoretical communities aimed, on the one hand, at a characterization of the noise, and, on the other hand, at understanding and eventually reducing noise effects. From a complementary perspective, nanodevices are sensitive probes of the noise characteristics and therefore may provide important insights into its microscopic origin.

In this review we describe the current state of theoretical work on $1/f$ noise in nanodevices with emphasis on implications for solid-state quantum information. We focus on superconducting systems and refer to other implementations, in particular, those based on semiconductors, whenever physical analogies and/or formal similarities are envisaged.

Previous reviews on $1/f$ noise mainly focused on resistivity fluctuations of conducting materials (Dutta and Horn, 1981; Weissman, 1988; Kogan, 1996). Important questions have been addressed, such as universality of the mechanisms leading to conductivity fluctuations and the kinetic patterns leading to the $1/f$ spectral form. Detailed investigations in different materials (metals and semiconductors) failed to confirm the impression of universality and led instead to the conclusion of a variety of origins of $1/f$ conductance noise existing in diverse materials.

Recent experiments with superconducting circuits evidenced $1/f$ low-frequency fluctuations of physically different observables, thus providing new insight into noise microscopic sources. This is due to the fact that three fundamental types of superconducting qubits exist: flux, charge, and phase; for a recent review, see Clarke and Wilhelm (2008), Ladd *et al.* (2010) Steffen *et al.* (2011), and You and Nori (2011). The main difference between them is the physical observable where information is encoded: superconducting current, excess charge in a superconducting island, or the superconducting phase difference across a Josephson junction. Different observables couple more strongly to environmental variables of a different nature and therefore are sensitive probes of different noise sources. As a result, magnetic flux noise, polarization or "charge" noise and critical current noise with $1/f$ spectrum in some frequency range are presently routinely measured in the three implementations.

One scope of this review is to present the current understanding of the microscopic sources of $1/f$ noise in superconducting nanocircuits. Despite the fact that relevant mechanisms have been largely identified, in most solid-state nanodevices this problem cannot be considered as totally

settled (Sec. II). In some cases, available experiments do not allow one to draw solid conclusions and further investigation is needed. A number of basic features of the phenomenon are, however, agreed upon. According to previous reviews, $1/f$ noise results from a superposition of fluctuators (whose nature has to be specified case by case) having switching times distributed in a very broad domain (Dutta and Horn, 1981; Weissman, 1988; Kogan, 1996). Statistical properties of $1/f$ noise have been discussed by Kogan (1996). These properties are at the origin of $1/f$ noise-induced loss of coherence of solid-state qubits. For clarity, we recall here the basic definitions and specify their use in the context of the present review.

For a Gaussian random process all nonzero nth-order moments can be expressed in terms of the second-order moments, i.e., pair correlations. In general, statistical processes producing $1/f$ noise are non-Gaussian. This fact has several important implications. On the one hand, statistical correlations higher than the power spectrum should be considered in order to characterize the process; see Kogan (1996). On the other hand, deviations from Gaussian behavior are also expected to show up in the coherent quantum dynamics of solid-state qubits. In relevant regimes for quantum computation, where effects of noise are weak, it can be described by linear coupling to one or more operators of the quantum system. Under this condition, for Gaussian noise, random noise-induced phases acquired by a qubit obey the Gaussian distribution. We refer to a process as *Gaussian* whenever this situation occurs. As we see explicitly in Sec. III, even in cases where the noise can be considered as a sum of many statistically independent contributions, the distribution of the phases can be essentially non-Gaussian. A number of investigations aimed at predicting decoherence due to non-Gaussian $1/f$ noise are (Paladino *et al.* (2002), Grishin, Yurkevich, and Lerner (2005), Bergli, Galperin, and Altshuler (2006, 2009), Galperin *et al.* (2006, 2007), Burkard (2009), and Yurkevich *et al.* (2010) (more references can be found in Sec. III).

The other crucial property of $1/f$ noise is that it cannot be considered a Markovian random process. A statistical process is *Markovian* if one can make predictions for the future of the process based solely on its present state, just as well as one could do knowing the process's full history. We will see that even if the noise can be considered as a sum of Markovian contributions, the overall phase fluctuations of a qubit can be essentially non-Markovian. This is the case when non-Gaussian effects are important; see, e.g., Laikhtman (1985), where this issue was analyzed for the case of spectral diffusion in glasses. The consequence of $1/f$ noise being non-Markovian is that the effects of $1/f$ noise on the system evolution depend on the specific "quantum operation" and/or measurement protocol. In this review we illustrate various approaches developed in recent years to deal with the non-Markovian nature of $1/f$ noise starting both from microscopic quantum models and from semiclassical theories. We discuss the applicability range of the Gaussian approximation as well as deviations from the Gaussian behavior in connection with the problem of qubit dephasing.

A statistical process is *stationary* if all joint probability distributions are invariant for translations in time. To our knowledge, at the present there is no clear evidence of nonstationarity of the processes leading to $1/f$ noise (see the discussion in Sec. III).

Low-frequency noise is particularly harmful since it is difficult to filter out with finite-band filters. In recent years different techniques have been proposed, and sometimes experimentally tested, in order to limit the effect of low-frequency fluctuations. One successful strategy to increase phase-coherence times is to operate qubits at working points where low-frequency noise effects vanish to the lowest order; such operating conditions are called "optimal" point or "magic" point (Vion *et al.*, 2002). Further substantial improvement resulted from the use of dynamical techniques inspired by nuclear magnetic resonance (NMR) (Schlichter, 1992). In a quantum information perspective, any approach aimed at limiting decoherence should be naturally integrated with other functionalities as quantum gates. In addition, achieved fidelities should be sufficiently high to allow for the successful application of quantum error correction codes. The question about the best strategy to limit $1/f$ noise effects via passive or active stabilization is still open. We review the current status of the ongoing research along this direction in Sec. III.D.

Building scalable multiqubit systems is presently the main challenge toward the implementation of a solid-state quantum information processor (Nielsen and Chuang, 1996). The effect of $1/f$ noise in solid-state complex architectures is a subject of current investigation. Considerable improvement in minimizing sensitivity to charge noise has been reached via clever engineering. A new research area named *circuit quantum electrodynamics* (cQED) recently developed from the synergy of superconducting circuits technology and phenomena of the atomic and quantum optics realm. In this framework important further steps have been done. Among the newest we mention is the achievement of three-qubit entanglement with superconducting nanocircuits (Di Carlo *et al.*, 2010; Neeley *et al.*, 2010) which, in combination with longer qubit coherence, illustrate a potentially viable approach to factoring numbers (Lucero *et al.*, 2012), implementing quantum algorithms (Fedorov *et al.*, 2011; Mariantoni *et al.*, 2011), and simple quantum error correction codes (Chow *et al.*, 2012; Reed *et al.*, 2012; Rigetti *et al.*, 2012).

A. General features and open issues

Low-frequency noise is commonly attributed to so-called *fluctuators*. In a "minimal model," reproducing main features of $1/f$ noise, fluctuators are dynamic defects, which randomly switch between two metastable states (1 and 2); see, e.g., Dutta and Horn (1981), Weissman (1988), and Kogan (1996). Such a switching produces random telegraph (RT) noise. The process is characterized by the switching rates $\gamma_{1\to2}$ and $\gamma_{2\to1}$ for the transitions $1 \to 2$ and $2 \to 1$. Only the fluctuators with energy splitting E less than a few k_BT (T is temperature) contribute to the dephasing of a qubit, since the fluctuators with large level splitting are frozen in their ground states. As long as $E \lesssim k_BT$ the rates $\gamma_{1\to2}$ and $\gamma_{2\to1}$ are close in magnitude, and to describe the general features of decoherence one can assume that $\gamma_{1\to2} = \gamma_{2\to1} \equiv \gamma$, i.e., the fluctuations can be described as a RT process (Buckingham,

1989; Kirton and Uren, 1989; Kogan, 1996). A set of random telegraph fluctuators with exponentially broad distribution of relaxation rates γ produces noise with a $1/f$ power spectrum at $\gamma_{\min} \ll \omega = 2\ \pi f \ll \gamma_{\max}$. Here $\gamma_{\min}$ is the switching rate of the "slowest" fluctuator affecting the process, whereas $\gamma_{\max}$ is the maximal switching rate for fluctuators with energy difference $E \sim k_B T$. Random telegraph noise has been observed in numerous nanodevices based on semiconductors, normal metals, and superconductors (Ralls *et al.*, 1984; Rogers and Buhrman, 1984, 1985; Parman, Israeloff, and Kakalios, 1991; Peters, Dijkhuis, and Molenkamp, 1999; Duty *et al.*, 2004; Eroms *et al.*, 2006). Multistate fluctuators with a number of states greater than 2 were also observed (Bloom, Marley, and Weissman, 1993, 1994).

Various microscopic sources can produce classical random telegraph noise. Here we briefly summarize some of them in connection with charge, flux, and critical current noise and mention some recent key references; a detailed discussion is presented in Sec. II.

The obvious source of RT charge noise is a charge which jumps between two different locations in space. Various hypotheses about the actual location of these charges and the nature of the two states are still under investigation. The first attempt at constructing such a model in relation to qubit decoherence appeared in Paladino *et al.* (2002), where electron tunneling between a localized state in the insulator and a metallic gate was studied. The quantitative importance (in explaining observed spectra) of effects of hybridization between localized electronic states (at the trap) and electrodes extended states was pointed out by Grishin, Yurkevich, and Lerner (2005) and Abel and Marquardt (2008). Models considering the actual superconducting state of the electrodes have been studied by Faoro *et al.* (2005) and Faoro and Ioffe (2006), leading to predictions in agreement with the experimental observations of charge noise based on measurements of relaxation rates in charge qubits reported by Astafiev *et al.* (2004).

Studies of flux noise have a long history. Koch *et al.* (1983) demonstrated that flux rather than critical current noise limits the sensitivity of dc SQUIDs. The interest in this problem was recently renewed when it was realized that flux noise can limit the coherence in flux and phase superconducting qubits (Yoshihara *et al.*, 2006; Harris *et al.*, 2008). Two recent models for fluctuators producing low-frequency noise were suggested. Koch, DiVincenzo, and Clarke (2007) attribute flux noise to electrons hopping between traps, with spins having fixed, random orientations. de Sousa (2007) proposed that electrons flip their spins due to interaction with tunneling two-level systems (TLSs) and phonons. A novel mechanism, based on independent spin diffusion along the surface of a superconductor, was suggested by Faoro and Ioffe (2008). It seems to agree with experiments on measurements of the $1/f$ flux noise reported by Bialczak *et al.* (2007) and Sendelbach *et al.* (2008). Instead, recent measurements by Anton *et al.* (2013) appear to be incompatible with random reversal of independent surface spins, possibly suggesting a non-negligible spin-spin interaction (Sendelbach *et al.*, 2009).

The microscopic mechanism and the source of the fluctuations of the critical current in a Josephson junction are long-standing open problems. These fluctuations were initially attributed to charges tunneling or hopping between different localized states inside the barrier, forming glasslike TLSs. However, a more detailed comparison with experiments revealed an important problem: the noise spectrum experimentally observed by Van Harlingen *et al.* (2004) and Wellstood, Urbina, and Clarke (2004) was proportional to T^2, which is incompatible with the assumption of constant TLS density of states, or equivalently with any power-law dependence of relaxation rates for $E \lesssim k_B T$. The experiments by Eroms *et al.* (2006) on fluctuations in the normal state in small Al junctions [similar to those used in several types of qubits (Martinis *et al.*, 2002; Vion *et al.*, 2002; Chiorescu *et al.*, 2003)] brought a new puzzle. It turned out that the temperature dependence of the noise power spectrum in the normal state is linear, and the noise power is much less than that reported for large superconducting contacts. A plausible explanation of such behavior was proposed by Faoro and Ioffe (2007), who suggested that the critical current noise is due to electron trapping in shallow subgap states that might be formed at the superconductor-insulator boundary. Recently, measurements on $Al/AlO_x/Al$ junctions reported by Nugroho, Orlyanchik, and Van Harlingen (2013) showed an equivalence between the critical-current and normal-state resistance fractional noise power spectra, both scaling $\propto T$, suggesting the possibility of an upper limit to the additional noise contribution from electrons tunneling between weak Kondo states at subgap energies.

The dramatic effect of $1/f$ charge noise was already pointed out in the breakthrough experiment performed at the Nippon Electric Corporation and reported by Nakamura, Pashkin, and Tsai (1999), where time-domain coherent oscillations of a superconducting charge qubit were observed for the first time. This experiment has renewed the interest for charge noise and has stimulated a number of investigations aimed at explaining decoherence due to noise sources characterized by a $1/f$ power spectrum in some frequency range. The theoretical understanding of decoherence in solid-state single qubit gates is presently quite well established. Quite often in the literature the statistics of the fluctuations of the qubit parameters displaying $1/f$ spectrum is assumed to be Gaussian. This assumption is not *a priori* justified. In order to discuss the applicability range of the Gaussian approximation as well as deviations from the Gaussian behavior in connection with the problem of qubit dephasing, we consider in detail some of the above-mentioned models where the qubit response to typical manipulation protocols can be solved exactly.

Peculiar features originated from fluctuations with $1/f$ spectrum show up in the qubit dynamics superposed to effects due to high-frequency fluctuations (see Fig. 1). The intrinsic high-frequency cutoff of $1/f$ noise is in fact hardly detectable, with measurements typically extending to 100 Hz. Recently, charge noise up to 10 MHz has been detected in a single-electron transistor (SET) by Kafanov *et al.* (2008), and flux noise in the 0.2–20 MHz range has been measured by Bylander *et al.* (2011) with proper pulse sequences. Incoherent energy exchanges between system and environment, leading to relaxation and decoherence, occur at typical operating frequencies (about 10 GHz). Indirect measurements of noise spectrum in this frequency range (quantum noise) often suggest a "white" or Ohmic behavior (Astafiev *et al.*,

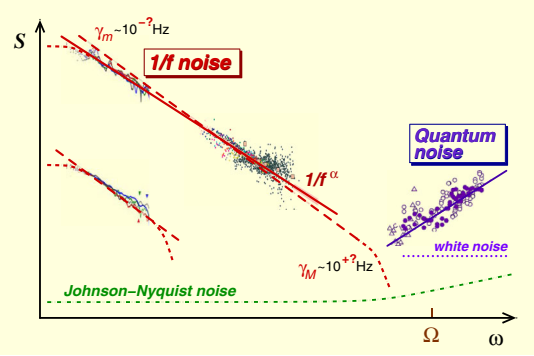

FIG. 1 (color online). Qualitative representation of the noise spectrum $S(\omega)$ [defined in Eq. (10)] on log-log scale. Lines correspond to the behavior expected in different frequency domains, and dots represent typical experimental observations in selected frequency ranges. Long-dashed lines indicate the $1/f$ dependence extending between the intrinsic low- and high-frequency cutoffs γ_m and γ_M, which in general are not known. The thick lines indicate the $1/f^{\alpha}$ dependence, with $\alpha \sim 0.9$. $1/f$ noise can be measured in different frequency windows using different detection techniques (different symbols and dots). For instance, $1/f$-type flux noise has been detected by a free-induction Ramsey interference experiment in the 0.01–100 Hz range (Yan *et al.*, 2012) and by noise spectroscopy by means of dynamical decoupling in the 0.2–20 MHz range (Bylander *et al.*, 2011). Fluctuations of flux, critical current, and charge correspond usually to different $1/f$ noise amplitudes and extend in different frequency ranges: top and bottom curves illustrate typical $1/f$ measurements of different variables in the same setup. At frequencies corresponding to the qubit splittings, $\Omega \sim 10^{10}$ Hz for superconducting qubits, the measured quantum noise is white or Ohmic (dotted and thin lines). The dash-dotted line indicates the linearly increasing Johnson-Nyquist noise.

2004; Ithier *et al.*, 2005). In addition, narrow resonances at selected frequencies (sometimes resonant with the nanodevice-relevant energy scales) have been observed (Cooper *et al.*, 2004; Simmonds *et al.*, 2004; Eroms *et al.*, 2006). In certain devices they originate from the circuitry (Van der Wal *et al.*, 2000) and may eventually be reduced by improving filtering. More often, resonances are signatures of the presence of spurious fluctuators which also show up in the time resolved evolution, unambiguously proving the discrete nature of these noise sources (Duty *et al.*, 2004). Fluctuators may severely limit the reliability of nanodevices (Falci *et al.*, 2005; Galperin *et al.*, 2006). An explanation of this rich physics is beyond phenomenological theories describing the environment as a set of harmonic oscillators. On the other hand, an accurate characterization of the noise sources might be *a priori* inefficient, since a microscopic description would require a large number of parameters. A road map to treat broadband noise which allows one to obtain reasonable approximations by systematically including only the relevant information on the environment, out of the large parametrization needed to specify it, has been proposed by Falci *et al.* (2005). The predictions obtained for the decay of the coherent signal are in agreement with observations in various superconducting implementations and different protocols, such as the decay of Ramsey fringes in charge-phase qubits (Vion *et al.*, 2002).

One successful strategy to increase phase-coherence times in the presence of $1/f$ noise is to operate close to the qubits' optimal points where low-frequency noise effects vanish to the lowest order. This strategy was first implemented in a device named "quantronium" (Vion *et al.*, 2002) and it is now applied to all types of superconducting qubits (except for phase qubits). Further substantial improvement resulted from the use of charge- or flux-echo techniques (Nakamura *et al.*, 2002; Bertet *et al.*, 2005). In NMR the spin echo removes the inhomogeneous broadening that is associated with, for example, variations of static local magnetic fields over the sample, changing the NMR frequency. In the case of qubits, the variation is in their energy-level splitting frequency from measurement to measurement. For some qubits defocusing is strongly suppressed by combining optimal point and echo techniques, thus providing further evidence of the fundamental role of $1/f$ noise. Dynamical decoupling, which uses sequences of spin flips to effectively average out the coupling to the environment, is another promising strategy (Falci *et al.*, 2004; Faoro and Viola, 2004; Bylander *et al.*, 2011). Optimized sequences limiting the blowup in resources involved in $1/f$ noise suppression (Uhrig, 2007; Lee, Witzel, and Das Sarma, 2008; Du *et al.*, 2009; Biercuk, Doherty, and Uys, 2011) as well as "optimal control theory" design of quantum gates (Montangero, Calarco, and Fazio, 2007; Rebentrost *et al.*, 2009) have recently been explored. The experimental realization of optimal dynamical decoupling in solid-state systems and the implementation of quantum gates with integrated decoupling in a scalable and/or hybrid architecture is an open problem.

B. Why is $1/f$ noise important for qubits?

We briefly discuss in which ways noise influences the operation of an elementary part of a quantum computer—a quantum bit (qubit). This topic is addressed in detail in Sec. III. The qubit can be described as a two-level system with the effective Hamiltonian

$$\hat{H}_q = \frac{\hbar}{2}(\epsilon\sigma_z + \Delta\sigma_x). \tag{1}$$

Here $\hbar\epsilon$ represents diagonal splitting of the individual levels, $\hbar\Delta$ represents their tunneling coupling, and $\sigma_{x,z}$ are the Pauli matrices. The physical meaning of the quantities ϵ and Δ depends on the specific implementation of the qubit. In its diagonalized form the qubit Hamiltonian (1) reads

$$\hat{H}_q = \frac{\hbar\Omega}{2}\sigma_{z'} \equiv \frac{\hbar\Omega}{2}(\cos\theta\sigma_z + \sin\theta\sigma_x), \tag{2}$$

where $\Omega = \sqrt{\epsilon^2 + \Delta^2}$ and the quantization axis $\sigma_{z'}$ forms an angle θ with σ_z. The Hamiltonian (1) corresponds to a pseudospin $1/2$ in a "magnetic field" $\mathbf{B}$, which can be time dependent:

$$\hat{H}_q = (\hbar/2)\mathbf{B}\cdot\boldsymbol{\sigma}, \qquad B_z \equiv \epsilon(t), \qquad B_x \equiv \Delta(t). \tag{3}$$

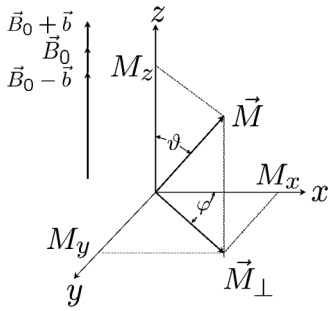

FIG. 2. Bloch vector representing the state of a qubit in the rotating (with angular frequency B_0) frame of reference. In the laboratory frame of reference it precesses around the z axis with (time-dependent) angular velocity B. The fluctuation of this velocity is $b(t)$.

Any state vector $|\Psi\rangle$ of the qubit determines the Bloch vector $\mathbf{M}$ through the density matrix

$$\rho = |\Psi\rangle\langle\Psi| = (1 + \mathbf{M}\cdot\boldsymbol{\sigma})/2. \tag{4}$$

The Schrödinger equation turns out to be equivalent to the precession equation for the Bloch vector:

$$\dot{\mathbf{M}} = \mathbf{B}\times\mathbf{M}. \tag{5}$$

The problem of decoherence arises when the magnetic field is a sum of a controlled part $\mathbf{B}_0$ and a fluctuating part $\mathbf{b}(t)$ which represents the noise, i.e., the field is a stochastic process $\mathbf{B}(t) = \mathbf{B}_0 + \mathbf{b}(t)$, determined by its statistical properties. The controlled part $\mathbf{B}_0$ is not purely static—to manipulate the qubit one has to apply certain high-frequency pulses of $\mathbf{B}_0$ in addition to the static fields applied between manipulation steps. In this language, the role of the environment is that it creates a stochastic field $\mathbf{b}(t)$, i.e., stochastic components of $\epsilon(t)$ and $\Delta(t)$. These contributions destroy coherent evolution of the qubit making its *coherence time* finite.

We consider first the simple case of "longitudinal noise," where $\mathbf{b}\|\mathbf{B}_0$, and let the z axis lie along the common directions of $\mathbf{B}_0$ and $\mathbf{b}$ (see Fig. 2). In the physics of magnetic resonance, this situation is called *pure dephasing* because the z component of the Bloch vector M_z is conserved during the process. As long as the time evolution of $\mathbf{M}$ is governed by Eq. (5), the length $|\mathbf{M}| = \sqrt{M_x^2 + M_z^2} \equiv M$ is also conserved, while the length $|\langle\mathbf{M}\rangle|$ of the vector $\mathbf{M}$ averaged over the stochastic process $\mathbf{b}(t)$ decays. The description of this decay is the main objective of the decoherence theory. In the case of pure dephasing, this will be the decay of the components M_x and M_y. It is convenient to introduce a complex combination $m_+ = (M_x + iM_y)/M$. Equation (5) can be written in terms of m_+ as $\dot{m}_+ = iBm_+$ with solution

$$m_+(t) = e^{i\phi(t)}m_+(0), \quad \phi(t) \equiv \int_0^t B(t')dt'. \tag{6}$$

Here we assumed that the variable $B(t)$ is a classical one, i.e., the order of times in the products $B(t_1)B(t_2)\cdots B(t_n)$ is not important. The solution has to be averaged over the stochastic process $b(t)$. We define the phase $\phi(t)$ accumulated by m_+ during the time t as the sum of regular ϕ_0 and stochastic $\varphi(t)$ parts:

$$\phi(t) = \phi_0(t) + \varphi(t), \quad \phi_0(t) = B_0 t, \quad \varphi(t) = \int_0^t b(t')dt'$$

and obtain $\langle m_+(t)\rangle = e^{i\phi_0}\langle e^{i\varphi(t)}\rangle m_+(0)$. The stochastic phase φ is the integral of the random process $b(t)$. The Bloch vector precesses around the z axis with the angular velocity that has random modulation $b(t)$. In the Gaussian approximation the only relevant statistical characteristic of $b(t)$ is the correlation function $\langle b(t_1)b(t_2)\rangle = S_b(|t_1 - t_2|)$ [we assume that $b(t)$ is a stationary random process]. The function $S_b(t)$ decays at $|t| \to \infty$ and the scale of this decay is the correlation time. If the integration time t strongly exceeds the correlation time, the random phase φ is a sum of many uncorrelated contributions. According to the central limit theorem such a sum has a Gaussian distribution,

$$p(\varphi) = \frac{1}{\sqrt{2\pi\langle\varphi^2\rangle}}\exp\left(-\frac{\varphi^2}{2\langle\varphi^2\rangle}\right), \tag{7}$$

independently of the details of the process. Therefore, the Gaussian distribution should be valid as soon as t exceeds the correlation time of the noise. In Sec. III.A.1.a we further discuss this conclusion. As follows from Eq. (7),

$$\langle e^{i\varphi}\rangle = \int p(\varphi)e^{i\varphi}d\varphi = e^{-\langle\varphi^2\rangle/2}, \tag{8}$$

$$\langle\varphi^2\rangle = \int_0^t dt_1\int_0^t dt_2 S_b(|t_1 - t_2|). \tag{9}$$

Representing $S_b(\tau)$ by its Fourier transform,

$$S_b(\omega) = \frac{1}{\pi}\int_0^\infty dt S_b(t)\cos\,\omega t, \tag{10}$$

that is just the *noise spectrum*, and using Eq. (9) we obtain

$$\langle\varphi^2(t)\rangle = 2\int_0^\infty d\omega\left(\frac{\sin\,\omega t/2}{\omega/2}\right)^2 S_b(\omega). \tag{11}$$

Therefore, the signal decay given by Eq. (8) is determined (in the Gaussian approximation) only by the noise spectrum $S_b(\omega)$. For large t, the identity $\lim_{a\to\infty}(\sin^2 ax/\pi ax^2) = \delta(x)$ implies that $\langle\varphi^2(t)\rangle = 2\pi t S_b(0)$ and thus

$$\langle e^{i\varphi(t)}\rangle = e^{-t/T_2^*}, \quad T_2^{*-1} = \pi S_b(0). \tag{12}$$

Thus, the Gaussian approximation leads to exponential decay of the signal at large times, the decrement being given by the noise power at zero frequency. Equation (12) shows that the pure dephasing is determined by the noise spectrum at low frequencies. In particular, at $S_b(\omega) \propto 1/\omega$ the integral in Eq. (11) diverges; cf. with further discussion of a spin echo.

The time dependence of $\langle m_+\rangle \propto \langle e^{i\varphi}\rangle$ characterizes decay of the so-called free induction signal (Schlichter, 1992). The free induction decay (FID) is the observable NMR signal generated by nonequilibrium nuclear spin magnetization

precessing about the magnetic field. This nonequilibrium magnetization can be induced generally by applying a pulse of resonant radio frequency close to the Larmor frequency of the nuclear spins. In order to extract it in qubit experiments, one usually has to average over many repetitions of the same qubit operation. Even in setups that allow single-shot measurements (Astafiev *et al.*, 2004), each repetition gives one of the two qubit states as the outcome. Only by averaging over many repeated runs can one see the decay of the average as described by the free induction signal. The problem with this is that the environment has time to change its state between the repetitions, and thus we average not only over the stochastic dynamics of the environment during the time evolution of the qubit, but over the initial states of the environment as well. As a result, the free induction signal decays even if the environment is too slow to rearrange during the operation time. This is an analog of the inhomogeneous broadening of spectral lines in magnetic resonance experiments. This analogy also suggests ways to eliminate the suppression of the signal by the dispersion of the initial conditions. One can use the well-known echo technique (Mims, 1972) when the system is subjected to a short manipulation pulse (the so-called π pulse) with duration τ_1 at time τ_{12}. The duration τ_1 of the pulse is chosen to be such that it switches the two states of the qubit. This is equivalent to reversing the direction of the Bloch vector and thus effectively reversing the time evolution after the pulse as compared with the initial one. As a result, the effect of any static field is canceled and decay of the echo signal is determined only by the dynamics of the environment during time evolution. The decay of the two-pulse echo can be expressed as $\langle m_+^{(e)}(2\tau_{12})\rangle$ (Mims, 1972), where

$$\langle m_+^{(e)}(t)\rangle \equiv \langle e^{i\psi(t)}\rangle, \quad \psi(t) = \left(\int_0^{\tau_{12}} - \int_{\tau_{12}}^{t}\right) b(t')dt'. \quad (13)$$

The finite correlation time of $b(t)$ again leads to the Gaussian distribution of $\psi(t)$ at large enough t with

$$\langle \psi^2(2\tau_{12})\rangle = 8\int_0^\infty d\omega \left(\frac{\sin^2(\omega\tau_{12}/2)}{\omega/2}\right)^2 S_b(\omega). \quad (14)$$

This variance can be much smaller than $\langle\varphi^2\rangle$ given by Eq. (11), especially if $S_b(\omega)$ is singular at $\omega\to 0$. Although the integral (14) is not divergent in the case of $1/f$ noise, the time dependence of the echo signal is sensitive to the low-frequency behavior of S_b. Therefore, the low-frequency noise strongly affects coherent properties of qubits.

Along the simplified model discussed above, the component $\mathbf{M}_z$ of the magnetic moment which is parallel to the magnetic field $\mathbf{B}$ does not decay because longitudinal fluctuations of the magnetic field do not influence its dynamics. In a realistic situation it also decays in time, the decay time being referred to as relaxation time and conventionally denoted T_1. This occurs when the stochastic field $\mathbf{b}(t)$ has a component perpendicular to the controlled part $\mathbf{B}_0$. Relaxation processes also induce another decay channel for the M_x and M_y components on a time scale denoted T_2. We suppose that the stochastic field is $\mathbf{b}(t) = b(t)\hat{z}$, while $\mathbf{B}_0 = \Delta\hat{x} + \epsilon\hat{z}$. Due to the nonisotropic interaction term, the effect of noise on the qubit phase-coherent dynamics depends on the angle θ. When $\theta = 0$ the interaction is longitudinal and we obtain the already discussed pure dephasing condition. When $\theta \neq 0$ the stochastic field also induces transitions between the qubit eigenstates. As a result, if the noise has a spectral component at the qubit energy splitting, this interaction induces inelastic transitions between the qubit eigenstates, i.e., incoherent emission and absorption processes. This is easily illustrated for a weak amplitude noise treated in the Markovian approximation. Approaches developed in different areas of physics, as the Bloch-Redfield theory (Bloch, 1957; Redfield, 1957), the Born-Markov master equation (Cohen-Tannoudji, Dupont-Roc, and Grynberg, 1992), and the systematic weak-damping approximation in a path-integral approach (Weiss, 2008), lead to exponential decay with time scales

$$1/T_1 = \pi\sin^2\theta S_b(\Omega), \quad (15)$$

$$1/T_2 = 1/2T_1 + 1/T_2^*, \quad (16)$$

where the adiabatic or pure dephasing term of Eq. (12), in the general case, reads $1/T_2^* = \pi\cos^2\theta S_b(0)$. Even if the above formulas do not hold for $1/f$ noise, which would lead to a singular dephasing time, they indicate that the diverging adiabatic term containing $S_b(0)$ may be eliminated (in lowest order) if the qubit operates at $\theta = \pi/2$, or equivalently when the noise is "transverse," $\mathbf{b}\perp\mathbf{B}_0$. In the context of quantum computing with superconducting systems, this condition (of reduced sensitivity to $1/f$ noise) is usually referred to as an "optimal point" (Vion *et al.*, 2002). In this case $T_2 = 2T_1$, which is the upper limit to the dephasing time. We return to this issue in Sec. III.B.

II. PHYSICAL ORIGIN OF $1/f$ NOISE IN NANODEVICES

A. Basic models for the $1/f$ noise

Studies of the noise with the spectral density $\propto\omega^{-1}$ have a long history; see, e.g., Kogan (1996) for a review. This behavior at low frequencies is typical for many physical systems, such as bulk semiconductors, normal metals and superconductors, strongly disordered conductors, as well as devices based on these materials. One observes, in practically all cases, an increase of the spectral density of the noise with decreasing frequency $f \equiv \omega/2\pi$ approximately proportional to $1/f$ down to the lowest experimentally achievable frequencies. Therefore, the noise of this type is referred to as $1/f$ noise (the term "flicker noise" proposed by Schottky is now rarely used).

$1/f$ noise poses many puzzles. Is the noise spectrum decreasing infinitely as $f\to 0$ or does it saturate at small frequencies? What are the sources of the $1/f$ noise? Why do many systems have very similar noise spectra at low frequencies? Is this phenomenon universal and does a unified theory exist? Those and many other questions stimulated interest to the $1/f$ noise from a fundamental point of view. This interest is also supported by the crucial importance of such a noise for all applications based on dc and low-frequency response.

Usually, the observed $1/f$ noise of the electrical current is a quadratic function of the applied voltage in uniform Ohmic

conductors. This indicates that the noise is caused by fluctuation in the sample resistance, which are independent of the mean current. Therefore, the current just "reveals" the fluctuations. Although the low-frequency noise spectrum seems to be rather universal the noise intensity differs a great deal in different systems depending not only on the material, but also on the preparation technology, heat treatment, etc. These facts lead to the conclusion that in many cases the $1/f$ noise is *extrinsic*, i.e., caused by some dynamic defects.

In the simplest case, when the kinetics of fluctuations is characterized by a single relaxation rate γ, the correlation function of a fluctuating quantity $x(t)$ is proportional to $e^{-\gamma|t|}$. Then the spectral density is a Lorentzian function of frequency,

$$S_x(\omega) \propto \mathcal{L}_\gamma(\omega) \equiv \frac{1}{\pi}\frac{\gamma}{\omega^2+\gamma^2}. \tag{17}$$

In more general cases, the kinetics of $x(t)$ is a superposition of several, or even many, relaxation processes with different rates. In general, a continuous distribution of the relaxation rates $\mathcal{P}_x(\gamma)$ may exist. Then the noise spectral density can be expressed as

$$S_x(\omega) \propto \int_0^\infty d\gamma \mathcal{P}_x(\gamma)\mathcal{L}_\gamma(\omega). \tag{18}$$

Equation (18) describes nonexponential kinetics with $\mathcal{P}_x(\gamma)d\gamma$ the contribution of the processes with relaxation rates between γ and $\gamma + d\gamma$ to the variance

$$\overline{(\delta x)^2} = 2\int_0^\infty d\omega S_x(\omega) \propto \int_0^\infty d\gamma \mathcal{P}_x(\gamma). \tag{19}$$

If $\mathcal{P}_x(\gamma) \propto \gamma^{-1}$ in some window $\gamma_0 \gg \gamma_{\min}$, but very small outside this interval, then, according to Eq. (18), one gets $S_x(\omega) \propto \omega^{-1}$ in the frequency domain $\gamma_0 \gg \omega \gg \gamma_{\min}$ (Surdin, 1939). Following a model of this type, one has to specify the processes responsible for the noise, which depend on the specific properties of the system under consideration. Several types of kinetic processes were indicated as able to produce the $1/f$ noise. Among them are activated processes with different relaxation rates exponentially dependent on the inverse temperature $\gamma = \gamma_0 e^{-E/k_BT}$, where γ_0 is some attempt frequency and the distribution of activation energies $\mathcal{F}(E)$ is smooth in a sufficiently broad domain. Then the distribution of the relaxation rates has the required form since $\mathcal{P}_x(\gamma) = \mathcal{F}_x(E)|\partial\gamma/\partial E|^{-1} = \mathcal{F}_x(E)(k_BT/\gamma)$ (van der Ziel, 1950).

If the kinetics of the fluctuations is controlled by tunneling processes, then the relaxation rates depend approximately exponentially on the width and height of the tunneling barrier. If the distribution of these parameters is almost constant in a wide interval, then again the distribution of the relaxation rates will be proportional to $1/\gamma$. In particular, McWhorter (1957) suggested that fluctuation of the number of carriers in a surface layer of a semiconductor arises from the exchange of electrons between this layer and the traps lying in the oxide layer covering the surface, or on the outer surface of the oxide. Since the electron transfer takes place via tunneling, the characteristic relaxation rate exponentially depends on the distance x between the surface and trap $\gamma = \gamma_0 e^{-x/\lambda}$. Since the distances x vary with a scatter $\gg \lambda$, the distribution of relaxation times is exponentially wide. This model has been extensively used to interpret $1/f$ noise in field-effect transistors. However, the model failed to explain observed small rates γ in the devices with a relatively thin insulator layer.

There exist special low-energy excitations in amorphous materials, in particular, in all dielectric and metallic glasses. They result in anomalous temperature dependencies of the heat capacity and the thermal conductivity at low temperatures, as well as specific features of the sound absorption; see, e.g., Black (1981), Hunklinger and von Schickfus (1981), and Galperin, Gurevich, and Kozub (1989) for a review. According to this model, atoms or groups of atoms exist that can occupy two positions. Therefore, their energy as a function of some configuration coordinate can be represented as a double-well potential, as shown in Fig. 3.

The model of TLSs formulated by Anderson, Halperin, and Varma (1972) and Phillips (1972) contains two parameters—the asymmetry U of the potential (which is approximately equal to the difference between the minima) and the tunnel matrix element λ, characterizing the strength of the barrier which can be estimated as

$$\Lambda = \hbar\omega_0 e^{-\lambda}, \tag{20}$$

where ω_0 is the frequency of the intrawell vibrations. Thus the interlevel spacing E of a TLS (which is its excitation energy) is given by

$$E = \sqrt{U^2+\Lambda^2}. \tag{21}$$

The transitions of atoms or group of atoms between these levels and the change in the levels' relative occupancy with varying temperature or under acoustic vibrations are responsible for the low-temperature properties of structural glasses. The same type of low-energy excitations were also found in amorphous metals and ionic conductors; see Black (1981) for a review.

Due to disorder, the TLSs have different values of U and λ. Physical considerations lead one to assume that the distribution of U and λ, $\mathcal{P}(U,\lambda)$, is almost constant in the region $\lambda \gg 1$, $U \ll \hbar\omega_0$ important for the effects observed in the experiments. Therefore it is assumed that in this region $\mathcal{P}(U,\lambda) = P_0$. Here P_0 is a constant, which can be found by comparison with experiments (Black, 1978; Halperin, 1976).

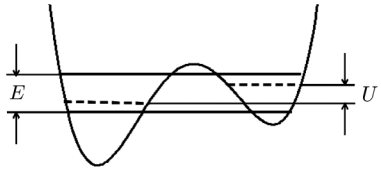

FIG. 3. Schematic diagram of the potential energy of a two-level tunneling system vs a configuration coordinate. U is the distance between the single-well energy levels, characterizing asymmetry of the potential. E is the difference between the lowest energy levels in a two-well potential with the account of tunneling below the barrier.

The rate of transitions between the two levels of a TLS is determined by interactions with phonons (in insulating solids), or with electrons (in metals). Assuming that fluctuations of the diagonal splitting U are most important, we can describe the interaction between the TLS and the environment as

$$\mathcal{H}_{\text{TLS-env}} = g'\hat{c}\tau_z, \tag{22}$$

where $\hat{c}$ is an operator in the Hilbert space of the environment depending on the specific interaction mechanism. It is convenient to diagonalize the TLS Hamiltonian,

$$\mathcal{H}_{\text{TLS}} = \tfrac{1}{2}(U\tau_z + \Lambda\tau_x), \tag{23}$$

where τ_i are the Pauli matrices, by rotating the TLS Hilbert space. Then

$$\mathcal{H}_{\text{TLS}} = (E/2)\tau_z, \tag{24}$$

$$\mathcal{H}_{\text{TLS-env}} = g'\hat{c}\left(\frac{U}{E}\tau_z + \frac{\Lambda}{E}\tau_x\right). \tag{25}$$

The interlevel transitions are described by the second term in the interaction Hamiltonian (25). Therefore, the relaxation rate for the deviation of the occupancy numbers of the levels from the equilibrium ones is proportional to $(\Lambda/E)^2$ (Jäckle, 1972; Black and Gyorffy, 1978):

$$\gamma = \gamma_0(E)\left(\frac{\Lambda}{E}\right)^2, \quad \gamma_0(E) \propto E^a \coth\left(\frac{E}{2k_BT}\right). \tag{26}$$

The quantity $\gamma_0(E)$ has the meaning of a *maximal* relaxation rate for the TLSs with given interlevel spacing E. The exponent a depends on the details of the interaction mechanism; its typical values are 3 (for the interaction with phonons) and 1 (for the interaction with electrons). Using Eq. (26) one obtains the distribution of the relaxation rates as

$$\mathcal{P}(\gamma, E) = \frac{E}{2U\gamma}\mathcal{P}(U, \lambda) = \frac{P_0}{2\gamma\sqrt{1-\gamma/\gamma_0}} \approx \frac{P_0}{2\gamma} \tag{27}$$

(here we have taken into account that small relaxation rates require small tunnel couplings of the wells, $\Lambda \ll U \simeq E$). Therefore, owing to the exponential dependence of γ on the tunneling parameter λ ($\gamma \propto e^{-2\lambda}$) and approximately uniform distribution in λ, the distribution with respect to γ is inversely proportional to γ in an exponentially broad interval, as is characteristic of systems showing $1/f$ noise.

Spontaneous transitions between the levels of the TLSs can lead to fluctuations of macroscopic properties, such as resistance of disordered metals (Kogan and Nagaev, 1984b; Ludviksson, Kree, and Schmid, 1984), density of electron states in semiconductors and metal-oxide-semiconductor structures (Kogan and Nagaev, 1984a), etc. These fluctuations have $1/f$ spectrum.

The mechanism of $1/f$ noise in hopping insulators has been investigated by several theoretical groups. It was first suggested (Shklovskii, 1980; Kogan *et al.*, 1981) that the $1/f$ noise in the nearest-neighbor-hopping transport is associated with electronic traps, in a way similar to McWhorter's idea of $1/f$ noise in metal-oxide-semiconductor field-effect transistors (McWhorter, 1957). Each trap consists of an isolated donor within a spherical pore of the large radius r. Such rare configurations form fluctuators, which have two possible states (empty or occupied) switching back and forth with the very slow rate defined by the tunneling rate of an electron out or into the pore.

According to Burin *et al.* (2006), two-level fluctuators can also be formed by different many-electron configurations having close energies. In this case, giant relaxation times necessary for $1/f$ noise are provided by a slow rate of simultaneous tunneling of many localized electrons and by large activation barriers for their consecutive rearrangements. The model qualitatively agrees with the low-temperature observations of $1/f$ noise in p-type silicon and GaAs. Several other models of the $1/f$ noise have been reviewed by Kogan (1996).

B. $1/f$ noise and random telegraph noise

In many systems comprising such semiconductor devices as p-n junctions, metal-oxide-semiconductor field-effect transistors, point contacts and small tunnel junctions between the metals, small semiconductor resistors or small metallic samples, the resistance switches at random between two (or several) discrete values. The time intervals between switchings are random, but the two values of the fluctuating quantity are time independent. This kind of noise is now usually called random telegraph noise (RTN); see Kogan (1996) for a review.

Statistical properties of RTNs in different physical systems are rather common. First, the times spent by the device in each of the states are much longer than the microscopic relaxation times. Therefore, the memory of the previous state of the system is erased, and the random process can be considered as a discrete Markovian process. Such a process (for a two-state system) is characterized by the equilibrium probabilities p_1 and $p_2 = 1 - p_1$ of finding the system, respectively, in the first and in the second state, as well as transition probabilities per unit time $\gamma_{1\to2}$ and $\gamma_{2\to1}$. The spectral density of a random quantity, which switches between the two states x_1 and x_2, can be easily derived as [cf. Kogan (1996)]

$$S_x(\omega) = \frac{(x_1 - x_2)^2}{4\cosh^2(E/2k_BT)}\mathcal{L}_\gamma(\omega), \tag{28}$$

where $\gamma \equiv \gamma_{1\to2} + \gamma_{2\to1}$. Therefore each RT process contributes a Lorentzian line to the noise spectrum.

RTN was observed in numerous small-size devices. At low temperatures, usually only one or few telegraph processes were observed. However, at higher temperatures (or at higher voltages applied to the device) the number of contributing telegraph processes increased. Typically, at high enough temperatures discrete resistance switching is not observed. Instead a continuous $1/f$ noise is measured. This behavior was interpreted by Rogers and Buhrman (1984, 1985) as a superposition of many uncorrelated two-state telegraph fluctuators with various relaxation rates γ. The increase of temperature leads to an increase in the number of contributing fluctuators and discrete switchings become indistinguishable.

A different interpretation was suggested by Ralls and Buhrman (1991), and references therein. This interpretation is based on interaction between the fluctuators leading to a deviation from the simple Lorentzian spectrum. Moreover, the system of interacting defects may pass to another metastable state where different defects play the role of active fluctuators. This interpretation is based on the observation of RTN in metallic nanobridges where the record of resistance at room temperature is still composed of one or two telegraph processes, but their amplitudes and characteristic switching rates change randomly in time. According to this interpretation, the system of interacting dynamic defects is similar to a glass, particularly, to a spin glass with a great number of metastable states between which it is incessantly wandering.

Despite great progress in the $1/f$ noise physics, for the major part of systems showing $1/f$ and/or random telegraph noise, the actual sources of the low-frequency fluctuations remain unknown: this is the main unsolved problem. Next we discuss some simple models in connection with devices for quantum computation.

C. Superconducting qubits and relevant noise mechanisms

Circuits presently being explored combine in variable ratios the Josephson effect and single Cooper-pair charging effects. When the Coulomb energy is dominant, the "charge circuits" can decohere from charge noise generated by the random motion of offset charges (Zimmerli *et al.*, 1992; Zorin *et al.*, 1996; Nakamura *et al.*, 2002). Conversely, when the Josephson energy is dominant, these "flux circuits" are sensitive to external flux and its noise (Wellstood, Urbina, and Clarke, 1987b; Mooij *et al.*, 1999; Friedman *et al.*, 2000). For the intermediate-energy regime, a circuit designed to be insensitive to both the charge and flux bias has recently achieved long coherence times ($\lesssim$500 ns), demonstrating the potential of superconducting circuits (Cottet *et al.*, 2002; Vion *et al.*, 2002). The third type is the phase qubit, which consists of a single Josephson junction current biased in the zero voltage state (Martinis *et al.*, 2002; Yu *et al.*, 2002). In this case, the two quantum states are the ground and first excited states of the tilted potential well, between which Rabi oscillations have been observed.[1]

In the case of charge qubits, the coherence times have been limited by low-frequency fluctuations of background charges in the substrate which couple capacitively to the island, thus dephasing the quantum state (Nakamura *et al.*, 2002). Flux and phase qubits are essentially immune to fluctuations of charge in the substrate, and, by careful design and shielding, can also be made insensitive to flux noise generated by either the motion of vortices in the superconducting films or by external magnetic noise. The flux-charge hybrid, operating at a proper working point, is intrinsically immune to both charge and flux fluctuations. However, all of these qubits remain sensitive to fluctuations in the Josephson coupling energy and hence in the critical current of the tunnel junctions at low frequency f. These fluctuations lead to variations in the level splitting frequency over the course of the measurement and hence to dephasing.

1. Charge noise in Josephson qubits

The importance of the charge noise was recognized after careful spin-echo-type experiments applied to an artificial TLS utilizing a charge degree of freedom of a small superconducting electrode—a so-called single-Cooper-pair box (CPB) (Nakamura, Chen, and Tsai, 1997; Bouchiat *et al.*, 1998).

To explain the main principle behind this device, we consider a small superconductor grain located close to a (gate) metallic electrode. The ground state energy of such a grain depends in an essential way on the number of electrons on it. Two contributions to such a dependence are given by the electrostatic Coulomb energy $E_C(n)$ determined by the extra charge accumulated on the superconducting grain and the so-called parity term Δ_n (Tuominen *et al.*, 1992, 1993; Eiles, Martinis, and Devoret, 1993; Hekking *et al.*, 1993; Lafarge *et al.*, 1993; Matveev *et al.*, 1993; Glazman *et al.*, 1994; Hergenrother, Tuominen, and Tinkham, 1994; Joyez *et al.*, 1994; Matveev, Glazman, and Shekhter, 1994). The latter originates from the fact that only an even number of electrons can form a Bardeen-Cooper-Schrieffer (BCS) ground state of a superconductor (which is a condensate of paired electrons) and therefore in the case of an odd number of electrons n one unpaired electron should occupy one of the quasiparticle states (Averin and Nazarov, 1992).[2]

The energy cost of occupying a quasiparticle state, which is equal to the superconducting gap Δ_0, brings a new scale to bear on the number of electrons that a small superconducting grain can hold. Taking the above into account, one presents the ground state energy $U_0(n)$ in the form (Hekking *et al.*, 1993; Matveev *et al.*, 1993; Glazman *et al.*, 1994; Matveev, Glazman, and Shekhter, 1994),

$$U_0(n) = E_C\left(n - \frac{q}{e}\right)^2 = \Delta_n, \quad \Delta_n = \begin{cases} 0 & \text{even } n, \\ \Delta_0 & \text{odd } n. \end{cases} \tag{29}$$

Here q is the charge induced on the grain by the gate electrode. One can see from Eq. (29) that if $\Delta_0 > E_C$ only an even number of electrons can be accumulated in the ground state of the superconducting grain. Moreover, for special values of the gate voltage corresponding to $q = (2n+1)e$ a degeneracy of the ground state occurs with respect to changing the total number of electrons by one single Cooper pair. An energy diagram illustrating this case is presented in Fig. 4. The occurrence of such a degeneracy brings about an important opportunity to create a quantum hybrid state at low temperatures which will be a coherent mixture of two ground states, differing by a single Cooper pair:

$$|\Psi\rangle = \alpha_1|2n\rangle + \alpha_2|2(n+1)\rangle. \tag{30}$$

[1] A more detailed description can be found in the reviews by Clarke and Wilhelm (2008), Makhlin, Schön, and Shnirman (2001), and Xiang *et al.* (2013).

[2] Averin and Nazarov (1992), Ref. [7], indicates that the original idea belongs to K. A. Matveev.

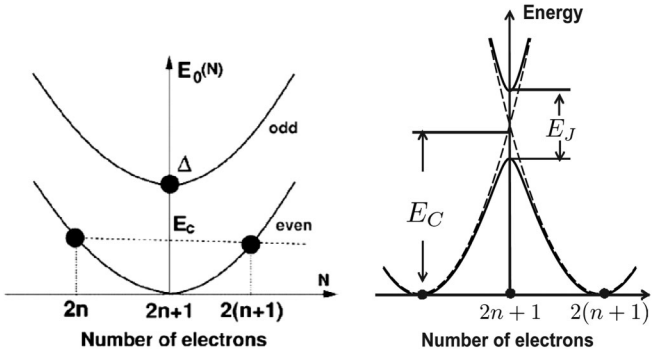

FIG. 4. Left panel: The energy diagram for the ground state of a superconducting grain with respect to charge for the case $\Delta_0 > E_C$. For a certain bias voltage when $q = (2n+1)e$, ground states differing by only one single Cooper pair become degenerate. Right panel: Energy of a Cooper-pair box with account of the Josephson tunneling.

The idea of the device is presented in Fig. 5, where the superconducting dot is shown to be in tunneling contact with a bulk superconductor. A gate electrode is responsible for lifting the Coulomb blockade of Cooper-pair tunneling (by creating the ground state degeneracy discussed above). This allows the delocalization of a single Cooper pair between two superconductors. Such a hybridization results in a certain charge transfer between the bulk superconductor and the grain. At the charge degeneracy point $q = (2n+1)e$, the Josephson tunneling produces an avoided crossing between the degenerate levels corresponding to the symmetrical and antisymmetrical superpositions $|2n\rangle \pm |2(n+1)\rangle$. As a result, the terms are split by an energy $E_J \ll E_C$. Far from this point the eigenstates are very close to being charge states.

To summarize, in a single-Cooper-pair box all electrons form Cooper pairs and condense in a single macroscopic ground state separated from the quasiparticle states by the superconducting gap Δ_0. The only low-energy excitations are transitions between the charge number states $|2n\rangle$, which are

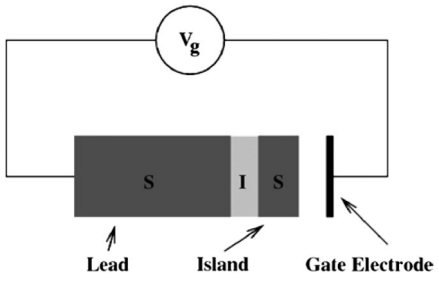

FIG. 5. Schematic diagram of a single-Cooper-pair box. An island of superconducting material is connected to a larger superconducting lead via a weak link. This allows coherent tunneling of Cooper pairs between them. For a nanoscale system, such quantum fluctuations of the charge on the island are generally suppressed due to the strong charging energy associated with a small grain capacitance. However, by appropriate biasing of the gate electrode it is possible to make the two states $|2n\rangle$ and $|2(n+1)\rangle$, differing by one Cooper pair, have the same energy (degeneracy of the ground state). This allows the creation of a hybrid state $|\Psi\rangle = \alpha_1|2n\rangle + \alpha_2|2(n+1)\rangle$.

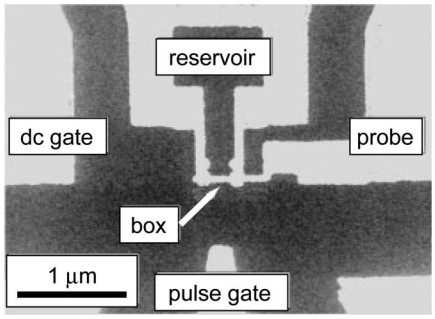

FIG. 6. Single-Cooper-pair box with a probe junction—micrograph of the sample. The electrodes were fabricated by electron-beam lithography and shadow evaporation of Al on a SiN_x insulating layer (400 nm thick) above a gold ground plane (100 nm thick) on the oxidized Si substrate. The "box" electrode is a $700 \times 50 \times 15$ nm Al strip containing $\sim 10^8$ conduction electrons. Adapted from Nakamura, Pashkin, and Tsai, 1999.

the states with an excess number of Cooper pairs in the box due to Cooper-pairs tunneling if Δ_0 is larger than the single-electron charging energy of the box E_C. The fluctuations of n are strongly suppressed if E_C exceeds both the Josephson energy E_J and the thermal energy k_BT. Then we get back to the Hamiltonian (1) with $\hbar\epsilon = E_C(n - q/e)^2$ (where q is the induced charge) and $\hbar\Delta = E_J$, i.e., the Josephson energy of the split Josephson junction between the box and the superconducting reservoir; see Fig. 5. Therefore, ϵ can be tuned through the gate voltage determining the induced charge. The Josephson junction is usually replaced by a dc SQUID with low inductance. E_J (and, consequently, Δ) is then adjusted by applying the appropriate magnetic flux. A realistic device is shown Fig. 6 (Nakamura, Pashkin, and Tsai, 1999).

Nakamura *et al.* (2002) compared the decay of the normalized echo signal (see Fig. 7) with the expression by Cottet *et al.* (2001):

$$\langle e^{i\varphi}\rangle = \exp\left[-\frac{1}{2\hbar^2}\int_{\omega_{\min}}^{\infty} d\omega S_\epsilon(\omega)\left(\frac{\sin^2(\omega\tau/4)}{\omega/4}\right)^2\right], \quad (31)$$

where $S_\epsilon(\omega)$ is the spectrum of the noise in the interlevel spacing $\hbar\epsilon$ of the qubit. The latter is expressed through the

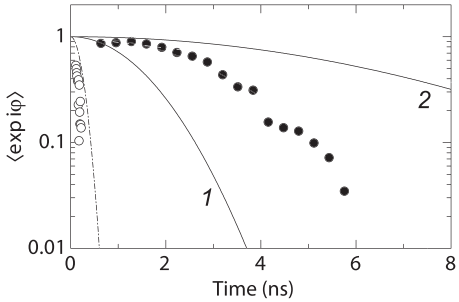

FIG. 7. Decay of the normalized amplitude of the echo signal (filled circles) and the free induction decay signal (open circles) compared with estimated decoherence factors $\langle e^{i\varphi}\rangle$ due to charge noise with the spectrum α/ω. Here $\sqrt{\alpha} \times 10^3 e^{-1}$ is 1.3 for line 1 and 0.3 for line 2. Adapted from Nakamura *et al.*, 2002.

charge noise $S_e(\omega)$ as $S_\epsilon(\omega) = (4E_C/e)^2 S_e(\omega)$. The charge noise spectrum was determined by a standard noise measurement on the same device used as a single-electron transistor. It can be expressed as $S_e(\omega) = \alpha/\omega$ with $\alpha = (1.3 \times 10^{-3} e)^2$. The estimate following from Eq. (31), with the mentioned value of α and $\omega_{\min} = 2\pi/t_{\max}$ being the low-frequency cutoff due to the finite data-acquisition time $t_{\max}$ (20 ms), is shown in Fig. 7 (solid line 1). Solid line 2 in the same figure corresponds to $\alpha = (3.0 \times 10^{-4} e)^2$. Note that Eq. (31) is based on the assumption that the fluctuations are Gaussian; it predicts that at small delay time τ the echo signal decays as $\ln\langle e^{i\varphi}\rangle \propto -\tau^2$. In Sec. III this assumption and the ensuing prediction is further discussed.

Astafiev *et al.* (2004) studied decoherence of the Josephson charge qubit by measuring energy relaxation and dephasing with the help of a single-shot readout. Both quantities were measured at different charges induced at the single-Cooper-pair box by the gate electrode. The decoherence was determined from decay of the coherent oscillations related to the noise spectrum as

$$\ln\langle e^{i\varphi}\rangle = -\frac{\epsilon^2}{2[(\hbar\epsilon)^2 + E_J^2]} \int_{\omega_{\min}}^{\infty} d\omega S_\epsilon(\omega) \left[\frac{\sin(\omega t/2)}{\omega/2}\right]^2. \quad (32)$$

Based on the dependence of the decoherence rate on the induced charge shown in Fig. 8 and on estimates of the noise, they concluded that the source of decoherence is charge noise having a $1/f$ spectrum. Another conclusion is that the energy relaxation rate Γ_1 is also determined by low-frequency noise of the same origin. This conclusion is drawn from the observed $\Gamma_1 \propto E_J^2/[(\hbar\epsilon)^2 + E_J^2]$ dependence. The importance of $1/f$ charge noise for decoherence in the so-called quantronium quantum bit circuit (Cottet *et al.*, 2002) was emphasized by Ithier *et al.* (2005).

To verify the hypothesis about the common origin of the low-frequency $1/f$ noise and the quantum f noise recently measured in the Josephson charge qubits, Astafiev *et al.* (2006) studied the temperature dependence of the $1/f$ noise amplitude and decay of coherent oscillations. The $1/f$ noise was measured in the SET regime. In the temperature domain 50 mK–1 K they demonstrated $\propto T^2$ dependence; see Fig. 9. The measurements of the noise were accompanied by measurements of the decay rate of the coherent oscillations away from the degeneracy point ($\hbar\epsilon \gg E_J$). The decay of the oscillations was fitted according to Eq. (32) yielding at small times the dependence $\langle e^{-i\varphi}\rangle \propto e^{-t^2/2T_2^{*2}}$. The results turned out to be consistent with the strength of the $1/f$ noise observed in transport measurements. To explain the quadratic temperature dependence of the $1/f$ noise they assumed that this dependence originated from two-level fluctuators with the density of states linearly dependent on the interlevel spacing. We discuss this assumption later while considering models for the noise-induced decoherence. Recently, measurements of charge noise in a SET showed a linear increase with temperature (between 50 mK and 1.5 or 4 K) above a voltage-dependent threshold, with a low-temperature saturation below 0.2 K (Gustafsson *et al.*, 2012). They concluded that this result is consistent with thermal interaction between SET electrons and TLSs residing in the immediate vicinity of the device. The possible defects include residue of Al grains formed around the perimeter of the SET island and leads during the two-angle evaporation (Kafanov *et al.*, 2008), as well as interface states between metal of the SET and its surrounding oxides (Choi *et al.*, 2009).

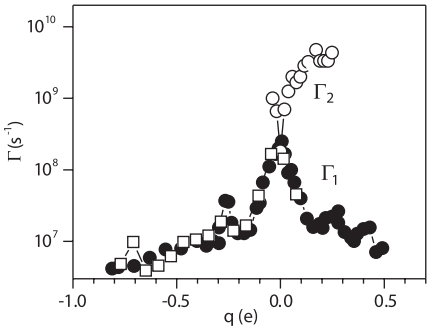

FIG. 8. Energy relaxation rate Γ_1 (closed circles and open squares) and phase decoherence rate $\Gamma_2 = T_2^{-1}$ (open circles) vs gate induced charge q. Adapted from Astafiev *et al.*, 2004.

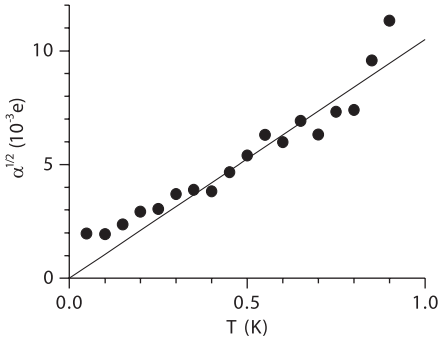

FIG. 9. Temperature dependence of the amplitudes $\alpha^{1/2}$, which can be approximated as $\alpha^{1/2} = (1.0 \times 10^{-2}\, e/\mathrm{K})T$. Adapted from Astafiev *et al.*, 2006.

Although the obvious source of RT charge noise is a charged particle which jumps between two different locations in space, less clear is where these charges are actually located and what are the two states. The first attempt of constructing such a model in relation to qubit decoherence appeared in Paladino *et al.* (2002), where electrons tunneling between a localized state in the insulator and a metallic gate was studied. This model was further studied by Grishin, Yurkevich, and Lerner (2005), Abel and Marquardt (2008), and Yurkevich *et al.* (2010). Later, experimental results (Astafiev *et al.*, 2004) indicated a linear dependence of the relaxation rate on the energy splitting of the two qubit states. One also has to take into account that in the experimental setup there is no normal metal in the vicinity of the qubit: all gates and leads should be in the superconducting state at the temperatures of experiment. These two facts suggest that the model (Paladino *et al.*, 2002) was not directly applicable to explain the decoherence in charge qubits (Nakamura *et al.*, 2002) and favored a model with superconducting electrodes (Faoro *et al.*, 2005). In this model, the two electrons of a Cooper pair are split and tunnel separately to some localized states in the insulator [see Fig. 10 for an illustration of this (model III) and other models]. A constant density of these localized states gives a linearly increasing density of occupied pairs, in agreement with

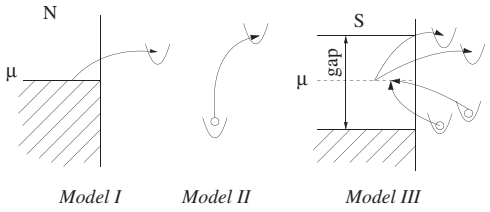

FIG. 10. Three possible models for the fluctuating charges: model I, electrons jumping between a localized state and a normal metal, as discussed by Paladino *et al.* (2002), Grishin, Yurkevich, and Lerner (2005), and Abel and Marquardt (2008); model II, electrons jumping between localized states; and model III, electrons jumping between localized states and a superconductor, as discussed by Faoro *et al.* (2005).

experiments (Astafiev *et al.*, 2004). This model was criticized (Faoro and Ioffe, 2006) because it required an unreasonably high concentration of localized states, and a more elaborate model involving Kondo-like traps was proposed. However, it was shown (Grishin, Yurkevich, and Lerner, 2005; Abel and Marquardt, 2008) that allowance for quantum effects of hybridization between the electronic states localized at the traps and extended states in the electrodes relaxes the above requirement. At present it seems that no solid conclusions can be drawn based on the available experiments.

As we have seen, the "standard" Cooper-pair boxes are rather sensitive to low-frequency noise from electrons moving among defects. This problem can be partly relaxed in more advanced charge qubits, such as transmon (Koch, DiVincenzo, and Clarke, 2007) and quantronium (Vion *et al.*, 2002). The transmon is a small Cooper-pair box where the Josephson junction is shunted by a large external capacitor to increase E_C and by increasing the gate capacitor to the same size. The role of this shunt is played by a transmission line, and therefore the qubit is called the *transmon*. The main idea is to increase the ratio E_J/E_C making the energy bands shown in Fig. 5 (right panel) almost flat. For this reason, the transmon is weakly sensitive to low-frequency charge noise at all operating points. This eliminates the need for individual electrostatic gate and tuning to a charge degeneracy point. A complementary proposal for using a capacitor to modify the E_J/E_C ratio in superconducting flux qubits was given by You *et al.* (2007).

At the same time, the large gate capacitor provides strong coupling to external microwaves even at the level of a single photon, greatly increasing coupling for cQED. The schematics of the suggested device is shown in Fig. 11, reprinted from Blais *et al.* (2004), where authors present a detailed discussion of cQED devices. Koch, DiVincenzo, and Clarke (2007) considered possible sources of dephasing and energy relaxation in transmon devices. In particular, the contributions of the charge, flux, and critical current to the dephasing rate T_2^{-1} were estimated. These (quite favorable) estimates are based on Eqs. (11) and (12), which follow from assuming Gaussian statistics of the noise. In some cases, the decoherence is predicted to be limited by the energy relaxation $T_2 \sim 2T_1$, which occurs due to dielectric losses (Martinis *et al.*, 2005) and quasiparticle tunneling (Lutchin, Glazman, and Larkin, 2005, 2006). Catelani *et al.* (2011) developed a general theory for the qubit decay rate induced by quasiparticles. They studied its dependence on the magnetic flux used to tune

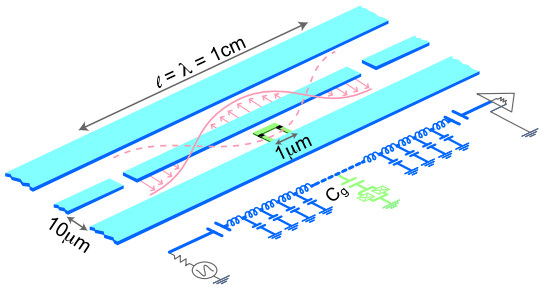

FIG. 11 (color online). Schematic layout and equivalent lumped circuit representation of proposed implementation of cavity QED using superconducting circuits. The 1D transmission line resonator consists of a full-wave section of a superconducting coplanar waveguide, which may be lithographically fabricated using conventional optical lithography. A Cooper-pair box qubit is placed between the superconducting lines and is capacitively coupled to the center trace at a maximum of the voltage standing wave, yielding a strong electric dipole interaction between the qubit and a single photon in the cavity. The box consists of two small ($\approx 100 \times 100$ nm^2) Josephson junctions, configured in a $\approx 1\,\mu$m loop to permit tuning of the effective Josephson energy by an external flux Φ_{ext}. Input and output signals are coupled to the resonator, via the capacitive gaps in the center line, from 50 Ω transmission lines, which allow measurements of the amplitude and phase of the cavity transmission, and the introduction of dc and rf pulses to manipulate the qubit states. From Blais *et al.*, 2004.

the qubit properties in devices such as the phase and flux qubits, the split transmon, and the fluxonium. Recently Hassler, Akhmerov, and Beenakker (2011) proposed using a transmon qubit to perform parity-protected rotations and readout of a topological qubit. The advantage over an earlier proposal using a flux qubit is that the coupling can be switched on and off with exponential accuracy, promising a reduced sensitivity to charge noise.

Interestingly, transmon qubits allow one to perform flux-noise spectroscopy at frequencies near 1 GHz using the phenomenon of measurement-induced qubit excitation in cQED (Slichter *et al.*, 2012). The extracted values agree with a $1/f^{\alpha}$ power-law fit below 1 Hz extracted from Ramsey spectroscopy and around 1–20 MHz deduced from Rabi oscillation decay. The above technique can be used to measure different types of qubit dephasing noise (charge, flux, or critical current noise, depending on the type of qubit used) at frequencies ranging from a few hundred MHz to several GHz, depending on the system parameters chosen.

Barends *et al.* (2013) demonstrated a planar, tunable superconducting qubit with energy relaxation times up to 44 μs. This was achieved by using a geometry based on a planar transmon (Houck *et al.*, 2007; Koch, DiVincenzo, and Clarke, 2007) and designed to both minimize radiative loss and reduce coupling to materials-related defects. They reported a fine structure in the qubit energy lifetime as a function of frequency, indicating the presence of a sparse population of incoherent, weakly coupled two-level defects. The suggested qubit (called "Xmon" because of its special geometry) combines facile fabrication, straightforward connectivity, fast control, and long coherence.

Finally, we mention an alternative single Cooper-pair circuit based on a superconducting loop coupled to an LC

resonator used for dispersive measurement analogously to cQED qubits and insensitive to offset charges. The circuit, named fluxonium, consists of a small junction shunted with the Josephson kinetic inductance of a series array of large-capacitance tunnel junctions, thereby ensuring that all superconducting islands are connected to the circuit by at least one large junction (Manucharyan *et al.*, 2009). The array of Josephson junctions with appropriately chosen parameters can perform two functions simultaneously: short circuit the offset charge variations of a small junction and protect the strong nonlinearity of its Josephson inductance from quantum fluctuations.

2. Flux and phase qubits

A flux qubit (see, e.g., Fig. 12), consists of a micrometer-sized loop with three or four Josephson junctions. The energy of each Josephson junction can be expressed as $E_J^{(i)}(1-\cos\delta_i)$, where $E_J^{(i)}$ is the Josephson energy of the ith junction while δ_i is the phase drop on the junction. The phase drops on the junctions are related by $\sum_i \delta_i + 2\pi(\Phi/\Phi_0) = 2\pi n$, where n is an integer number. Here Φ is the magnetic flux embedded in the loop while $\Phi_0 = \pi\hbar c/e$ is the magnetic flux quantum. To get the total energy one should add the charging energy of each junction $Q_i^2/2C_i$ and magnetic energy $(\Phi-\Phi_b)^2/2L$, where Φ_b is the bias flux created by external sources. Neglecting charging energies and magnetic energy of the loop and assuming that $E_J^{(1)} = E_J^{(2)} \equiv E_J$, $E_J^{(3)} = \alpha E_J$, one can express the total energy of the qubit as

$$u(\boldsymbol{\delta}) = 2 - \cos\delta_1 - \cos\delta_2 + \alpha[1+\cos(\varphi-\delta_1-\delta_2)], \tag{33}$$

where $u(\boldsymbol{\delta}) \equiv U(\delta_1,\delta_2)/E_J$, $\varphi \equiv \pi(2\Phi-\Phi_0)/\Phi_0$. The energy is a periodic function of δ_1 and δ_2 with a period of 2π. At $\varphi \ll 1$ and $\alpha > 1/2$ each elementary cell contains two close minima, the barrier between them being small. In the eigenbasis of the states representing these minima the qubit is then described by the effective Hamiltonian (1), where the

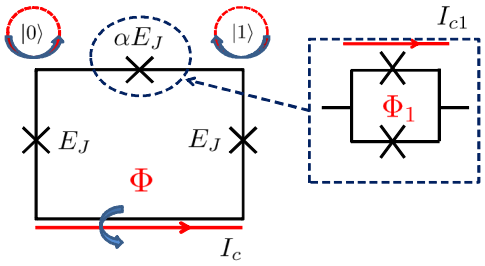

FIG. 12 (color online). A superconducting loop with three Josephson junctions (crosses) encloses a flux Φ that is supplied by an external magnet. Two junctions have a Josephson coupling energy E_J, and the third junction has αE_J, where $\alpha = 0.75$. This system has two (meta)stable states $|0\rangle$ and $|1\rangle$ with opposite circulating persistent current. The level splitting is determined by the offset of the flux from $\Phi_0/2$. The barrier between the states depends on the value of α. The qubit is operated by resonant microwave modulation of the enclosed magnetic flux by a superconducting control line I_c. From Mooij *et al.*, 1999.

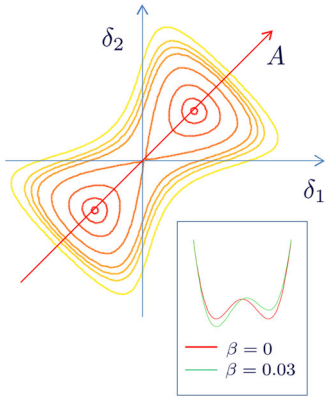

FIG. 13 (color online). Plot $u(\boldsymbol{\delta})$ for $\alpha = 0.75$. The inset shows the potential profile along the line A for different $\beta \equiv (2\Phi-\Phi_0)/\Phi_0$. The potential is symmetric for $\beta = 0$.

asymmetry $\hbar c$ can be tuned by the embedded magnetic flux Φ. Figure 13 shows the plot $u(\boldsymbol{\delta})$ for $\alpha = 0.75$. The inset shows the potential profile along the line A for different $\beta \equiv (2\Phi-\Phi_0)/\Phi_0$. To tune the tunneling parameter Δ, one can replace the third junction by two Josephson junctions connected in parallel, as shown in Fig. 12 (inset). The Josephson energy of this circuit can be tuned by the magnetic flux through the second loop, which in turn can be tuned by an external current-carrying line. Quantum superpositions of these states are obtained by pulsed microwave modulation of the enclosed magnetic flux by currents in control lines. Such a superposition was demonstrated by Friedman *et al.* (2000) and Van der Wal *et al.* (2000).

Although fabricated Josephson circuits exhibit a high level of static and dynamic charge noise due to charged impurities, the magnetic background is much more clean and stable. The flux qubits can be driven individually by magnetic microwave pulses; measurements can be made with superconducting magnetometers (SQUIDs). They are decoupled from charges and electrical signals, and the known sources of decoherence allow for a decoherence time of more than 1 ms. Entanglement is achieved by coupling the flux, which is generated by the persistent current, to a second qubit. The qubits are small (of the order of 1 mm) and can be individually addressed and integrated into large circuits. However, they are slower than the charge qubits. As it follows from Eq. (33), fluctuations of two parameters—magnetic flux Φ and Josephson energies $E_J^{(i)}$ (or Josephson critical currents $J_C^{(i)}$)—are important for the operation of flux qubits.

Phase qubits (Martinis *et al.*, 2002) are designed around a 10 μm scale Josephson junction in which the charging energy is very small, thus providing immunity to charge noise. Although still sensitive to flux, the circuit retains the quality of being tunable, and calculations indicate that decoherence from flux noise is small. The main part of a phase qubit is a current-biased Josephson junction, which can be characterized by the potential energy

$$U(\delta) = -E_J[\cos\delta + (I/I_J)\delta]. \tag{34}$$

Because the junction bias current I is typically driven close to the critical current I_J the tilted washboard potential (34) can

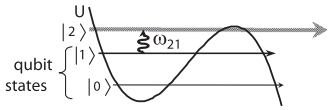

FIG. 14. Cubic potential U showing qubit states and a measurement scheme. Adapted from Martinis *et al.*, 2002.

be well approximated by a cubic potential with the barrier height

$$\Delta U(I) = (4\sqrt{2}/3)E_J[1 - I/I_J]^{3/2}.$$

Therefore, the barrier can be tuned by the bias current; at $I \to I_J$ it vanishes. The bound quantum states $|n\rangle$ with energy E_n (see Fig. 14) can be observed spectroscopically by resonantly inducing transitions with microwaves at frequencies $\omega_{mn} = (E_m - E_n)/\hbar$. The qubit state can be manipulated with dc and microwave pulses at frequency ω_{10} of the bias current. The measurement of the qubit state utilizes the escape from the cubic potential via tunneling. To measure the occupation probability p_1 of state $|1\rangle$, microwave pulses at frequency ω_{21} driving a $1 \to 2$ transition were used. The large tunneling rate then causes state $|2\rangle$ to rapidly tunnel. Since the potential profile depends on E_J, i.e., on the Josephson critical current, as well as on the bias current through the junction, their fluctuations are important. Unlike the other qubits, the phase qubit does not have a degeneracy point. Below we briefly discuss main noise sources in flux and phase qubits.

a. Flux noise

The origin of magnetic flux noise in SQUIDs with a power spectrum of the $1/f$ type has been a puzzle for over 20 years. The noise magnitude, a few $\mu\Phi_0$ $\mathrm{Hz}^{1/2}$ at 1 Hz, scales slowly with the SQUID area and does not depend significantly on the nature of the thin-film superconductor or the substrate on which it is deposited. The substrate is typically silicon or sapphire, which are insulators at low temperature (Wellstood, Urbina, and Clarke, 1987b). Flux noise of a similar magnitude is observed in flux (Yoshihara *et al.*, 2006; Kakuyanagi *et al.*, 2007) and phase (Bialczak *et al.*, 2007) qubits. The near insensitivity to the device area of the noise magnitude (normalized by the device area) (Wellstood, Urbina, and Clarke, 1987b; Bialczak *et al.*, 2007; Lanting *et al.*, 2009) suggests that the origin of the noise is local.

Koch, DiVincenzo, and Clarke (2007) proposed a model in which electrons hop stochastically between traps with different preferential spin orientations. They found that the major noise contribution arises from electrons above and below the superconducting loop of the SQUID or qubit, and that an areal density of about 5×10^{13} cm^{-2} unpaired spins is required to account for the observed noise magnitude. de Sousa (2007) proposed that the noise arises from spin flips of paramagnetic dangling bonds at the Si-SiO_2 interface. Assuming an array of localized electrons, Faoro, Kitaev, and Ioffe (2008) suggested that the noise results from electron spin diffusion. The model was extended by Faoro, Ioffe, and Kitaev (2012) where it was shown that in a typical random configuration some fractions of spins form strongly coupled pairs behaving as two-level systems. Their switching dynamics is driven by the high-frequency noise from the surrounding spins, resulting in low-frequency $1/f$ noise in the magnetic susceptibility and other physical quantities.

Sendelbach *et al.* (2008) showed that thin-film SQUIDs are paramagnetic, with a Curie ($\propto T^{-1}$) susceptibility. Assuming the paramagnetic moments arise from localized electrons, they deduced an areal density of 5×10^{13} cm^{-2}. Subsequently, Bluhm *et al.* (2009) used a scanning SQUID microscope to measure the low-T paramagnetic response of (nonsuperconducting) Au rings deposited on Si substrates, and reported an areal density of 4×10^{13} cm^{-2} for localized electrons. Paramagnetism was not observed on the bare Si substrate.

Choi *et al.* (2009) proposed that the local magnetic moments originate in metal-induced gap states (MIGS) (Louie and Cohen, 1976) localized by potential disorder at the metal-insulator interface. At an ideal interface, MIGS are states in the band gap that are evanescent in the insulator and extended in the metal (see Fig. 15). At a metal-insulator interface there are inevitably random fluctuations in the electronic potential. The MIGS are particularly sensitive to these potential fluctuations, and a significant fraction of them with single occupancy becomes strongly localized near the interface, producing the observed paramagnetic spins. The local moments interact via mechanisms such as direct superexchange and the Ruderman-Kittel-Kasuya-Yosida (RKKY) interaction between themselves, and Kondo exchange with the quasiparticles in the superconductor. This system, in principle, can exhibit a spin-glass transition. However, experiments (Harris *et al.*, 2008) suggest that at $T > 55$ mK the spins are in thermal equilibrium and exhibit a $1/T$ (Curie law) static susceptibility. To explain the observed $1/f^{\alpha}$ $(0.6 < \alpha < 1)$ noise spectrum of the magnetic flux they suggest that in this region one can use the fluctuation-dissipation theorem leading to the conclusion that fluctuations of the electronic momenta have also a $1/f^{\alpha}$ spectrum. Unfortunately, without knowing the form of the interaction between the spins, one cannot derive this behavior theoretically—this is still an open question.

Recently Sank *et al.* (2012) measured the dependence of qubit phase coherence and flux noise on inductor loop geometry. They concluded that while wider inductor traces do not change either the flux-noise power spectrum or the qubit dephasing time, increased inductance leads to a simultaneous increase in both. Another important result is the absence of scaling with the trace aspect ratio. Anton *et al.* (2013) performed flux-noise measurements as a function of temperature in 10 dc SQUIDs with systematically varied

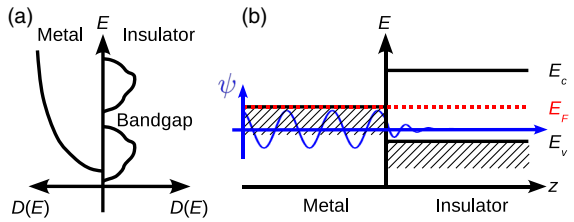

FIG. 15 (color online). (a) Schematic density of states. (b) MIGS at a perfect interface with energy in the band gap are extended in the metal and evanescent in the insulator. Adapted from Choi *et al.*, 2009.

geometries. Measurements have shown that α increases as the temperature is lowered. Moreover, for a given SQUID the spectrum pivoted about a nearly fixed frequency as the temperature was changed. The mean-square flux noise, inferred by integrating the power spectra, was found to rapidly grow with temperature and, at given T, to be approximately independent of the outer dimension of a given SQUID. They argued that those results are incompatible with a model based on the random reversal of independent, surface spins and considered the possibility that the spins form clusters (Sendelbach *et al.*, 2009); see Sec. III.B.2. An interpretation in terms of a spin-diffusion constant increasing with temperature is instead proposed by Lanting *et al.* (2013).

b. Critical current noise

Noise of the Josephson critical current in various superconducting qubits incorporating Josephson junctions was investigated in detail by Van Harlingen *et al.* (2004). They considered critical-current fluctuations caused by charge trapping at defect sites in the tunneling barrier and compared their contribution to the dephasing time with that of the flux noise due to hopping of the vortices through the SQUID loop (see Fig. 16). This mechanism can usually be made negligible in devices fabricated with linewidths less than approximately $\sqrt{\Phi_0/B}$ for which vortex trapping in the line is suppressed (Dantsker *et al.*, 1996); here B is the field in which the device is cooled. The trapped charges block tunneling through a region of the junction due to the Coulomb repulsion, effectively modulating the junction area. In general, a single-charge fluctuator produces a two-level, telegraph noise in the critical current of a junction characterized by the lifetimes τ_u in the untrapped state (high critical current), and τ_t in the trapped state (low critical current). This produces a Lorentzian peak in the power spectral density with a characteristic rate $\gamma = \tau_u^{-1} + \tau_t^{-1}$. Experiments on dynamics of such fluctuators and their lifetimes (Rogers and Buhrman, 1984, 1985; Wakai and Van Harlingen, 1986) provide strong evidence that the dominant charges enter the barrier from one electrode and exit to the other (voltage dependence), and that the fluctuators exhibit a crossover from thermal activation to tunneling behavior at about 15 K. In the tunneling regime, the fluctuating entity has been shown to involve an atomic mass, suggesting that ionic reconfiguration plays an important role in the tunneling process (Galperin, Gurevich, and Kozub, 1989). Although interactions between traps resulting in multiple-level hierarchical kinetics have been observed (Wakai and Van Harlingen, 1987), usually the traps can be considered to be local and noninteracting. In this limit, the coexisting traps produce a distribution of Lorentzian features that superimpose to give a $1/f$-like spectrum. Careful analysis of the influence of the noise in the Josephson critical current on different qubit designs and various data acquisition schemes has led (Van Harlingen *et al.*, 2004) to the conclusion that, although there is strong evidence that the noise derives from a superposition of random telegraph signals produced by charge trapping and untrapping processes, the origin of $1/f$ noise in the critical current of Josephson junctions is still not fully understood. In particular, the origin of the $\propto T^2$ dependence of the noise power observed by Wellstood, Urbina, and Clarke (1987a, 1987b, 2004) remains puzzling. To account for this behavior Shnirman *et al.* (2005) suggested that the density of states for two-level fluctuators is proportional to their interlevel spacing E. This assumption was supported with a microscopic model by Faoro *et al.* (2005). However, detailed measurements by Eroms *et al.* (2006) showed that, in shadow-evaporated $Al/AlO_x/Al$ tunnel junctions utilized in many superconductor-based qubits, the noise power is $\propto T$ between 150 and 1 K rather than $\propto T^2$. The observed spectral density saturates below 0.8 K due to individual strong two-level fluctuators. Interestingly, the noise spectral density at 4.2 K is 2 orders of magnitude lower than expected from the literature survey of Van Harlingen *et al.* (2004). Recently, measurements in $Al/AlO_x/Al$ Josephson junctions reported by Nugroho, Orlyanchik, and Van Harlingen (2013) showed an equivalence between the fractional noise power spectra of the critical current S_{I_c}/I_c^2 and the normal-state resistance S_{R_n}/R_n^2 with a linear temperature dependence down to the lowest temperatures measured, consistent with Eroms *et al.* (2006). Both fractional power spectra displayed an inverse scaling with the junction area down to $A \lesssim 0.04\ \mu m^2$ at $T = 2$ K. The estimated TLS density is consistent with observations from qubit energy spectroscopy (Martinis *et al.*, 2005) and glassy systems (Phillips, 1987). Similar noise characteristics have been observed in junctions with AlO_x and Nb electrodes (Pottorf, Patel, and Lukens, 2009). These properties suggest that the noise sources are insensitive to the barrier interfaces and that the main contribution comes from TLSs buried within the amorphous AlO_x barrier.

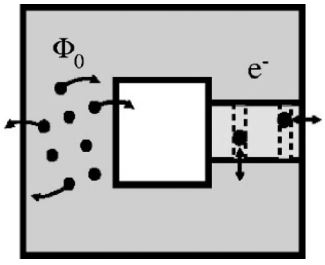

FIG. 16. Flux modulation from vortices hopping into and out of a loop, and critical-current modulation from electrons temporarily trapped at defect sites in the junction barrier. Adapted from Van Harlingen *et al.*, 2004.

The role of the critical current noise is conventionally allowed for by introducing a coupling term into the Hamiltonian (Simmonds *et al.*, 2004; Faoro *et al.*, 2005; Ku and Yu, 2005; Shnirman *et al.*, 2005; Faoro and Ioffe, 2006). A simple microscopic model relevant to $Al/AlO_x/Al$ was developed by Constantin and Yu (2007). This model leads to the scaling of the $1/f$ noise with the junction thickness as $\propto L^5$. The results are in reasonable agreement with corresponding experimental values of Zimmerli *et al.* (1992), Zorin *et al.* (1996), and Eroms *et al.* (2006). However, to the best of our knowledge, the predicted scaling has not yet been verified.

c. Decoherence in Josephson qubits from dielectric losses

As mentioned in Sec. II.A, amorphous materials contain low-energy excitations behaving as two-level tunneling systems. These states are responsible for low-temperature thermal and kinetic properties of structural glasses, in particular, for specific heat and dielectric losses. Due to interaction with their environment, the TLSs switch between their states producing low-frequency noise. These noises act on a qubit reducing its coherence time.

Martinis *et al.* (2005) pointed out that the noises produced by TLSs in amorphous parts of qubit devices are of primary importance. The reason is that crossover wiring in complex superconducting devices requires an insulating spacer that is typically made from amorphous SiO_2 deposited by chemical vapor deposition (CVD). They performed a variety of microwave qubit measurements and showed that the results are well modeled by loss from resonant absorption of two-level defects. Dielectric loss (loss tangent) in a system formed by a superconductor lead and a 300 nm thick CVD SiO_2 layer was measured at $f \sim 6$ GHz and $T = 25$ mK $\ll \hbar\omega/k_B$. Generally, two mechanisms contribute to the dissipation induced by the two-level defects. The first (resonant) is due to direct microwave-induced transitions between the TLS's level with subsequent emission of phonons. The second one is due to the relaxation-induced lag in phase between the nonequilibrium level populations and the driving ac electric field. One can expect that at $\hbar\omega \gg k_B T$ the first mechanism should dominate (Hunklinger and von Schickfus, 1981). A hallmark of the resonant absorption is its strong dependence on the amplitude of the applied ac electric field. This dependence is due to a decrease of the difference between the occupancies of the upper and lower levels with the field amplitude increase. The theoretical prediction for the loss tangent β is (von Schickfus and Hunklinger, 1977)

$$\beta = \frac{\pi \bar{P}(ed)^2}{3\varkappa} \frac{\tanh(\hbar\omega/2k_B T)}{\sqrt{1+\omega_R^2 T_1 T_2}}. \tag{35}$$

Here $\bar{P}$ is the TLS density of states each having a fluctuating dipole moment ed and relaxation times T_1 and T_2, $\varkappa$ is the dielectric constant, while $\omega_R = e\mathcal{E}d/\hbar$ is the TLS Rabi frequency corresponding to the ac field amplitude $\mathcal{E}$. Equation (35) is derived under the assumption that distributions of interlevel spacings and logarithms of the relaxation times of the TLSs are smooth. The theory fits the experimental data well with parameters compatible with previous measurements of bulk SiO_2 (von Schickfus and Hunklinger, 1977). The above results are consistent with previous measurements of an AlO_x capacitor by Chiorescu *et al.* (2004).

A key difference between tunnel junctions and bulk materials is that tunnel junctions have small volume, and the assumption of a continuous distribution of defects is incorrect. Instead, dielectric loss must be described by a sparse bath of discrete defects. Indeed, individual defects were measured spectroscopically with the phase qubit (Cooper *et al.*, 2004; Simmonds *et al.*, 2004; Lisenfeld *et al.*, 2010a, 2010b). They are observed as avoided crossings in the plots of the occupation probability versus qubit bias. A qualitative trend is that small-area qubits show fewer splittings than do large-area qubits, although larger splittings are observed in the smaller junctions. It follows from a quantitative analysis of the number of resonances that couple to the qubit that at large area the decoherence rate is compatible with the loss tangent of a bulk material.

Based on the obtained results, Martinis *et al.* (2005) formulated the following trends for making devices with long coherence times: (i) the usage of small-area junctions where the number of two-level defects is small, (ii) the usage of simple designs with no lossy dielectrics directly connected to the qubit junction, and (iii) trying to find insulating materials with low dielectric losses.

A way to eliminate the effects of low-frequency charge (and flux) noise is to operate the system close to the degeneracy point [$\epsilon = 0$ in the Hamiltonian (1)]. Indeed, since the distance between the energy levels is $\hbar\Omega = \hbar\sqrt{\epsilon^2 + \Delta^2}$, the fluctuation part $\hbar\delta\epsilon(t)$ of the potential energy $\hbar\epsilon(t)$ creates the additional shift

$$\delta\Omega(t) = \frac{\epsilon}{\Omega}\delta\epsilon(t) + \frac{1}{2}\frac{\Delta^2}{\Omega^3}[\delta\epsilon(t)]^2. \tag{36}$$

Therefore, at $\epsilon = 0$ the charge noise vanishes in the linear approximation and only second-order contributions are important. For a charge qubit, the degeneracy point corresponds to the induced charge $q = e$, while for a flux qubit this point corresponds to an integer number of the half-flux quanta in the loop. This idea of tuning the device to the *double* degeneracy point where the qubit is insensitive to both the charge and flux noise was implemented in the *quantronium* device (Cottet *et al.*, 2002; Vion *et al.*, 2002; Ithier *et al.*, 2005).

The main principle behind the device is shown in Fig. 17. The CPB involves two Josephson junctions with a capacitance

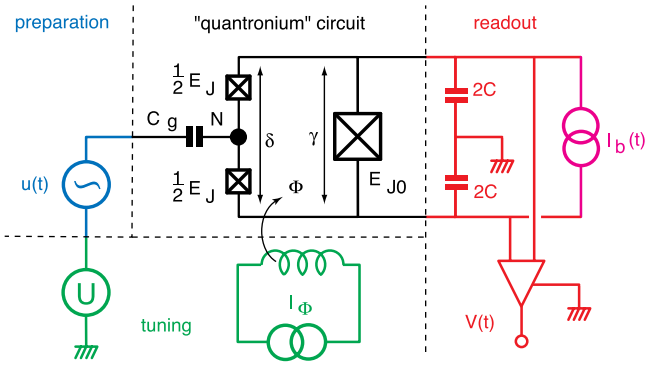

FIG. 17 (color online). Idealized circuit diagram of the quantronium, a quantum-coherent circuit with its tuning, preparation, and readout blocks. The circuit consists of a CPB island (black node) delimited by two small Josephson junctions (crossed boxes) in a superconducting loop. The loop also includes a third, much larger Josephson junction shunted by a capacitance C. The Josephson energies of the box and the large junction are E_J and E_{J0}. The Cooper pair number N and the phases δ and γ are the degrees of freedom of the circuit. A dc voltage U applied to the gate capacitance C_g and a dc current I_Φ applied to a coil producing a flux Φ in the circuit loop tune the quantum energy levels. Microwave pulses $u(t)$ applied to the gate prepare arbitrary quantum states of the circuit. The states are read out by applying a current pulse $I_b(t)$ to the large junction and by monitoring the voltage $V(t)$ across it. From Vion *et al.*, 2002.

C_g connected to the island separating them. The junctions are connected to a third, larger junction, with a larger Josephson energy, to form a superconducting loop threaded by a magnetic flux Φ. To achieve insensitivity to the charge noise the qubit is operated at $N_g \equiv C_g U/(2e) = 0.5$, where the energy levels have zero slope and the energy-level splitting is E_J. Insensitivity to the flux noise is achieved by applying an integer number of half-flux quanta to the loop. Therefore, a double degeneracy point can be achieved by tuning dc gate voltage U and the current I_Φ. To measure the qubit state one has to shift the qubit from this point. This was achieved by the current pulse $I_b(t)$ applied to the loop, which produces a clockwise or counterclockwise current in the loop, depending on the state of the qubit. The direction of the current is determined by the third (readout) junction since the circulating current either adds or subtracts from the applied current pulse. As a result, the readout junction switches out of the zero-voltage state at different values of the bias current. Thus, the state of the qubit was determined by measuring the switching currents. In the quantronium, much longer relaxation and decoherence times can be achieved compared with conventional CPB.

D. Semiconductor-based qubits

Here we briefly discuss main trends in designing the qubits based on semiconductors and semiconductor devices. One can find more detailed discussion in the reviews by Hanson *et al.* (2007), Chirolli and Burkard (2008), Liu, Yao, and Sham (2010), and Zak *et al.* (2010).

1. Spin qubits

It is natural to choose the electron spin as the two-state system that encodes the qubit. In modern semiconductor structures the spin of the electron can have a much longer coherence time than the charge degrees of freedom. However, it is not easy to isolate, control, and manipulate the spin degree of freedom of an electron to a degree required for quantum computation. A successful and promising device for the physical implementation of electron spin-based qubits is the semiconductor quantum dot (Loss and DiVincenzo, 1998).

The quantum dots (QDs) considered for implementation of quantum algorithms are confined regions of semiconductor materials coupled with reservoirs by tunable tunnel barriers. The height of the barriers, and consequently the rates for tunneling through the barriers on and off the dot, can be controlled via the application of gate electrodes. The dots are actually quantum boxes having discrete energy levels, their positions with respect to the chemical potential of the reservoir can be also tuned by electrostatic potentials. Therefore, QDs can be considered as tunable artificial atoms. Coulomb interactions between the electrons (or holes) occupying the dot's levels determine the energy cost for adding an extra electron. Because of this cost, the electron transport through the dot can be strongly suppressed at low temperatures (the so-called Coulomb blockade). Since the energy cost can be tuned by gate electrodes, the QD devices are promising for many applications.

Among many types of quantum dots, devices based on lateral III-V semiconductor QDs are of special interest. Such

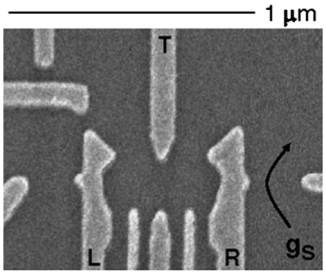

FIG. 18. Scanning electron microscopy (SEM) image of a double quantum dot device. A quantum point contact with conductance g_S senses a charge on the double dot. From Petta *et al.*, 2008.

devices are usually fabricated from heterostructures of GaAs and AlGaAs grown by molecular beam epitaxy. In such heterostructures the electron motion can be confined to a thin layer along the interface forming a two-dimensional electron gas (2DEG) with high mobility ($\sim 10^5$–10^7 cm^2/V s) and low density ($\sim 10^{11}$ cm^{-2}). The low density results in a relatively long Fermi wavelength ($\sim$40 nm) and a large screening length. Therefore, the 2DEG can be locally depleted by an electrostatic field applied to a metal gate electrode allowing one to design quantum devices similar to that shown in Fig. 18. When the lateral size of the dot is comparable with the Fermi wavelength the distance between the discretized energy levels becomes larger than the temperature (at temperatures of tens of millikelvins), and quantum phenomena become important.

Spin relaxation and dephasing in quantum dots: Two kinds of environment turn out to affect mainly the dynamics of an electron spin in a quantum dot, the phonons in the lattice, and the spins of atomic nuclei in the quantum dot.

Starting from Khaetskii and Nazarov (2000, 2001), the phonon-induced relaxation was extensively studied. It turns out that the lattice phonons do not couple directly to the spin degree of freedom. However, even without the application of external electric fields, the breaking of inversion symmetry in GaAs gives rise to spin-orbit (SO) interaction, which couples the spin and the orbital degrees of freedom. These orbital degrees of freedom, being coupled to the phonons, provide an indirect coupling between the electron spin and the phonons, which constitute a large dissipative bosonic reservoir and provide a source of decoherence and relaxation. Short time correlations in the phonon bath induce a Markovian dynamics of the electron spin, with well-defined relaxation and decoherence times T_1 and T_2.

As discussed in Sec. I.B, in the Bloch picture, pure dephasing arises from longitudinal fluctuations of the magnetic field, while a perturbative treatment of the SO interaction gives rise, within first order, to a fluctuating magnetic field perpendicular to the applied magnetic field. As a consequence the decoherence time T_2 is limited only by its upper bound T_1, $T_2 = 2T_1$.

Hyperfine interaction was first taken into consideration as a source of decoherence for an electron spin confined in a quantum dot by Burkard, Loss, and DiVincenzo (1999). This interaction is important since in a $\sim$40 nm GaAs quantum dot the wave function of an electron overlaps with approximately

10^5 nuclei. The electron spin and the nuclear spins in the dot couple via the Fermi contact hyperfine interaction, which creates entanglement between them and strongly influences the electron spin dynamics. It turns out that long-time correlations in the nuclear spin system induce a non-Markovian dynamics of the electron spin, with nonexponential decay in time of the expectation values of the electron spin components.

The relative importance of the above decoherence mechanisms depends on the external magnetic field: the phonon-induced relaxation rate of the electron spin is enhanced by an applied magnetic field, whereas the influence of the hyperfine interaction is reduced by a large Zeeman splitting.

In this review, we do not focus on decoherence in semiconductor spin qubits, which has been extensively reviewed, e.g., by Chirolli and Burkard (2008). More recent papers related to random telegraph or $1/f$ noise address charge traps near the interface of a Si heterostructure (Culcer, Hu, and Das Sarma, 2009), as well as nearby two-level charge fluctuators in a double dot spin qubit (Ramon and Hu, 2010).

2. Charge qubits

In semiconductor systems, a charge qubit can be formed by isolating an electron in a tunnel-coupled double quantum dot (DQD) (Hayashi *et al.*, 2003; Fujisawa, Hayashi, and Sasaki, 2006). Here we discuss a DQD consisting of two lateral QDs, which are coupled to each other through a tunnel barrier. Each QD is also connected to an electron reservoir via a tunnel junction. The operation of such a device can be analyzed from its electric circuit model shown in Fig. 19. The transport properties of a semiconductor DQD have been studied extensively (Grabert and Devoret, 1991; Kouwenhoven *et al.*, 1997; van der Wiel *et al.*, 2002). Each tunnel barrier has a small coupling capacitance C_i as well as a finite tunneling coupling T_c, and single-electron transport through the DQD can be measured. The tunneling rates for the left and right tunnel barriers are denoted as Γ_L and Γ_R, respectively. In addition, the DQD is connected to gate voltages V_l and V_r via capacitors C_l and C_r, respectively, so that the local electrostatic potential of each dot can be controlled independently. The energy difference between the electrochemical potentials μ_L and μ_R of the left and right reservoirs corresponds to the

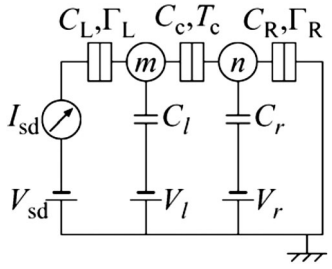

FIG. 19. Electric circuit model of a DQD containing m and n electrons in the left and right dots, respectively. The two QDs are coupled to each other via a tunnel junction, and each dot is connected to an electron reservoir via a tunnel junction. The electrostatic potential of the left (right) quantum dot is controlled by the gate voltage V_l (V_r) through the capacitance C_l (C_r). Adapted from Fujisawa, Hayashi, and Sasaki, 2006.

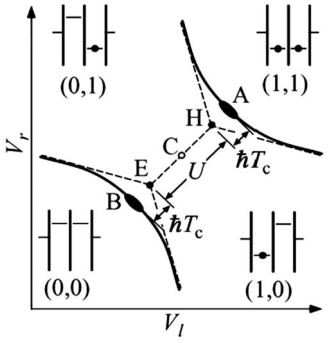

FIG. 20. Fragment from the stability diagram. Adapted from Fujisawa, Hayashi, and Sasaki, 2006.

applied source—drain voltage V_{sd}. The stable charge configuration (m,n), with m electrons on the left QD and n electrons on the right one, minimizes the total energy in all capacitors minus the work that has been done by the voltage sources. This energy can be estimated from the equivalent circuit in Fig. 19; see, e.g., Heinzel (2007), Sec. 9.3. A fragment of the stability diagram in the V_l-V_r plane is shown in Fig. 20.

When the tunneling coupling T_c is negligibly small, the boundaries of the stable charge states appear as a honeycomb pattern, a part of which is shown by dashed lines. The triple points E and H of three charge states are separated by a length corresponding to the interdot Coulomb energy U. Electrons pass through three tunnel barriers sequentially in the vicinity of triple points. On the other hand, the tunneling process at H can be viewed as a hole transport, as the unoccupied state (hole) moves from the right to the left (not shown in the diagram).

When the tunneling coupling is significantly large, the charging diagram deviates from the honeycomb pattern as shown by solid lines in Fig. 20. Due to quantum repulsion of the levels, the minimum distance between A and B is increased by the coupling energy $\hbar\Delta = \hbar T_c$ from its original value U.

The idealized dynamics of the qubit can be described assuming that each dot has a single energy level ϵ_i. Then the effective Hamiltonian can be expressed in the form (1) with $\hbar\epsilon = \epsilon_L - \epsilon_R$ and $\Delta = T_c$. The parameters of the Hamiltonian can be tuned by the gate voltages.

Coherent control of a GaAs charge qubit has been demonstrated (Hayashi *et al.*, 2003; Fujisawa *et al.*, 2004), along with correlated two-qubit interactions (Shinkai *et al.*, 2009). In these experiments each dot contained a few tens of electrons, potentially complicating the qubit level structure. In addition, the dots were strongly coupled with the leads typically limiting coherence times to ~1 ns (due to quantum cotunneling).

A coherent control of tunable GaAs charge qubit containing a single electron was demonstrated by Petersson *et al.* (2010) (see Fig. 21). The gate electrodes are arranged in a triple QD geometry and deplete 2DEG in the GaAs/AlGaAs heterostructure (Petta, Lu, and Gossard, 2010). The DQD was formed using the left and middle dots of the structure, while the right side of the device was configured as a noninvasive quantum point contact (QPC) charge detector. The device operated near the $(1,0)-(0,1)$ charge transition, where

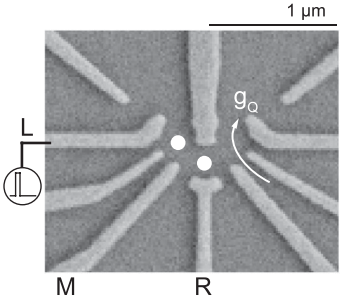

FIG. 21. Scanning electron microphotograph of a device similar to the one measured. Adapted from Petersson *et al.*, 2010.

(n_L, n_R) denote the absolute number of electrons in the left and right dots. The level detuning $\hbar\epsilon$ was adjusted by the voltage V_R on the gate R, while the tunnel splitting $\hbar\Delta$ was adjusted by the voltage V_M on the gate M. The coherence time was extracted as a function of the detuning (from the charge degeneracy point) voltage, the maximal value being ~7 ns. The result is ascribed to $1/f$ noise, whose influence is analyzed along the Gaussian assumption.

In spite of the successful manipulation of a single-charge qubit, the qubit is actually influenced by uncontrolled decoherence, which is present even in the Coulomb blockade regime. Several possible decoherence mechanisms were discussed.

First, background charge $(1/f)$ noise in the sample and electrical noise in the gate voltages cause fluctuation of the qubit parameters ϵ and Δ, which gives rise to decoherence of the system (Paladino *et al.*, 2002; Hayashi *et al.*, 2003; Itakura and Tokura, 2003). The amplitude of low-frequency fluctuation in $\hbar\epsilon$ is estimated to be about 1.6 μeV, which is obtained from low-frequency noise in the single-electron current, or 3 μeV, which is estimated from the minimum linewidth of an elastic current peak at the weak coupling limit (Fujisawa *et al.*, 1998). Low-frequency fluctuations in $\hbar\Delta$ are relatively small and estimated to be about 0.1 μeV for $\hbar\Delta = 10$ μeV, assuming local potential fluctuations in the device (Jung *et al.*, 2004). Actually, the ϵ fluctuation explains the decoherence rate observed at the off-resonant condition ($\epsilon \gtrsim \Delta$). $1/f$ is usually attributed to a set of bistable fluctuators, each of which produced a Lorentzian spectrum. However, the microscopic origin of the charge fluctuators is not fully understood, and their magnitude differs from sample to sample, even when samples are fabricated in the same batch. It was shown (Jung *et al.*, 2004) that fluctuations in ϵ can be reduced by decreasing the temperature as suggested by a simple phenomenological model where the activation energy of the traps is uniformly distributed in the energy range of interest. Cooling samples very slowly with positive gate voltage is sometimes effective in reducing charge fluctuation at low temperature (Pioro-Ladrière *et al.*, 2005). They suggested that the noise originates from a leakage current of electrons that tunnel through the Schottky barrier under the gate into the conduction band and become trapped near the active region of the device. According to Buizert *et al.* (2008), an insulated electrostatic gate can strongly suppress ubiquitous background charge noise in Schottky-gated GaAs/AlGaAs devices. This effect is explained by reduced leakage of electrons from the Schottky gates into the semiconductor through the Schottky barrier. A similar result was recently reported in Schottky gate-defined QPCs and DQDs in Si/SiGe heterostructures with a global top gate voltage (Takeda *et al.*, 2013). By negatively biasing the top gate, $1/f^2$ switching noise is suppressed in a homogeneous $1/f$ charge noise background. It is suggested that this technique may be useful to eliminate dephasing of qubits due to charge noise via the exchange interaction (Culcer, Hu, and Das Sarma, 2009).

In contrast, the decoherence at the resonant condition ($\epsilon = 0$) is dominated by other mechanisms. Although the first-order tunneling processes are forbidden in the Coulomb blockade regime, higher-order tunneling, namely, cotunneling, processes can take place and decohere the system (Eto, 2001). Actually, the cotunneling rate estimated from the tunneling rates is close to the observed decoherence rate and may thus be a dominant mechanism in the present experiment (Eto, 2001). However, since one can reduce the cotunneling effect by making the tunneling barrier less transparent, it is possible to eventually eliminate it.

The electron-phonon interaction is an intrinsic decoherence mechanism in semiconductor QDs. Spontaneous emission of an acoustic phonon persists even at zero temperature and causes an inelastic transition between the two states (Fujisawa *et al.*, 1998). The phonon emission rate at the resonant condition $\epsilon = 0$ cannot be directly estimated from the experimental data on the FID-type protocols, but it may be comparable to the observed decoherence rate. Strong electron-phonon coupling is related to the fact that the corresponding phonon wavelength is comparable to the size of the QD (Fujisawa *et al.*, 1998; Brandes and Kramer, 1999). In this sense, electron-phonon coupling may be reduced by optimizing the size of QD structures. In addition, polar semiconductors, such as GaAs, exhibit a piezoelectric type of electron-phonon coupling, which is significant for low-energy excitations (< 0.1 meV for GaAs). Nonpolar semiconductors, such as Si or carbon-based molecules, may be preferable for reducing the phonon contribution to the decoherence.

III. DECOHERENCE DUE TO $1/f$ NOISE

During the last decade we witnessed extraordinary progress in quantum devices engineering reaching a high level of isolation from the local electromagnetic environment. Under these conditions, the material-inherent sources of noise play a crucial role. While the microscopic noise sources may have different physical origin, as elucidated in Sec. II, their noise spectral densities show similar $1/f$-type behavior at low frequencies. Material-inherent fluctuations with $1/f$ spectrum represent the main limiting factor to quantum coherent behavior of the present generation of nanodevices. This fact has stimulated great effort in understanding and predicting decoherence due to $1/f$ noise and to the closely related RT noise.

There are two characteristic features that make any prediction of decoherence due to $1/f$ noise quite complicated. First, stochastic processes with $1/f$ spectrum are long-time correlated. The spectral density of the noise increases with

decreasing frequency down to the lowest experimentally accessible frequencies. The measurement frequency band is limited either by frequency filters or simply by the finite duration of each realization of the random process, set by the measurement time t_m. In particular, during t_m some of the excitations responsible for the noise may not reach the equilibrium. For this reason $1/f$ noise is considered a nonequilibrium phenomenon for which fluctuation-dissipation relations may not hold (Galperin, Altshuler, and Shantsev, 2004).[3]

The existence of relaxation times longer than any finite measurement time t_m also poses the question of stationarity of $1/f$-type noise, a problem that has attracted much attention (Kogan, 1996). For a stationary process repeated measurements yield the same power spectrum $S_x(\omega)$, within experimental accuracy. In some systems variations of the spectrum or its "wandering" have been reported (Weissman, 1993; Kogan, 1996). However, this effect could be attributed to the finite measuring time, or to nonequilibrium initial conditions for different measurements due to the fact that some degrees of freedom do not completely relax between successive measurements. The long relaxation times may correspond to rare transitions of the system, overcoming high energy barriers, from one "valley" in phase space to another one in which the spectrum of relaxation times $\tau < t_m$ is different. Several experiments tried to reveal a possible nonstationarity of $1/f$ noise [see Kogan (1996) and references therein], but no clear manifestation of nonstationarity has been found.

Second, in general $1/f$ noise cannot be assumed to be a Gaussian random process. Even if the probability density function of many $1/f$ processes resembles a Gaussian form (which is necessary, but not sufficient to guarantee Gaussianity), clear evidence demonstrating deviations from a Gaussian random behavior has been reported; for a review, see Weissman (1988), Sec. III.A, and Kogan (1996), Sec. 8.2.2. The explanation of the variety of observed behaviors stems from the fact that the mechanisms of $1/f$ noise may be different in various physical systems, implying that their statistical properties may strongly differ.

As a consequence, the two standard approximations allowing simple predictions for the evolution of open quantum systems, namely, the Markovian approximation and the modelization of the environment as a bath of harmonic oscillators, cannot be straightforwardly applied when the power spectrum of the noise is of $1/f$ type.[4] In the context of quantum computation, the implication of long-time correlations of the stochastic processes is that the effects of $1/f$ noise on the system evolution depend on the specific quantum operation performed and/or on the measurement protocol. Some protocols show signatures of the non-Gaussian nature of the process, whereas for others a Gaussian approximation captures the main effects at least on a short time scale (Makhlin and Shnirman, 2004; Rabenstein, Sverdlov, and Averin, 2004; Falci *et al.*, 2005).

In this section we illustrate various approaches developed in recent years to address the problem of decoherence due to noise sources having $1/f$ spectrum, considering both microscopic quantum models and semiclassical theories. We start addressing the decohence problem in single-qubit gates driven by dc pluses or by ac fields, and then we consider more complex architecture needed to implement the set of universal gates. To cast these problems in a general framework, we introduce here the Hamiltonian of a nanodevice plus environment on a phenomenological basis. In some cases this general structure is derived from a microscopic description of the device, including the most relevant environmental degrees of freedom. A convenient general form for the Hamiltonian is

$$\hat{H}_{\rm tot} = \hat{H}_0 + \hat{H}_c(t) + \hat{H}_n(t) + \hat{H}_R + \hat{H}_I, \tag{37}$$

where $\hat{H}_0 + \hat{H}_c(t)$ describes the driven closed system, the classical noise affecting the system is included in $\hat{H}_n(t)$, and $\hat{H}_R + \hat{H}_I$ represents the quantum environment and its interaction with the system. The structure of this general Hamiltonian can be justified as follows. The macroscopic Hamiltonian of the device $\hat{H}_0[\mathbf{q}]$ is an operator acting onto a N-dimensional Hilbert space $\mathbb{H}$. It depends on a set of parameters $\mathbf{q}$, which fix the bias (operating) point and account for tunability of the device. The eigenstates of $\hat{H}_0[\mathbf{q}]$, $\{|\phi_i(\mathbf{q})\rangle : i = 1, \ldots, N\}$, form the "local basis" of the "laboratory frame," where $\hat{H}_0 = \sum_{i=1}^{N} E_i(\mathbf{q})|\phi_i(\mathbf{q})\rangle\langle\phi_i(\mathbf{q})|$. External control is described by a time-dependent term. In a one-port design, the driving field $A(t)$ couples to a single time-independent system operator $\hat{Q}$,

[3]The typical examples are $1/f$ voltage fluctuations in uniform conductors resulting from resistance fluctuations which are detected by a current and are proportional to the current squared. To observe them one has to bring the device out of equilibrium where the fluctuation-dissipation theorem is not necessarily valid. This may not be the case in some magnetic systems. For instance, experiments in spin glasses evidenced magnetic noise with $1/f$ spectrum satisfying, within experimental accuracies, fluctuation-dissipation relations. Despite being nonergodic, in these systems magnetic noise is with satisfactory accuracy a thermal and equilibrium one. The mechanism of magnetic fluctuations is, however, not yet clear. The problem of kinetics of spin glasses, determined by both many-body competing interactions and disorder, is extremely complicated and beyond the scope of this review. In connection with $1/f$ noise it has been addressed by Kogan (1996).

[4]Note that the *Markovian approximation* for the reduced dynamics of a quantum system is applicable provided that the noise correlation time τ_c and the system-bath coupling strength v satisfy the condition $v\tau_c \ll 1$ (Cohen-Tannoudji, Dupont-Roc, and Grynberg, 1992). Physically, the quantum system very weakly perturbs the environment; thereby memory of its previous states is quickly lost. If $1/f$ noise is produced by superposition of RT processes, each of which is a discrete Markov process, some of them should have very long correlation times. "Sufficiently slow" fluctuators would violate the above inequality (see the discussion in Sec. III.A.1). Therefore, the Markovian approximation may not be applicable to the reduced system evolution. For $1/f$ noise, a signature of the failure of the Markovian approximation is the divergence of the adiabatic decoherence rate $1/T_2^*$, Eq. (16). For more general situations see, e.g., Laikhtman (1985).

$$\hat{H}_c(t) = A(t)\hat{Q}, \tag{38}$$

which is Hermitian and traceless. In general, control is operated via the same ports used for biasing the system and accounted for by time-dependent parameters $\mathbf{q}$. It is convenient to split $\mathbf{q}$ in a slow part $\mathbf{q}(t)$, which includes static bias, and the fast control parameter $\mathbf{q}_c(t)$ as $\mathbf{q} \to \mathbf{q}(t) + \mathbf{q}_c(t)$. Accordingly, we write

$$\hat{H}_0[\mathbf{q}(t) + \mathbf{q}_c(t)] := \hat{H}_0[\mathbf{q}(t)] + \hat{H}_c(t), \tag{39}$$

where $\hat{H}_c(t)$ describes (fast) control; in relevant situations it can be linearized in $\mathbf{q}_c(t)$, yielding the structure of Eq. (38).[5] At this stage the interaction with the complicated environment of microscopic degrees of freedom in the solid state can be introduced in a phenomenological way. We first consider classical noise usually acting through the same ports used for control and that can be modeled by adding a stochastic component $\delta\mathbf{q}(t)$ to the drive. Again, we split slow and fast noise $\delta\mathbf{q}(t) \to \delta\mathbf{q}(t) + \mathbf{q}_f(t)$ and include the slow part in $\hat{H}_0[\mathbf{q}] \to \hat{H}_0[\mathbf{q}(t) + \delta\mathbf{q}(t)]$. The same steps leading to Eq. (39) yield the noisy Hamiltonian

$$\hat{H}_{\rm tot} = \hat{H}_0[\mathbf{q}(t) + \delta\mathbf{q}(t)] + \hat{H}_c(t) + H_f(t), \tag{40}$$

where $H_f(t)$ describes a short-time correlated stochastic process. "Quantization" of this term $H_f(t) \to \hat{E}\,\hat{Q} + \hat{H}_R = \hat{H}_I + \hat{H}_R$ yields the phenomenological system-environment Hamiltonian in the form of Eq. (37), where $\hat{H}_0[\mathbf{q}(t)] + H_n(t) \equiv \hat{H}_0[\mathbf{q}(t) + \delta\mathbf{q}(t)]$, $\hat{E}$ operates on the environment, and $\hat{H}_R$ is its Hamiltonian (plus possibly suitable counterterms).

When the nanodevice operates as a qubit, $\hat{H}_0[\mathbf{q}]$ can be projected onto the eigenstates and it can be cast in the form Eq. (1), where both the level splitting Ω and the polar angle θ shown in Fig. 2 depend on the set of parameters $\mathbf{q}$. For simplicity, we suppose that a single parameter is used to fix the bias point q. We can write Eq. (40) as

$$\hat{H}_{\rm tot} = \frac{\hbar}{2}\vec{\Omega}[q + \delta q(t)] \cdot \vec{\sigma} + \hat{H}_c(t) + \hat{H}_I + \hat{H}_R. \tag{41}$$

Expanding $\vec{\Omega}[q + \delta q(t)]$ about the fixed bias q, we obtain

$$\hat{H}_{\rm tot} = \frac{\hbar}{2}\vec{\Omega}(q) \cdot \vec{\sigma} + \delta q(t)\frac{\partial\hbar\vec{\Omega}}{\partial q} \cdot \vec{\sigma} + \hat{H}_c(t) + \hat{H}_I + \hat{H}_R, \tag{42}$$

and if bias q controls only one qubit component, for instance, $\Omega_z(q)$, then Eq. (42) reduces to the commonly used form

$$\hat{H}_{\rm tot} = \frac{\hbar\Omega_x}{2}\sigma_x + \frac{\hbar}{2}[\Omega_z(q) + E(t) + \hat{E}]\sigma_z + \hat{H}_c(t) + \hat{H}_R. \tag{43}$$

Here the qubit working point is parametrized by the angle θ_q which is tunable via the bias q, $\tan\theta_q = \Omega_x/\Omega_z(q)$, the classical noise term is $E(t) = 2\delta q(t)\partial\Omega_z/\partial q$, and we have consistently set $\hat{Q} = \sigma_z$ in $\hat{H}_I$.

From a physical point of view, the phenomenological Hamiltonian (43) treats on different footings fast environmental modes exchanging energy with the system and slow modes responsible for dephasing. The fast modes, responsible for spontaneous decay, must be treated quantum mechanically and included in $\hbar\hat{E}\sigma_z/2 + \hat{H}_R$. Slow modes can be accounted for classically and included in $H_n(t) \equiv \hbar E(t)\sigma_z/2$. This term yields the longitudinal fluctuating part $\mathbf{b}(t)$ of a magnetic field formed by an external part $\mathbf{B}_0$ plus an "internal" classical stochastic component, as introduced in Eq. (3). Results of measurements involve both quantum and classical ensemble averaging. From the technical point of view, effects of quantum noise described by $\hat{H}_I + \hat{H}_R$ can be studied by weak coupling master equations (Bloch, 1957; Redfield, 1957; Cohen-Tannoudji, Dupont-Roc, and Grynberg, 1992; Weiss, 2008), which lead to exponential decay of both the diagonal (populations) and off-diagonal (coherences) elements of qubit density matrix elements in the $\hat{H}_q$ eigenbasis. The corresponding time scales T_1 and T_2 are given by Eqs. (15) and (16), respectively.

The weak coupling master equation approach fails in dealing with slow noise as $H_n(t)$, which describes low-frequency (e.g., $1/f$) noise. An important feature of superconducting nanodevices is that the Hamiltonian $\hat{H}_0[q]$ can be tuned in a way such that symmetries (usually parity) are enforced. At such symmetry points $\partial E_i/\partial q = 0$ and selection rules hold for the matrix elements Q_{ij} in the local basis. In these symmetry points the device is well protected against low-frequency noise, and the system is said to operate at optimal points (Vion *et al.*, 2002; Chiorescu *et al.*, 2004). In general, noise affecting solid-state devices, as described by $H_n(t)$ and $\hat{H}_I + \hat{H}_R$ in Eq. (40), has a broadband colored spectrum. Therefore, approaches suitable to deal with noise acting on very different time scales are required. This topic will be discussed in Sec. III.B.1.b.

To start with, we analyze the effect of $1/f$ noise on the qubit's evolution under pure dephasing conditions. As discussed in Sec. I.B, in some situations the Gaussian approximation does not apply. In these cases knowledge of only the noise power spectrum $S(\omega)$ is not sufficient since noise sources with identical power spectra can have different decohering effects on the qubit. Therefore, it is necessary to specify the model for the noise source in more detail. In Sec. III.A we illustrate dephasing by the *spin-fluctuator* (SF) model, which can be solved exactly under general conditions. When we depart from pure dephasing, i.e., when the noise-system interaction is not longitudinal, no exact analytic solution for the time evolution of the system is available even for the spin-fluctuator model. Different exact methods have been proposed which lead to approximate solutions in relevant regimes.

[5]Note that while $\hat{Q}$ is an observable and does not depend on the local basis, its matrix representation does. The physical consequence is that the effectiveness of the fast control $\mathbf{q}_c(t)$ in triggering transitions depends also on the slow $\mathbf{q}(t)$, a feature of artificial atoms which is the counterpart of tunability.

In Sec. III.B we present approximate approaches proposed to predict dephasing due to $1/f$ noise described as a classical stochastic process. Approaches based on the adiabatic approximation (Falci *et al.*, 2005; Ithier *et al.*, 2005) allow simple explanations of peculiar nonexponential decay reported in different experiments with various setups (Cottet *et al.*, 2001; Vion *et al.*, 2002; Martinis *et al.*, 2003; Van Harlingen *et al.*, 2004; Ithier *et al.*, 2005; Bylander *et al.*, 2011; Chiarello *et al.*, 2012; Sank *et al.*, 2012; Yan *et al.*, 2012). These approaches also predict the existence of operating conditions where leading order effects of $1/f$ fluctuations are eliminated also for complex architectures, analogously to the single qubit optimal point. The effect of $1/f$ noise in solid-state complex architectures is a subject of current investigation (Storcz *et al.*, 2005; Hu *et al.*, 2007; D'Arrigo *et al.*, 2008; Paladino *et al.*, 2009, 2010, 2011; Bellomo *et al.*, 2010; Brox, Bergli, and Galperin, 2012; D'Arrigo and Paladino, 2012). Considerable improvement in minimizing sensitivity to charge noise has been reached via clever engineering, in particular, in the cQED architecture; see Sec. II.C.1. Recently, highly sensitive superconducting circuits have been used as "microscopes" for probing characteristic properties of environmental fluctuators. Recent progress in the ability of direct control of these microscopic quantum TLSs has opened a new research scenario where they may be used as naturally formed qubits. These issues will be addressed in Sec. III.C.

In the final part of this section we present current strategies to reduce effects of $1/f$ noise based on techniques developed in NMR (Schlichter, 1992). The open question about the best strategy to limit $1/f$ noise effects via open or closed loop control is discussed and we review the current status of the ongoing research along this direction.

A. Spin-fluctuator model

In the following we use a simple classical model according to which the quantum system, qubit, is coupled to a set of two-state fluctuators. The latter randomly switch between their states due to interaction with a thermal bath, which can be only weakly directly coupled to the qubit. Since we are interested only in the low-frequency noise generated by these switches, they will be considered as classical. (The situations where quantum effects are of importance is discussed separately.) The advantage of this approach, which is often referred to as the spin-fluctuator model, is that the system qubit plus fluctuators can be described by a relatively simple set of stochastic differential equations, which in many cases can be exactly solved. In particular, many results can be borrowed from earlier work on magnetic resonance (Klauder and Anderson, 1962; Hu and Walker, 1977; Maynard, Rammal, and Suchail, 1980), on spectral diffusion in glasses (Black and Halperin, 1977), as well as works on single-molecule spectroscopy (Moerner, 1994; Geva, Reilly, and Skinner, 1996; Moerner and Orrit, 1999; Barkai, Jung, and Silbey, 2001).

The interaction of electrons with two-state fluctuators was previously used for evaluation of the effects of noise on various systems (Kogan and Nagaev, 1984b; Kozub, 1984; Ludviksson, Kree, and Schmid, 1984; Galperin, Gurevich, and Kozub, 1989; Galperin and Gurevich, 1991; Galperin, Zou, and Chao, 1994; Hessling and Galperin, 1995). It was recently applied to the analysis of decoherence in qubits (Paladino *et al.*, 2002; Falci, Paladino, and Fazio, 2003; Paladino, Faoro, and Falci, 2003; Falci *et al.*, 2004, 2005; Galperin, Altshuler, and Shantsev, 2004; Bergli, Galperin, and Altshuler, 2006, 2009; Galperin *et al.*, 2006; Martin and Galperin, 2006). Various quantum and non-Markovian aspects of the model were addressed by Paladino *et al.* (2002), Galperin, Altshuler, and Shantsev (2003), de Sousa *et al.* (2005), DiVincenzo and Loss (2005), Grishin, Yurkevich, and Lerner (2005), Abel and Marquardt (2008), Coish, Fischer, and Loss (2008), Lutchyn *et al.* (2008), Burkard (2009), Culcer, Hu, and Das Sarma (2009), and Yurkevich *et al.* (2010).

1. Exact results at pure dephasing

In Sec. I.B we discussed a simple model of so-called pure dephasing, when the diagonal splitting ϵ of a qubit represented by the Hamiltonian (1) fluctuates in time and $\Delta = 0$. The resulting expression (11) for the FID was obtained assuming that the fluctuations obey the Gaussian statistics. To approach specific features of the $1/f$ noise we take into account that such a noise can be considered as a superposition of random telegraph processes. To begin with we consider decoherence due to a single random telegraph process.

a. Dephasing due to a single RT fluctuator

A random telegraph process is defined as follows (Buckingham, 1989; Kirton and Uren, 1989). Consider a classical stochastic variable $\chi(t)$, which at any time takes the values $\chi(t) = \pm 1$. It is thus suitable for describing a two-state fluctuator that can find itself in one of two (meta)stable states, 1 and 2, and once in a while it makes a switch between them. The switchings are assumed to be uncorrelated random events with rates $\gamma_{1\to 2}$ and $\gamma_{2\to 1}$, which can be different. For simplicity, we limit ourselves to a symmetric RT process $\gamma_{1\to 2} = \gamma_{2\to 1} = \gamma/2$. The extension to the general case can be easily made (Itakura and Tokura, 2003). The number k of switches that the fluctuator experiences within a time t follows a Poisson distribution

$$P_k(t) = \frac{(\gamma t)^k}{2^k k!} e^{-\gamma t/2}. \tag{44}$$

The number of switches k determines the number of times the function $\chi(t)$ changes its sign contributing $(-1)^k$ to the correlation function $C(t) \equiv \langle \chi(t)\chi(0)\rangle$. Therefore,

$$C(t) = e^{-\gamma t/2} \sum_{k=0}^{\infty} (-1)^k \frac{(\gamma t)^k}{2^k k!} = e^{-\gamma t}, \quad t \geq 0. \tag{45}$$

The RT process results in a fluctuating field $\mathbf{b}(t) = \mathbf{b}\chi(t)$ applied to the qubit. The magnitude $b = |\mathbf{b}|$ together with the switching rate γ characterizes the fluctuator. Using Eq. (10) it is possible to find the power spectrum of the noise generated by the ith fluctuator:

$$S_i(\omega) = b_i^2 \mathcal{L}_{\gamma_i}(\omega), \tag{46}$$

with $\mathcal{L}_{\gamma_i}(\omega)$ given by Eq. (17). Equation (46) corresponds to the high-temperature limit $E \ll k_B T$ of Eq. (28) with $x_1 - x_2 = 2b_i$. Thus, together with the considerations reported in Sec. II.B, we conclude that telegraph fluctuators provide a reasonable model for the $1/f$ noise.

Single shot measurements and FID: Using Eq. (5) we now discuss how a single RT fluctuator affects a qubit. We assume that the fluctuator does not feel any feedback from the qubit and thus the RT function $\chi(t)$ equals to $+1$ or -1 with the probability $1/2$ regardless of the direction of the Bloch vector $\mathbf{M}$. One can show that under this assumption the probability to find the angle φ (see Fig. 2) at time t, $p(\varphi, t)$, satisfies the following second-order differential equation (Bergli, Galperin, and Altshuler, 2009):

$$\ddot{p} + \gamma \dot{p} = b^2 \partial_\varphi^2 p, \tag{47}$$

which is known as the telegraph equation. We can always choose the x direction such that $\varphi = 0$ at $t = 0$, so $p(\varphi, 0) = \delta(\varphi)$. The second initial condition,

$$\dot{p}(\varphi, 0) = \pm 2b \partial_\varphi p(\varphi, 0),$$

can be derived from the integral equation for $p(\varphi, t)$ (Bergli, Galperin, and Altshuler, 2009). After averaging over the fluctuator's initial state, $\dot{p}(\varphi, 0) = 0$.

The FID is given as $\langle m_+ \rangle = \langle e^{i\varphi} \rangle = \int d\varphi p(\varphi, t) e^{i\varphi}$. The differential equation and initial conditions for this quantity can be obtained multiplying Eq. (47) by $e^{i\varphi}$ and integrating over φ. In this way we obtain

$$\langle \ddot{m}_+ \rangle + \gamma \langle \dot{m}_+ \rangle = -b^2 \langle m_+ \rangle \tag{48}$$

with initial conditions $\langle m_+(0) \rangle = 1$, $\langle \dot{m}_+(0) \rangle = 0$. The solution of Eq. (48) with these initial conditions is

$$\langle m_+ \rangle = (2\mu)^{-1} e^{-\gamma t/2} [(\mu + 1) e^{\gamma \mu t/2} + (\mu - 1) e^{-\gamma \mu t/2}], \quad \mu \equiv \sqrt{1 - (2b/\gamma)^2}. \tag{49}$$

In the context of decoherence due to discrete noise sources affecting superconducting qubits Eq. (49) was first reported by Paladino *et al.* (2002), where it was derived as the high-temperature limiting form of a real-time path-integral result. Equation (49) also follows by direct averaging the qubit coherence over the stochastic bistable process $\mathbf{b}(t) = \mathbf{b}\chi(t)$, i.e., by evaluation of the time average $\mathcal{Z}(t) = \langle\langle \exp[-i \int_0^t dt' b(t')] \rangle\rangle$. The last two approaches do not necessarily assume a thermal equilibrium initial condition for the fluctuator at the initial time $t = 0$. Thus, results also depend on the initial population difference between the two states $\chi = \pm 1$, δp_0. When this quantity is fixed to one of the classical values $+1$ or -1, we obtain the effect of noise only during the qubit quantum evolution, i.e., in an "ideal" single shot measurement. The result takes the form given by Eq. (49) with the prefactors of the two exponentials $\mu \pm 1$ replaced by $\mu \pm 1 \mp i \delta p_0 2b/\gamma$. The FID results by further averaging over the initial conditions, i.e., by replacing δp_0 with $\langle \delta p_0 \rangle = \delta p_{\mathrm{eq}}$, where the thermal equilibrium value δp_{eq} is consistently set to zero in the regime $E \ll k_B T$. Both the single shot and the free induction signals demonstrate qualitatively different behaviors for large and small values of the ratio $2b/\gamma$. This is easily seen from Eq. (49). At $b \gg \gamma$ one can consider the qubit as a quantum system experiencing beatings between the states with different splittings $B_0 \pm b$, the width of these states being $\gamma/2$. In the opposite limiting case $b \ll \gamma$, the energy-level splitting is self-averaged to a certain value, the width being b^2/γ. This situation was extensively discussed in connection with the magnetic resonance and is known as the motional narrowing of spectral lines (Klauder and Anderson, 1962). Different behaviors of the FID amplitudes depending on the ratio $2b/\gamma$ are illustrated in Fig. 22.

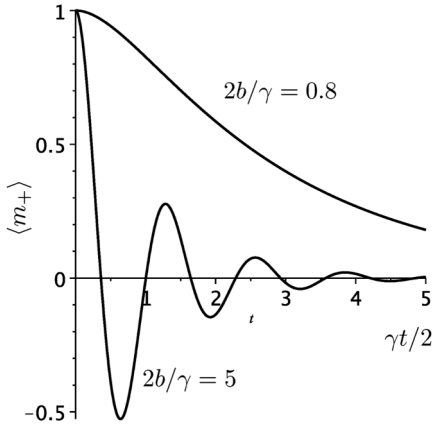

FIG. 22. Time dependence if the FID amplitude for $2b/\gamma = 0.8$ and 5.

Thus, one can discriminate between *weakly coupled* fluctuators $2b/\gamma \ll 1$ and *strongly coupled* fluctuators (in the other regimes) (Paladino *et al.*, 2002), which influence the qubit in different ways. Figure 23 shows the decay factor $\Gamma(t) = -\ln[|\langle m_+ \rangle(t)|]$ for different values of $2b/\gamma$ normalized in such a way that the Gaussian decay factor $\Gamma^G(t) \equiv \langle \varphi^2 \rangle/2$

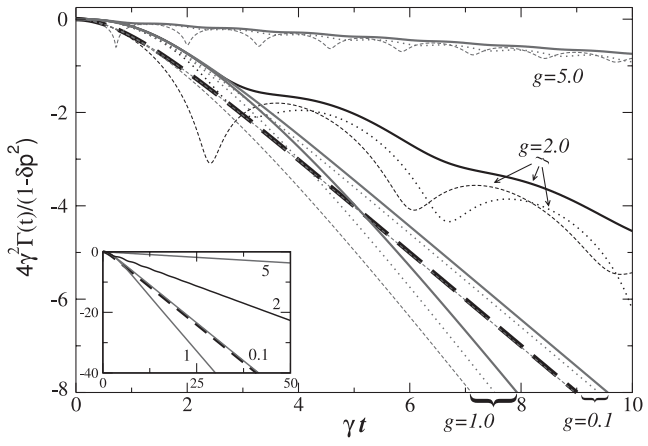

FIG. 23. Reduced $\Gamma(t)$ due to fluctuators prepared in a stable state ($\delta p_0 = 1$, solid lines and $\delta p_0 = -1$, dotted lines) and in a thermal mixture ($\delta p_0 = 0$, dashed lines) for the indicated values of $g = 2b/\gamma$. Inset: Longer time behavior for stable state preparation. The curves are normalized in such a way that the oscillator approximation for all of them coincides (thick dashed line). Adapted from Paladino, Faoro, and Falci, 2003.

[see Eqs. (8) and (11)] is the same for all curves. Both the single-shot and FID signals are reported. Substantial deviations are clearly observed, except in the presence of a weakly coupled fluctuator. In particular, a fluctuator with $2b/\gamma > 1$ induces a slower dephasing compared to an oscillator environment with the same $S_b(\omega)$, a sort of saturation effect. Recurrences at times comparable with $1/2b$ are visible in $\Gamma(t)$. In addition, strongly coupled fluctuators show memory effects. This is clearly seen considering different initial states for the fluctuator, corresponding to the single shot and FID measurement schemes. This is already seen in the short-time behavior $\gamma t \ll 1$, relevant for quantum operations which need to be performed before the signal decays to a very low value. In the limit $\gamma t \ll 1$, $\Gamma^G(t) \approx b^2(1-\delta p_{\rm eq}^2)t^2/2$, whereas

$$\Gamma(t) \approx b^2\left[\frac{1-\delta p_0^2}{2}t^2 + \frac{1+2\delta p_0 \delta p_{\rm eq} - 3\delta p_0^2}{6}\gamma t^3\right]. \quad (50)$$

In a single shot process, $\delta p_0 = \pm 1$, and $\Gamma(t) \propto t^3$, showing that a fluctuator is stiffer than a bath of oscillators. On the other hand, for repeated measurements $\delta p_0 = \delta p_{\rm eq}$ and for very short times we recover the Gaussian result. This is due to the fact that inhomogeneous broadening due to the uncontrolled preparation of the fluctuator at each repetition adds to the effect of decoherence during the time evolution and results in a faster decay of $\Gamma(t)$.

The difference between Eq. (49) and the result (12) based on the Gaussian assumption is further elucidated considering the long-time behavior. Substituting Eq. (46) for the noise spectrum into Eq. (12) one obtains

$$1/T_2^{*(G)} = b^2/\gamma. \quad (51)$$

This result should be valid for times much longer than the correlation time of the noise, which is γ^{-1}. Expanding Eq. (49) at long times we find that FID also decays exponentially (or the beatings decay exponentially at $b > \gamma$). However, the rate of decay is parametrically different from Eq. (51):

$$\frac{1}{T_2^*} = \frac{\gamma}{2}\left(1 - {\rm Re}\sqrt{1-\frac{4b^2}{\gamma^2}}\right). \quad (52)$$

At $b \ll \gamma$, Eq. (52) coincides with the Gaussian result. Shown in Fig. 24 are the dephasing rates $1/T_2^{(G)}$ and $1/T_2$ given by Eqs. (51) and (52), respectively. Again we see that the Gaussian approximation is valid only in the limit $b \ll \gamma$. The main effect of a strongly coupled fluctuator is a static energy shift, the contribution to the qubit decoherence rate saturates at $\sim\gamma$, and at $b \gtrsim \gamma/2$ the Gaussian assumption overestimates the decay rate. Apparently, this conclusion is in contradiction with the discussion in Sec. I.B following from the central limiting theorem. According to this theorem $p(\varphi, t)$ always tends to a Gaussian distribution with time-dependent variance provided that the time exceeds the correlation time of the noise. To resolve this apparent contradiction, we analyze the shape of the distribution function $p(\varphi, t)$, following from the telegraph equation (47) with initial conditions $p(\varphi, 0) = \delta(\varphi)$, $\dot{p}(\varphi, 0) = 0$. This solution is (Bergli, Galperin, and Altshuler, 2006)

$$\begin{aligned} p(\varphi,t) = {} & (1/2)e^{-\gamma t/2}[\delta(\varphi+bt)+\delta(\varphi-bt)] \\ & + [\gamma/b\nu(t)]e^{-\gamma t/2}[\Theta(\varphi+bt)-\Theta(\varphi-bt)] \\ & \times \{I_1[\nu(t)\gamma t/2] + \nu(t) I_0[\nu(t)\gamma t/2]\}. \end{aligned} \quad (53)$$

Here $I_\beta(x)$ is the modified Bessel function, $\nu(t) = \sqrt{1-(\varphi/bt)^2}$, while $\Theta(x) = 1$ at $x > 0$ and 0 at $x < 0$ is the Heaviside step function. This distribution for various t shown in Fig. 25 consists of two delta functions and a central peak. The delta functions represent the finite probability for a fluctuator to remain in the same state during time t. As time increases, the weight of the delta functions decreases and the central peak broadens. At long times, this peak acquires a Gaussian shape. Indeed, at $\gamma t \gg 1$ one can use an asymptotic form of the Bessel function $I_\beta(z) \approx (2\pi z)^{-1/2}e^z$, as $z \to \infty$. In addition, at $t \gg \varphi/b$ we can also expand $\sqrt{1-(\varphi/bt)^2}$ and convince ourselves that the central peak is described by the Gaussian distribution (7) with $\langle\varphi^2\rangle = 2b^2t/\gamma$. If the

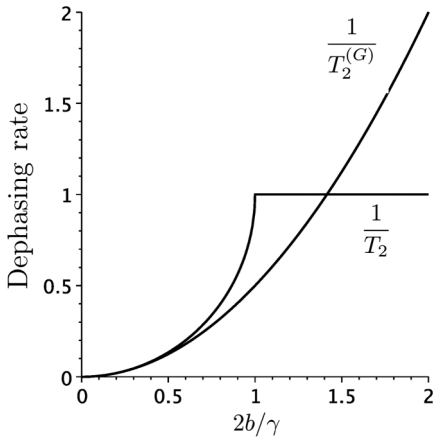

FIG. 24. Comparison of the dephasing rate T_2^{-1} for a single random telegraph process and the corresponding Gaussian approximation. Adapted from Bergli, Galperin, and Altshuler, 2009.

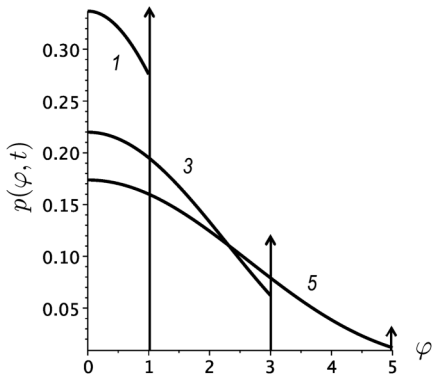

FIG. 25. The distribution (53) for $2b/\gamma = 1$ and $\gamma t/2 = 1$, 3, and 5 (numbers at the curves). Only the part with positive φ is shown; the function is symmetric. The arrows represent the delta functions (not to scale). Adapted from Bergli, Galperin, and Altshuler, 2009.

qubit-fluctuator coupling is weak, $b \ll \gamma$, this Gaussian part of $p(\varphi,t)$ dominates the average $\langle e^{i\varphi}\rangle$ and the Gaussian approximation is valid. On the contrary, when the coupling is strong, $b > \gamma/2$, the average is dominated by delta functions at the ends of the distribution and the decoherence demonstrates a pronounced non-Gaussian behavior, even at long times ($t > 2/\gamma$).

Unfortunately, we are not aware of a way to measure the distribution $p(\varphi,t)$ in experiments with a single qubit. The reason is in the difference between the qubit that can be viewed as a pseudospin 1/2 and a classical Bloch vector $\mathbf{M}$. According to Eq. (4) the components M_x, M_y, M_z of $\mathbf{M}$ are connected with the mean component of the final state of the pseudospin. Therefore, to measure the value of the phase φ (argument of m_+) that corresponds to a given realization of the noise one should repeat the experimental shot with the same realization of the noise many times. This is impossible because each time the realization of noise is different. Therefore, the only observable in decoherence experiments is the average $\langle e^{i\varphi}\rangle$.

b. Echo

The analysis of the echo signal is rather similar: One has to replace $\langle m_+(t)\rangle$ taken from Eq. (49) by $\langle m_+^{(e)}(2\tau_{12})\rangle$ where [cf. with Laikhtman (1985)],

$$\langle m_+^{(e)}(t)\rangle = \frac{e^{-\gamma t/2}}{2\nu^2}[(\nu+1)e^{\gamma\nu t/2} - (\nu-1)e^{-\gamma\nu t/2} - 8b^2/\gamma^2]. \tag{54}$$

This result can also be obtained by direct calculation of the function $Z(2t|\eta) = \langle\langle \exp[-i\int_0^{2t} dt'\eta(t')b(t')]\rangle\rangle$, where $\eta(t') = 1$ for $0 < t' < t$ and $\eta(t') = -1$ for $t < t' < 2t$ (Falci, Paladino, and Fazio, 2003). To demonstrate non-Gaussian behavior of the echo signal we evaluate from Eq. (14) the variance $\langle\psi^2(2\tau_{12})\rangle$. We obtain [cf. with Bergli, Galperin, and Altshuler (2009)]

$$\langle\psi^2\rangle = (2b^2/\gamma^2)(2\gamma\tau_{12} - 3 + 4e^{-\gamma\tau_{12}} - e^{-2\gamma\tau_{12}}) \tag{55}$$

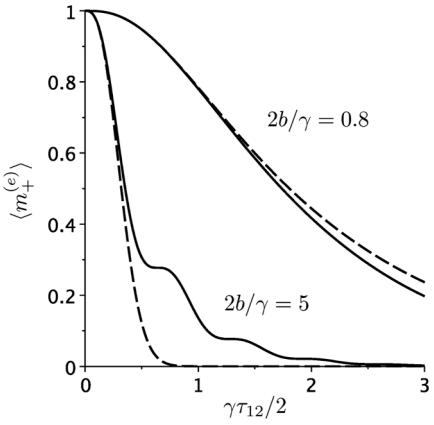

FIG. 26. Solid lines: The echo signal for different values of the ratio $2b/\gamma$, Eq. (54). Dashed lines: The calculations along the Gaussian approximation, Eq. (55). Adapted from Bergli, Galperin, and Altshuler, 2009.

with $\langle m_+^{(e)}\rangle = e^{-\langle\psi^2\rangle/2}$ as before. Comparison between the two results is shown in Fig. 26 for a weakly ($2b/\gamma = 0.8$) and a strongly ($2b/\gamma = 5$) coupled fluctuator. As discussed, the Gaussian approximation is accurate at $2b \lesssim \gamma$, while at $2b > \gamma$ the results are qualitatively different. In particular, the plateaus in the time dependence of the echo signal shown in Fig. 26 are beyond the Gaussian approximation. We believe that such a plateau was experimentally observed by Nakamura *et al.* (2002) (see Fig. 3 from that paper partly reproduced in Fig. 7). In the limit $b \gg \gamma$, $\sqrt{\gamma/\tau}$ Eq. (54) acquires a simple form:

$$\langle m_+^{(e)}(\tau)\rangle = e^{-\gamma\tau}[1 + (\gamma/2b)\sin 2b\tau]. \tag{56}$$

According to Eq. (56), the plateaulike features ($|\partial\langle m_+^{(e)}\rangle/\partial\tau| \ll 1$) occur at $b\tau \approx k\pi$ (where k is an integer) and their heights $\langle m_+^{(e)}\rangle \approx e^{-\pi k\gamma/b}$ exponentially decay with the number k. Experimentally measuring the height and the position of the first plateau, one can determine both the fluctuator coupling strength b and its switching rate γ. For example, the echo signal measured by Nakamura *et al.* (2002) shows a plateaulike feature at $\tau_{12} = 3.5$ ns at the height $\langle m_+^{(e)}\rangle = 0.3$, which yields $b \approx 143$ MHz and $\gamma/2 \approx 27$ MHz. If the fluctuator is a charge trap near a gate producing a dipole electric field, its coupling strength is $b = e^2(\mathbf{a}\cdot\mathbf{r})/r^3$. Using the gate-CPB distance $r = 0.5$ μm, we obtain a reasonable estimate for the tunneling distance between the charge trap and the gate $a \sim 20$ Å. A more extensive discussion can be found in Galperin *et al.* (2006). A similar analysis for an arbitrary qubit working point was reported by Zhou and Joynt (2010). The effect of RTN for an arbitrary working point is discussed in Sec. III.A.2.

c. Telegraph noise and Landau-Zener transitions

Driven quantum systems are exceedingly more complicated to study than stationary systems, and only few such problems have been solved exactly. An important exception is the Landau-Zener (LZ) transitions (Landau, 1932; Stueckelberg, 1932; Zener, 1932). In the conventional LZ problem, a TLS is driven by changing an external parameter in such a way that the level separation $\hbar\epsilon$ is a linear function of time $\epsilon(t) \equiv a^2 t$. Close to the crossing point of the two levels, an interlevel tunneling matrix element $\hbar\Delta$ lifts the degeneracy in an avoided level crossing. When the system is initially in the ground state, the probability to find it in the excited state after the transition is $e^{-\pi\Delta^2/2a^2}$. Hence, a fast rate drives the system to the excited state, while the system ends in the ground state when driven slowly.

In connection with decoherence of qubits, there has recently been increased interest in Landau-Zener transitions in systems coupled to an environment. This problem is of both theoretical interest and practical importance for qubit experiments (Sillanpää *et al.*, 2006). The noisy Landau-Zener problem was discussed by several (Kayanuma, 1984, 1985; Shimshoni and Gefen, 1991; Shimshoni and Stern, 1993; Nishino, Saito, and Miyashita, 2001; Pokrovsky and Sinitsyn, 2003; Wubs *et al.*, 2006; Pokrovsky and Sun, 2007; Saito *et al.*, 2007). Here we discuss the role of a classical telegraph fluctuator following Vestgården, Bergli, and Galperin (2008).

We model a driven qubit by the Hamiltonian (3) with $\epsilon(t) = a^2 t$ and $\Delta(t) \equiv \Delta + v\chi(t)$, where $\chi(t)$ is a RT process. Representing the density matrix as in Eq. (4) one can study the dynamics of the Bloch vector averaged over the realizations of the telegraph noise. To this end, one has to study the solution of the Bloch equation (5) in the presence of the magnetic fields $\mathbf{B}_\pm = \mathbf{B}_0 \pm \mathbf{v}(t)$. Introducing the partial probabilities $p_\pm(\mathbf{M}, t)$ to be in the state $\mathbf{M}$ at time t under rotations around $\mathbf{B}_+$ and $\mathbf{B}_-$, respectively, and defining

$$\mathbf{M}_\pm \equiv \int d^3M[p_+(\mathbf{M}, t) \pm p_-(\mathbf{M}, t)],$$

one arrives at the set of equations [cf. with Vestgården, Bergli, and Galperin (2008)]

$$\begin{aligned}\dot{\mathbf{M}}_+ &= \mathbf{M}_+ \times \mathbf{B}_0 + \mathbf{v} \times \mathbf{M}_-,\\ \dot{\mathbf{M}}_- &= \mathbf{M}_- \times \mathbf{B}_0 + \mathbf{v} \times \mathbf{M}_+ - \gamma \mathbf{M}_-.\end{aligned} \tag{57}$$

Here $\mathbf{M}_+$ is the average Bloch vector whose z component is related to the occupancy of the qubit's levels. To demonstrate the role of telegraph noise, we consider a simplified problem putting $\Delta = 0$. In this way we study the LZ transitions induced solely by the telegraph process. In this case, Eqs. (57) reduce to an integro-differential equation for $M_z \equiv M_{+z}$:

$$\dot{M}_z(t) = -v^2 \int_0^\infty dt_1 \cos\left[\frac{a^2 t_1(2t - t_1)}{2}\right] e^{-\gamma|t_1|} M_z(t - t_1). \tag{58}$$

Equation (58) can be easily analyzed for the case of fast noise $\gamma \gg a$. A series expansion in t_1 leads to the following solution of Eq. (58) with initial condition $M_z(0) = 1$:

$$M_z(\infty) = e^{-\pi v^2/a^2}. \tag{59}$$

This is the usual expression for the LZ transition probability with replacement $\Delta \to \sqrt{2}v$. This result holds for any noise correlated at short times ($\ll a^{-1}$), as shown by Pokrovsky and Sinitsyn (2003). Note that the result (59) can be obtained using the Gaussian approximation.

The case of a slow fluctuator with $\gamma \lesssim a$ leads to very different results which, for an arbitrary ratio v/a, require a numerical solution of the integro-differential equation (58).

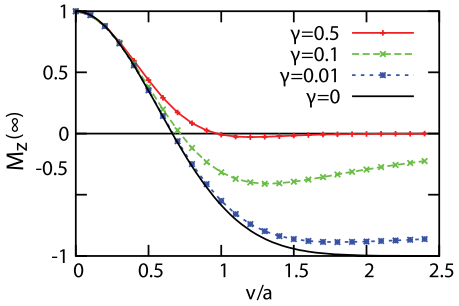

FIG. 27 (color online). $M_z(\infty)$ vs the ratio v/a for different switching rate γ (shown in units of a). Adapted from Vestgården, Bergli, and Galperin, 2008.

The result of such analysis is shown in Fig. 27. The static case $\gamma = 0$ is equivalent to the standard Landau-Zener transition with the noise strength $\sqrt{2}v$ replacing the tunnel coupling Δ between the diabatic levels. In the adiabatic limit $v \gg a$, we see that $M_z(\infty) \to -1$, which corresponds to the transition to the opposite diabatic state. In this case the dynamics is fully coherent, but since we average over the fluctuator's initial states, the Bloch vector asymptotically lies on the z axis of the Bloch sphere. At finite γ, the noise also stimulates Landau-Zener transitions; however, the transition probability decreases with increasing switching rate. Note that the curves cross the line $M_z(\infty) = 0$ at some v/a, which depends on γ. For this noise strength, the final state is at the center of the Bloch sphere, corresponding to full decoherence. However, increasing the noise strength beyond this point results in a final state with negative $M_z(\infty)$. Thus, we have the surprising result that, under some conditions, increasing the noise strength will also increase the system purity after the transition. The results for slow and strong noise cannot be obtained in the Gaussian approximation. These considerations point out that telegraph noises can facilitate LZ transitions. This process may prevent the implementation of protocols for adiabatic quantum computing.

d. Ensemble of fluctuators: Effects of $1/f$ noise

As a result of the above considerations, we concluded that the role of a fluctuator in decoherence of a qubit depends on the ratio between the interaction strength b and the correlation time γ^{-1} of the random telegraph process. *Weakly* coupled fluctuators, i.e., "weak" and relatively "fast" fluctuators for which $2b/\gamma \ll 1$, can be treated as a Gaussian noise acting on the qubit. On the contrary, the influence of *strongly* coupled fluctuators, i.e., "strong" and "slow" fluctuators for which $2b/\gamma \gtrsim 1$, is characterized by quantum beatings in the qubit evolution.

As seen, a set of fluctuators characterized by the distribution function $\mathcal{P}(\gamma) \propto 1/\gamma$ of the relaxation rates provides a realistic model for $1/f$ noise. Therefore, it is natural to study in which way the qubit is decohered by a sum of the contributions of many fluctuators $b(t) = \sum_i b_i \chi_i(t)$. A key question here is "Which fluctuators, weak or strong, are responsible for the qubit decoherence?" In the first case the noise can be treated as Gaussian, while in the second case a more accurate description is needed.

Here we analyze this issue using a simple model assuming that the dynamics of different fluctuators are not correlated, i.e., $\langle \chi_i(t)\chi_j(t')\rangle = \delta_{ij} e^{-\gamma_i|t-t'|}$. Under this assumption, the average $\langle m_+ \rangle$ is the product of the partial averages,

$$\langle m_+(t)\rangle = \prod_i \langle m_{+i}(t)\rangle = \exp\left(\sum_i \ln\langle m_{+i}(t)\rangle\right). \tag{60}$$

Since the logarithm of a product is a self-averaging quantity, it is natural to approximate the sum of logarithms $\sum_i \ln\langle m_{+i}(t)\rangle$ by its average value $-\mathcal{K}_m(t)$, where

$$\mathcal{K}_m(t) \equiv -\overline{\sum_i \ln\langle m_{+i}(t)\rangle}. \tag{61}$$

Here the bar denotes the average over both the coupling constants b of the fluctuators and their transition rates γ. Equation (61) can be further simplified when the total number $\mathcal{N}_T$ of thermally excited fluctuators is very large. Then we can replace $\overline{\sum_i \ln\langle m_{+i}(t)\rangle}$ by $\mathcal{N}_T\overline{\ln\langle m_+(t)\rangle}$. Furthermore, we can use the so-called Holtsmark procedure (Chandresekhar, 1943), i.e., to replace $\overline{\ln\langle m_+(t)\rangle}$ by $\overline{\langle m_+\rangle} - 1$ assuming that in the relevant time domain each $\langle m_{+i}\rangle$ is close to 1. Thus, $\mathcal{K}_m(t)$ is approximately equal to (Klauder and Anderson, 1962; Laikhtman, 1985; Galperin, Altshuler, and Shantsev, 2003, 2004)

$$\mathcal{K}_m(t) \approx \mathcal{N}_T[1 - \overline{\langle m_+(t)\rangle}] = \int dbd\gamma \mathcal{P}(b,\gamma)[1 - \langle m_+(b,\gamma|t)\rangle]. \quad (62)$$

Here $\langle m_{+i}\rangle$ is specified as $\langle m_+(b,\gamma|t)\rangle$, which depends on the parameters b and γ according to Eq. (49). The free induction signal is then $\exp[-\mathcal{K}_m(t)]$. Analysis of the echo signal is rather similar: one has to replace $\langle m_+(t)\rangle$ taken from Eq. (49) with Eq. (54).

To evaluate the time dependence of the free induction or echo signal, one has to specify the distribution function of the coupling constants b, i.e., partial contributions of different fluctuators to the random magnetic field $b(t)$. To start with, we consider the situation where the couplings b_i are distributed with a small dispersion around an average value $\bar{b}$. Under these conditions the total power spectrum reads

$$S(\omega) = \bar{b^2}\int_{\gamma_m}^{\gamma_M} d\gamma \frac{P_0}{2\gamma}\mathcal{L}_\gamma(\omega) \approx \frac{\mathcal{A}}{\omega}, \quad (63)$$

where the amplitude $\mathcal{A}$ can be expressed in terms of the number of fluctuators per noise decade, $n_d = \mathcal{N}_T \ln(10)/\ln(\gamma_M/\gamma_m)$, as follows $\mathcal{A} = \bar{b^2}P_0/4 = \bar{b^2}n_d/2\ln(10)$. The spectrum exhibits a crossover to ω^{-2} behavior at $\omega \sim \gamma_M$. In Fig. 28 we showed the results for a sample with a number of fluctuators per decade $n_d = 1000$ and with couplings distributed around $\bar{b}/(2\pi) = 4.6\times10^7$ Hz. Initial conditions $dp_{0j} = \pm1$ are distributed according to $\langle dp_{0j}\rangle = dp_{\rm eq}$, the equilibrium value. The different role played by weakly and strongly coupled fluctuators is illustrated considering sets with $\gamma_M/(2\pi) = 10^{12}$ Hz and different γ_m. In this case the dephasing is given by fluctuators with $\gamma_j > 2\pi\times10^7$ Hz $\approx 2\bar{b}/10$. The main contribution comes from three decades at frequencies around $\approx 2\bar{b}$. The overall effect of the strongly coupled fluctuators ($\gamma_j < 2\bar{b}/10$) is minimal, despite their large number. We remark that, while saturation of dephasing due to a single fluctuator is physically intuitive, it is not *a priori* clear whether this holds also for the $1/f$ case, where a large number ($\sim 1/\gamma$) of slow (strongly coupled) fluctuators is involved. The decay factor $\mathcal{K}_m(t)$ can be easily compared with the Gaussian approximation (11) (Paladino *et al.*, 2002). This approximation fails to describe fluctuators with $2b/\gamma \gg 1$. For instance, $\langle\varphi^2\rangle$ at a fixed t scales with the number of decades and does not show saturation. On the other hand, the Gaussian approximation becomes correct if the environment has a very large number of extremely weakly coupled fluctuators. This is shown in Fig. 29, where the power spectrum is identical for all curves but it is obtained by sets of fluctuators with different n_d and b_i. The Gaussian behavior is recovered for $t \gg 1/\gamma_m$ if n_d is large (all fluctuators are weakly coupled). If in addition we take $\langle dp_{0j}\rangle = dp_{\rm eq}$, $\mathcal{K}_m(t)$ approaches $\langle\varphi^2\rangle$ also at short times. Hence decoherence depends separately on n_d and $\bar{b}$, whereas in the Gaussian approximation only the combination $n_d\bar{b^2}$, which enters $S(\omega)$, matters. In other words, the characterization of the effect of slow sources of $1/f$ noise requires knowledge of moments of the bias fluctuations higher than $S(\omega)$. A more accurate averaging procedure considering $\langle\delta p_{0j}\rangle = \pm1$ for fluctuators, with $\gamma_i t_m < 1$ and $\langle\delta p_{0j}\rangle = \delta p_{\rm eq}$ for $\gamma_i t_m > 1$, shows that, for long measurement times $\bar{b}t_m \gg 1$, fluctuators with $\gamma < 1/t_m$ are saturated and therefore not effective, whereas other fluctuators, being averaged, give for short enough times

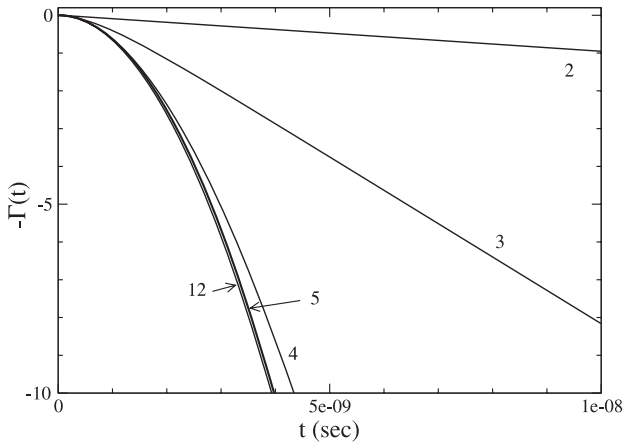

FIG. 28. The saturation effect of slow fluctuators for a $1/f$ spectrum and coupling distributed with $\langle\Delta b\rangle/\langle b\rangle = 0.2$. Labels indicate the number of decades included. Adapted from Paladino *et al.*, 2002.

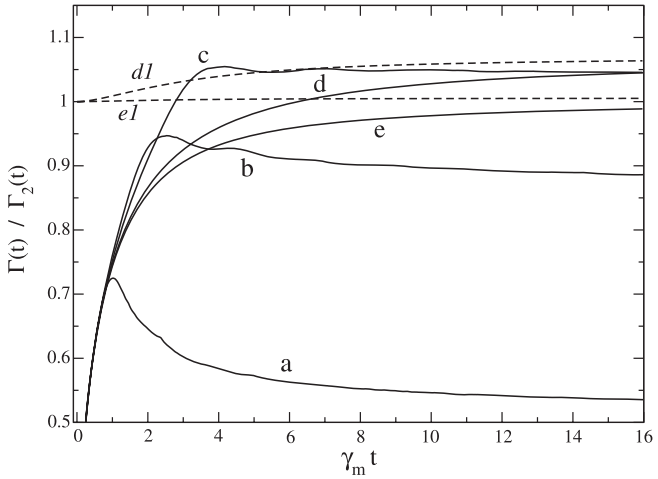

FIG. 29. Ratio $\mathcal{K}_m(t)/\langle\varphi^2\rangle \equiv \Gamma(t)/\Gamma_2(t)$ for $1/f$ spectrum between $\gamma_m/(2\pi) = 2\times10^7$ Hz and $\gamma_M/(2\pi) = 2\times10^9$ Hz with different numbers of fluctuators per decade: (a) $n_d = 10^3$, (b) $n_d = 4\times10^3$, (c) $n_d = 8\times10^3$, (d) and (d1) $n_d = 4\times10^4$, and (e) and (e1) $n_d = 4\times10^5$. Solid lines correspond to $\delta p_{0j} = \pm1$, and dashed lines correspond to equilibrium initial conditions (FID). Adapted from Paladino *et al.*, 2002.

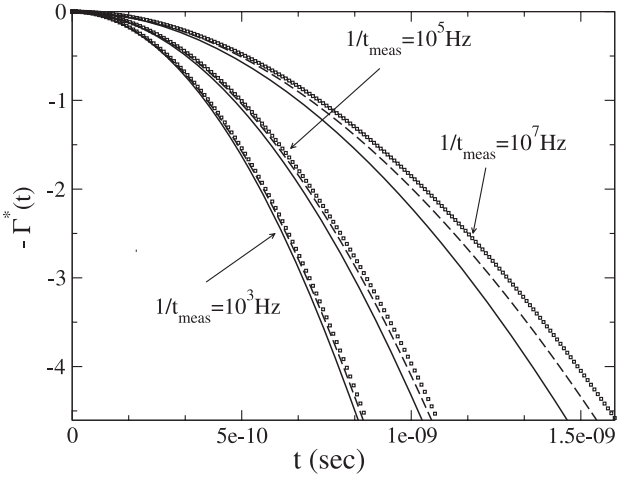

FIG. 30. Different averages over δp_{0j} for $1/f$ spectrum reproduce the effect of repeated measurements. They are obtained by neglecting (dotted lines) or accounting for (solid lines) the strongly correlated dynamics of $1/f$ noise. The noise level of Nakamura *et al.* (2002) is used, by setting $|\bar{b}|/(2\pi)=9.2\times10^6$ Hz, $n_d=10^5$, $\gamma_m/(2\pi)=1$ Hz, and $\gamma_M/(2\pi)=10^9$ Hz. Dashed lines are the oscillator approximation with a lower cutoff at $\omega=\min\{|\bar{b}|,1/t_m\}$. Adapted from Paladino, Faoro, and Falci, 2003.

$$\Gamma(t)\approx\int_{1/t_m}^{\infty}d\omega S(\omega)\left(\frac{\sin\omega t/2}{\omega/2}\right)^2. \tag{64}$$

This is illustrated in Fig. 30. The above considerations explain the often used approximate form (64) obtained from Eq. (11) with low-frequency cutoff at $1/t_m$ which was proposed by Cottet *et al.* (2001) and that we already mentioned in Sec. II.C, Eq. (32).

The echo signal obtained from Eq. (62) with Eq. (54) assuming that $\mathcal{P}(b,\gamma)\propto\gamma^{-1}\delta(b-\bar{b})\Theta(\gamma_m-\gamma)$ leads to the following time dependence when $\bar{b}\ll\gamma_M$ (Galperin *et al.*, 2007):

$$\mathcal{K}^{(e)}(t)=\begin{cases}\mathcal{A}\gamma_M t^3/6, & t\ll\gamma_M^{-1},\\ \ln(2)\mathcal{A}t^2, & \gamma_M^{-1}\ll t\ll\bar{b}^{-1},\\ \alpha(\mathcal{A}/\bar{b}^2)\bar{b}t, & \bar{b}^{-1}\ll t,\end{cases} \tag{65}$$

where $\alpha\approx6$. At small times, the echo signal behaves as in the Gaussian approximation, Eq. (14), where the t^3 dependence follows from the crossover of the spectrum from ω^{-1} to ω^{-2}. On the other hand, at large times $\bar{b}^{-1}\ll t$ the SF model dramatically differs from the Gaussian result which predicts $K_G^{(e)}(t)=\mathcal{A}\ln(2)t^2$. The origin of the non-Gaussian behavior comes from the already observed fact that decoherence is dominated by the fluctuators with $\gamma\approx2\bar{b}$. Indeed, very slow fluctuators produce slowly varying fields, which are effectively refocused in the course of the echo experiment. As to the "too fast" fluctuators, their influence is reduced due to the effect of motional narrowing. Since only the fluctuators with $\bar{b}\ll\gamma$ produce Gaussian noise, the noise in this case is essentially non-Gaussian. Only at times $t\ll\bar{b}^{-1}$, which are too short for these most important fluctuators to switch, the decoherence is dominated by the faster fluctuator contributions, and the Gaussian approximation turns out to be valid. Instead when $\bar{b}\gg\gamma_M$ all fluctuators are strongly coupled and the long-time echo decay is essentially non-Gaussian (Galperin *et al.*, 2007)

$$\mathcal{K}^{(e)}(t)=\begin{cases}\mathcal{A}\gamma_M t^3/6, & t\ll\bar{b}^{-1},\\ 4(\mathcal{A}/\bar{b}^2)\gamma_M t, & t\gg\bar{b}^{-1}.\end{cases} \tag{66}$$

Thus, the long-time behavior of the echo signal depends on the details of the noise model, the dependence on the high-frequency behavior of the spectrum being the first manifestation. Unfortunately, the measured signal is usually very weak at long times, making it difficult to figure out the characteristics of the noise sources in the specific setup. Indeed, echo signal data measured on a flux qubit in the experiment by Yoshihara *et al.* (2006) can be equally well fit assuming either a Gaussian statistics of the noise or a non-Gaussian model. The two models can in principle be distinguished analyzing the different dependence on the average coupling $\bar{b}$. Details of this analysis are given in Galperin *et al.* (2007), where a fit with the SF model for different working points indicates that Eq. (65) for the case $\bar{b}\ll\gamma_M$ gives an overall better fit. A similar experiment on a flux qubit has been reported in Kakuyanagi *et al.* (2007). Data for the echo decay rate in that case have been interpreted assuming Gaussian fluctuations of magnetic flux, and consistency with this model has been observed by changing the qubit working point. In general, echo procedures allow extraction of relevant information about the noise spectrum, like the noise amplitude (Yoshihara *et al.*, 2006; Galperin *et al.*, 2007; Kakuyanagi *et al.*, 2007; Zhou and Joynt, 2010), the noise sensitivity defined by Eq. (89) (Yoshihara *et al.*, 2006), or the average change of the flux in the qubit loop due to a single fluctuator flip (Galperin *et al.*, 2007). Similar possibilities can be provided by the real time qubit tomography (Sank *et al.*, 2012).

We now consider the role of the interaction strengths distribution b_i. Using the same model as for TLS in glasses (see Sec. II.A) we consider each fluctuator as a TLS with partial Hamiltonian

$$\hat{\mathcal{H}}_{\mathrm{F}}^{(i)}=\tfrac{1}{2}(U_i\tau_z+\Lambda_i\tau_x), \tag{67}$$

where τ_i is the set of Pauli matrices describing the ith TLS. The energy-level splitting for this fluctuator is $E_i=\sqrt{U_i^2+\Lambda_i^2}$. Fluctuators switch between their states due to the interaction with the environment, which is modeled as a thermal bath. It can represent a phonon bath as well as, e.g., electron-hole pairs in the conducting part of the system. Fluctuations of the environment affect the fluctuator through the parameters U_i and Λ_i. Assuming that fluctuations of the diagonal splitting U are most important, we describe fluctuators as TLSs in glasses; see Sec. II.A.

For the following, it is convenient to characterize fluctuators by the parameters E_i and $\theta_i=\arctan(\Lambda_i/U_i)$. The mutual distribution of these parameters can be written as (Laikhtman, 1985)

$$P(E,\theta)=P_0/\sin\theta,\quad 0\le\theta\le\pi/2, \tag{68}$$

which is equivalent to the distribution (27) of relaxation rates. To normalize the distribution one has to cut it off at small relaxation rates at a minimal value $\gamma_{\min}$ or cut off the distribution (68) at $\theta_{\min} = \gamma_{\min}/\gamma_0 \ll 1$. The distributions given by Eqs. (27) and (68) lead to the $\propto 1/\omega$ noise spectra at $\gamma_{\min} \ll \omega \ll \gamma_0$.

The variation of the qubit's energy-level spacing can be cast in the Hamiltonian, which [after a rotation similar to that leading to Eq. (25)] acquires the form

$$\hat{\mathcal{H}}_{\mathrm{qF}} = \hbar \sum_i b_i \sigma_z \tau_z^{(i)}, \qquad b_i = g(r_i) A(\mathbf{n}_i) \cos\theta_i. \tag{69}$$

Here $\mathbf{n}_i$ is the direction of the elastic or electric dipole moment of the ith fluctuator, and r_i is the distance between the qubit and the ith fluctuator. Note that in Eq. (69) we neglected the term $\propto \sigma_z \tau_x$. This can be justified as long as the fluctuator is considered to be a classical system. The functions $A(\mathbf{n}_i)$ and $g(r_i)$ are not universal.

The coupling constants b_i defined by Eq. (69) contain $\cos\theta_i$. Therefore they are statistically correlated with θ_i. It is convenient to introduce an uncorrelated random coupling parameter u_i as

$$u_i \equiv g(r_i) A(\mathbf{n}_i), \qquad b_i = u_i \cos\theta_i. \tag{70}$$

We also assume for simplicity that the direction $\mathbf{n}_i$ of a fluctuator is correlated neither with its distance from the qubit r_i nor to the tunneling parameter represented by the variable θ_i. This assumption allows us to replace $A(\mathbf{n}_i)$ by its average over the angles $\bar{A} \equiv \langle A(|\mathbf{n}|)\rangle_{\mathbf{n}}$.

Now we are ready to analyze the decoherence using Eq. (62). The question we address in this section is whether a special group of fluctuators responsible for decoherence does exist.

An interesting feature of the problem is that the result strongly depends on the decay of the coupling parameter $g(r)$ with the distance r, which usually can be described by a power law $g(r) = \bar{g}/r^s$. To illustrate this point, we compare two cases: (i) the fluctuators are distributed in three-dimensional space ($d = 3$) and (ii) the fluctuators are located in the vicinity of a two-dimensional manifold, e.g., in the vicinity of the interface between an insulator and a metal ($d = 2$). Using the distribution (68) of the relaxation rates one can express the distribution $\mathcal{P}(u,\theta)$ as

$$\mathcal{P}(u,\theta) = \frac{(\eta\cos\theta)^{d/s}}{u^{(d/s+1)}\sin\theta}, \quad \eta \equiv \frac{\bar{g}}{r_T^s}, \quad r_T \equiv \frac{a_d}{(P_0 k_B T)^{1/d}}. \tag{71}$$

Here we assumed that only the fluctuators with $E \lesssim k_B T$ are important for the decoherence since the fluctuators with $E \gtrsim k_B T$ are frozen in their ground states. The typical distance between such fluctuators is $r_T \equiv a_d (P_0 k_B T)^{-1/d}$, where a_d is a d-dependent dimensionless constant. In the following, for simplicity, we assume that

$$r_{\min} \ll r_T \ll r_{\max}, \tag{72}$$

where $r_{\min}$ ($r_{\max}$) are the distances between the qubit and the closest (most remote) fluctuator. In this case, $\eta \propto T^{s/d}$ is the typical value of the qubit-to-fluctuator coupling playing the role of the coupling parameter b. As soon as the inequality (72) is violated the decoherence starts to depend on either $r_{\min}$ or $r_{\max}$, i.e., becomes sensitive to particular mesoscopic details of the device.

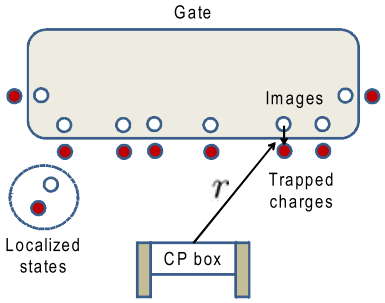

FIG. 31 (color online). Sketch of localized charges near an electrode in a Cooper pair box. Induced image charges create local dipoles that interact with the qubit.

We first consider the case when $d = s$, as it is for charged traps located near the gate electrode (where $s = d = 2$ due to the dipole nature of the field produced by a charge and its induced image, as shown in Fig. 31). In this case one can rewrite Eq. (62) as

$$\mathcal{K}_f(t) = \eta \int \frac{du}{u^2} \int_0^{\pi/2} d\theta \tan\theta f(u\cos\theta, \gamma_0 \sin^2\theta | t). \tag{73}$$

Here $f(v,\gamma|t)$ is equal either to $1 - \langle m_+(v,\gamma|t)\rangle$ or to $1 - \langle m_+^{(e)}(v,\gamma|t)\rangle$, depending on the manipulation protocol. Equation (62) together with Eqs. (49) and (54) allows one to analyze various limiting cases.

As an example, we consider the case of the two-pulse echo. To estimate the integral in Eq. (73) we look at asymptotic behaviors of the function f following from Eq. (54):

$$f^{(e)} \propto \begin{cases} t^3\gamma_0 \sin\theta (u\cos\theta)^2, & t \ll (\gamma_0 \sin\theta)^{-1}, \\ t^2 (u\cos\theta)^2, & (\gamma_0\sin\theta)^{-1} \ll t \ll u^{-1}, \\ tu\cos\theta, & u^{-1} \ll t. \end{cases} \tag{74}$$

Note that these dependences differ from those given by Eqs. (65) and (66). Splitting the regions of integration over u and θ according to the domains (74) of different asymptotic behaviors, one obtains (Galperin, Altshuler, and Shantsev, 2004)

$$\mathcal{K}^{(e)}(2\tau_{12}) \sim \eta\tau_{12} \min\{\gamma_0\tau_{12}, 1\}. \tag{75}$$

The dephasing time (defined for nonexponential decay as the time when $\mathcal{K} \sim 1$) for the two-pulse echo is thus given by

$$\tau_\varphi = \max\{\eta^{-1}, (\eta\gamma_0)^{-1/2}\}. \tag{76}$$

The result for $\gamma_0\tau_{12} \ll 1$ has a clear physical meaning [cf. with Laikhtman (1985)]: the decoherence occurs provided at least one of the fluctuators flips. Each flip provides a

contribution $\sim\eta t$ to the phase while $\gamma_0\tau_{12}$ is a probability for a flip during the observation time $\sim\tau_{12}$.

The result for long observation times $\gamma_0\tau_{12}\gg 1$ is less intuitive since in this domain the dephasing is non-Markovian; see Laikhtman (1985) for more details. In this case the decoherence is dominated by a set of *optimal* (most harmful) fluctuators located at some distance $r_{\rm opt}(T)$ from the qubit. This distance is determined by the condition

$$g(r_{\rm opt})\approx\gamma_0(T). \tag{77}$$

Although derivation of this estimate is rather tedious (Galperin, Altshuler, and Shantsev, 2004), it emerges naturally from the behavior of the decoherence in the limiting cases of strong ($b\gg\gamma$) and weak ($b\ll\gamma$) coupling. For strong coupling, the fluctuators are slow and the qubit's behavior is determined by quantum beatings between the states with $E\pm b$. Accordingly, the decoherence rate is $\sim\gamma$. In the opposite case, as discussed, the decoherence rate is $\sim b^2/\gamma$. Matching these two limiting cases one arrives at the estimate (77).

What happens if $d\neq s$? If the coupling decays as r^{-s} and the fluctuators are distributed in a d-dimensional space, then $r^{d-1}dr$ is transformed to $du/u^{1+d/s}$. Therefore, $\mathcal{P}(u)\propto 1/u^{1+d/s}$. As a result, at $d\le s$ the decoherence is controlled by the optimal fluctuators located at the distance $r_{\rm opt}$ provided they exist. If $d\le s$, but the closest fluctuator has $b_{\max}\ll\gamma_0$, then it is the quantity $b_{\max}$ that determines the decoherence. At $d>s$ the decoherence at large time is dominated by most remote fluctuators with $r=r_{\max}$. In the last two cases, $\mathcal{K}(t)\propto t^2$, and one can apply the results of Paladino *et al.* (2002), substituting for b either $b_{\min}$ or $b_{\max}$.

Since $r_{\rm opt}$ depends on the temperature, one can expect crossovers between different regimes as a function of temperature. A similar mesoscopic behavior of the decoherence rates was discussed for a microwave-irradiated Andreev interferometer (Lundin and Galperin, 2001). It is worth emphasizing that the result (75) for the long-range interaction cannot be reproduced by the Gaussian approximation. Indeed, if we expand the Gaussian approximation $e^{-\langle\psi^2\rangle/2}$ with $\langle\psi^2\rangle$ given by Eq. (55) in the same fashion as in Eq. (74) and then substitute into Eq. (73), the resulting integral over u will be divergent at its upper limit. Physically, this means the dominant role of nearest neighbors of the qubit. At the same time, the SF model implies that the most important fluctuators are those satisfying Eq. (77).

The existence of selected groups of fluctuators, out of an ensemble of many, which are responsible for decay of specific quantities, is closely related to the self-averaging property of the corresponding decay laws. Schriefl *et al.* (2006) analyzed a class of distribution functions of the form (71) with $0<d/s<2$. In this case the average over the coupling constants of the Lorentzian functions (46) diverges at the upper limit and the noise is dominated by the most strongly coupled fluctuators. The free induction decay has been found as non-self-averaging at both short and long times with respect to γ_0^{-1}. Non-self-averaging of the echo signal for $2\tau_{12}\gg\gamma_0^{-1}$ has also been demonstrated (Schriefl *et al.*, 2006).

e. Dephasing according to other phenomenological models

We remark that, beside the spin-fluctuator model, other stochastic processes have been considered for the description of fluctuations having $1/f$ spectral density. Here we mention an alternative phenomenological model, which has been discussed in connection with the problem of qubit dephasing. The motivation to consider these models comes from the observation of asymmetric telegraphic signals, with longer stays in the "down" state than in the "up" state, reported in tunnel junctions (Zimmerli *et al.*, 1992), in metal oxide semiconductor tunnel diodes (Buehler *et al.*, 2004), and of a spike field detected in a SET electrometer (Zorin *et al.*, 1996). In those cases the signal exhibits $1/f$ spectrum at low frequencies. This suggests a description of the $1/f$ noise in terms of a single asymmetric RT signal. (Schriefl *et al.* (2005a, 2005b) considered a phenomenological model for a $1/f^{\mu}$ classical intermittent noise. The model can be viewed as the intermittent limit of the sum of RT signals where the duration of each plateau of the RT signal $\tau_{\rm av}$ is assumed to be much shorter than waiting times between the plateaus. In this limit, the noise is approximated by a spike field consisting of delta functions whose heights x follow a Gaussian distribution or, more generally, a distribution with finite first and second moments $\bar{x}$ and $s\equiv(\bar{x^2})^{1/2}$, respectively, as illustrated in Fig. 32 (. The variance s plays the role of a coupling constant between the qubit and the stochastic process. A $1/f$ spectrum for the intermittent noise is recovered for a distribution of waiting times τ behaving as τ^{-2} at large times. Because the average waiting time is infinite, no time scale characterizes the evolution of the noise which is nonstationary. In the pure dephasing regime the relative phase between the qubit states performs a continuous time random walk (CTRW) (Haus and Kehr, 1987) as time goes on. Using renewal theory [see Feller (1962)], Schriefl *et al.* (2005a, 2005b) found an exact expression for the Laplace transform of the dephasing factor allowing analytical estimates in various limiting regimes and

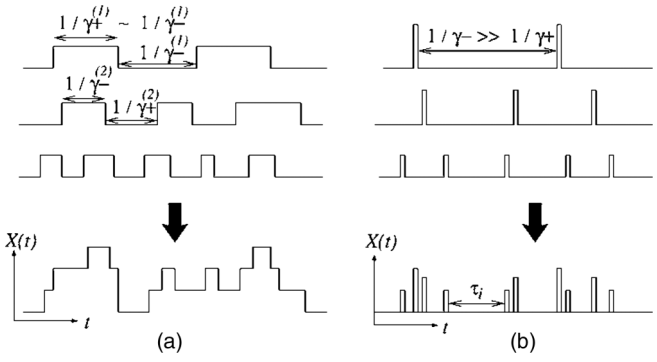

FIG. 32. (a) Low-frequency noise as a sum of the RT signals. The switching rates for the "up" and "down" states are comparable $\gamma_+\approx\gamma_-$ and $1/f$ noise results from a superposition of RT signals distributed as $\propto 1/\gamma$. (b) The intermittent limit corresponds to the limit where the noise stays in the down states most of the time ($\gamma_+\gg\gamma_-$). The intermittent noise can be approximated by a spike field with independent random waiting times and spike eighths. It gives a nonstationary $1/f^{\mu}$ spectrum depending on the plateaus distribution function. Adapted from Schriefl *et al.*, 2005a.

addressing the consequences of the CTRWs nonstationarity. The noise is initialized at time $t'=0$ and the coupling with the qubit is turned on at the preparation time t_p. The two qubit states accumulate a random relative phase between t_p and $t+t_p$ and nonstationarity manifests itself in the dependence of the dephasing factor, on the age of the noise t_p. This analysis shows that two dephasing regimes exist separated by a crossover coupling constant $s_c(t_p)=[2(\tau_{\rm av}/t_p)\ln(t_p/\tau_{\rm av})]^{1/2}$, strongly dependent on the preparation time t_p. For $s<s_c(t_p)$ dephasing is exponential and independent on t_p, whereas when $s>s_c(t_p)$ the dephasing time depends algebraically on t_p. Since $s_c(t_p)$ decays to zero with the noise age, any qubit coupled to the nonstationary noise will eventually fall in the regime $s>s_c(t_p)$.

Note that Schriefl *et al.* (2005a, 2005b) defined the dephasing factor as a configuration average over the noise, rather than a time average in a given configuration. The two averages do not coincide in general for nonstationary or aging phenomena. Thus one should be careful in comparing these results with experiments.

2. Decoherence due to the SF model at general working point

Here we discuss decoherence due to the spin-fluctuator model at a general operating point where

$$\hat{H}_{\rm tot}=\frac{\hbar}{2}[\Omega_x\sigma_x+\Omega_z(q)\sigma_z]+\frac{\hbar}{2}b\chi(t)\sigma_z. \tag{78}$$

As a difference with the pure-dephasing regime, no exact analytic solution is available under these conditions. Different approaches have been introduced to study the qubit dynamics leading to analytical approximations in specific limits and/or to (exact) numerical results.

A straightforward approach consists of solving the stochastic Schrödinger equation. Using the theory of stochastic differential equations (Brissaud and Frisch, 1974), a formal solution in Laplace space can be found which is however difficult to invert analytically. A numerical solution is instead feasible and the method can be extended to investigate the effect of an ensemble of fluctuators with proper distribution of parameters to generate processes having a $1/f$ power spectrum (Falci *et al.*, 2005). Cheng, Wang, and Joynt (2008) proposed a generalized transfer-matrix method. It reduces to the algebraic problem of the diagonalization of a 6×6 matrix whose eigenvalues give the decoherence "rates" entering the qubit dynamics. This approach also gives the system evolution on time scales shorter than the fluctuator correlation time. The transfer matrix method is suitable to address the dynamics under instantaneous dc pulses like those required in the spin-echo protocol. The method can in principle be extended to the case of many fluctuators, although the size of the matrices soon becomes intractable. Another approach consists in the evaluation of the quantum dynamics of a composite system composed of the qubit and one (or more) fluctuator(s), treated as quantum mechanical two-level systems (Paladino *et al.*, 2002; Paladino, Faoro, D'Arrigo, and Falci, 2003). This requires solving either the Heisenberg equations of motion or a master equation in the enlarged Hilbert space. Impurities

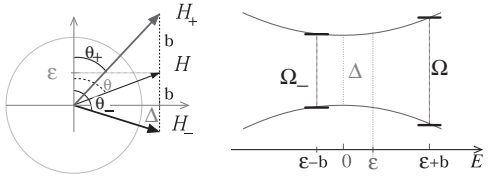

FIG. 33. Left panel: Qubit Bloch sphere. An isolated qubit defines the mixing angle $\theta=\arctan\{\Delta/\epsilon\}$, $H_\pm$ define $\theta_\pm=\arctan\{\Delta/(\epsilon\pm b)\}$. Right panel: Qubit energy bands $\pm\sqrt{E^2+\Delta^2}$: the energy splittings depend on the impurity state $\Omega_\pm=\sqrt{(\epsilon\pm b)^2+\Delta^2}$.

are traced out at the end of the calculation, when the high-temperature approximation for the fluctuator is also performed (Paladino *et al.*, 2002; Paladino, Faoro, D'Arrigo, and Falci, 2003). Both methods lead to analytic forms in a limited parameter regime and a numerical analysis is required in the more general case. Other approximate methods rely on the extension of the approach based on the evaluation of the probability distribution $p(\varphi,t)$ which is evaluated numerically (Bergli, Galperin, and Altshuler, 2006).

The main effects of a RT fluctuator coupled to a qubit via an interaction term of the form (78) can be simply illustrated as follows. The noise term $-b\chi(t)\sigma_z/2$ induces two effective splittings $\Omega_\pm=\sqrt{(\Omega_z\pm b)^2+\Omega_x^2}$ and correspondingly two values of the polar angle $\theta_\pm=\arctan[\Omega_x/(\Omega_z\pm b)]$, as illustrated in Fig. 33.

In the adiabatic limit $\gamma\sim|\Omega_+-\Omega_-|\ll\Omega_\pm$, and neglecting any qubit backaction on the fluctuator, the qubit coherence takes a form similar to the pure dephasing result Eq. (49). Here we report the average $\langle\sigma_y(t)\rangle$ (Paladino, Faoro, D'Arrigo, and Falci, 2003):

$$\langle\sigma_y(t)\rangle=-{\rm Im}\left[\frac{e^{i(\Omega+\gamma g/2)t}}{\alpha}\sum_{\pm}A(\pm\alpha)e^{-[(1\mp\alpha)/2]\gamma t}\right], \tag{79}$$

where $\alpha=\sqrt{1-g^2-2\,ig\delta p_{\rm eq}-(1-c^4)(1-\delta p_{\rm eq}^2)}$,

$$c=\cos[(\theta_--\theta_+)/2],\quad g=(\Omega_+-\Omega_-)/\gamma,$$

$$A(\alpha)=(\alpha+c^2-ig')\rho_{+-}^{(-)}(0)p_0+(\alpha+c^2+ig')\rho_{+-}^{(+)}(0)p_1,$$

with $g'=g+i\delta p_{\rm eq}(1-c^2)$ and $\rho_{+-}^{(\pm)}(0)$ are values at $t=0$ of the qubit coherences in the eigenbasis $|\pm\rangle_{\theta_\pm}$ of the qubit conditional Hamiltonians corresponding to $\chi=\pm1$. In the high-temperature regime, $\delta p_{\rm eq}\approx0$, and $\alpha\approx\sqrt{c^4-g^2}$. Thus the relevant parameter separating the weak-coupling from the strong-coupling regime is $g/c^2=(\Omega_+-\Omega_-)/c^2\gamma$. A fluctuator is weakly coupled if $g/c^2\ll1$ and strongly coupled otherwise. This condition depends on the qubit's operating point, and at $\theta=0$ we get $g/c^2=2b/\gamma$. Thus a fluctuator characterized by a set (b,γ) affects in a qualitatively different way the qubit dynamics depending on the qubit's operating point. In particular, a fluctuator turns from strongly to weakly coupled increasing θ from 0 to $\pi/2$, as illustrated in Fig. 34. From Eq. (79) it easy to see that a weakly coupled fluctuator induces an exponential decay with T_2 given by Eq. (16), whereas a strongly coupled fluctuator induces a saturation effect which is less effective at $\theta=\pi/2$ than at $\theta=0$

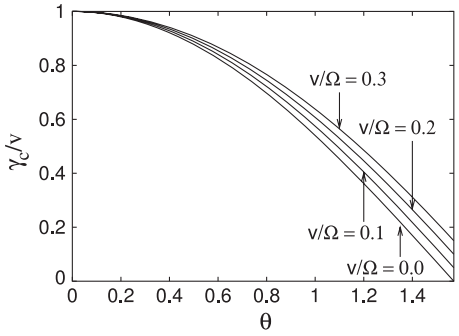

FIG. 34. The threshold value $\gamma_c/v \equiv (\Omega_+ - \Omega_-)/(2bc^2)$ for a fluctuator behaving as weakly coupled depends on the operating point ($v/\Omega \equiv 2b/\Omega$). Adapted from Paladino, Faoro, and Falci, 2003.

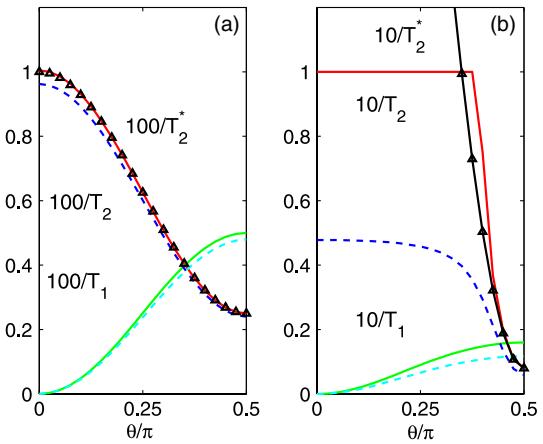

FIG. 35 (color online). Relaxation $1/T_1$ and dephasing $1/T_2$ rates (rescaled for visibility) as functions of θ. Triangles: $1/T_2^* = \cos^2\theta S(0)/2$ for a (a) weakly and (b) strongly coupled fluctuator. γ/Ω: (a) 0.5, (b) 0.1. b/Ω: (a) 0.1, (b) 0.3. The solid (dashed) lines correspond to a symmetric (slightly asymmetric) fluctuator. Adapted from Cheng, Wang, and Joynt, 2008.

(Paladino, Faoro, D'Arrigo, and Falci, 2003; Bergli, Galperin, and Altshuler, 2006; Cheng, Wang, and Joynt, 2008; Zhou and Joynt, 2010). The effect of strongly coupled fluctuators is more sensitive to deviations from the optimal point $\theta = \pi/2$. The dependence on the working point of the decoherence and relaxation times for a weakly and a strongly coupled fluctuator is shown in Fig. 35. The decay rates at $\theta = \pi/2$ have also been obtained by Itakura and Tokura (2003) by solving the stochastic differential equation.

a. Ensemble of fluctuators: Decoherence due to $1/f$ noise

All mentioned approaches become intractable analytically as soon as the number of fluctuators increases. Already in the presence of a few fluctuators a numerical solution is required. This difficulty and the physical scenario behind the mechanisms of dephasing due to $1/f$ noise at different operating points can be traced back to the dependence of the qubit splitting on the induced fluctuations [cf. with Eq. (36)], which we write here for $\Omega_\pm$:

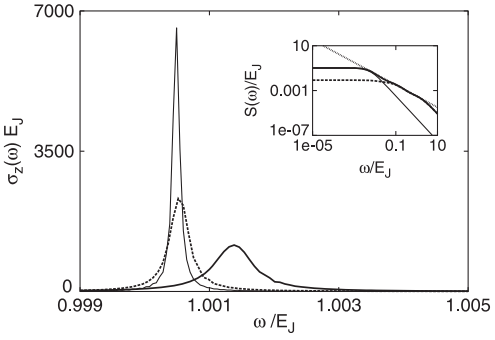

FIG. 36. The Fourier transform of $\langle\sigma_z(t)\rangle$ for a set of weakly coupled fluctuators plus a single strongly coupled fluctuator (thick line). The separate effect of the coupled fluctuator ($g = 8.3$, thin line) and the set of weakly coupled fluctuators (dotted line) is shown for comparison. Inset: corresponding power spectra. In all cases the noise level at $\Delta = E_J$ is fixed to the value $S(E_J)/E_J = 3.18 \times 10^{-4}$ [from typical $1/f$ noise amplitude in charge qubits (Zorin *et al.*, 1996; Covington *et al.*, 2000; Nakamura *et al.*, 2002) extrapolated at GHz frequencies]. Adapted from Paladino *et al.*, 2002.

$$\delta\Omega_\pm \approx \pm\frac{\Omega_z}{\Omega}b + \frac{1}{2}\frac{\Omega_x^2}{\Omega^3}b^2. \tag{80}$$

Far from the optimal point, the leading term is linear in the coupling b. This is the only effect left at pure dephasing $\Omega_x = 0$, and it is also the reason why an exact formula is available under this condition both in the case of a single fluctuator and in the presence of an ensemble of fluctuators. In this last case the phase-memory functional for any number of fluctuators is found by simply multiplying the phase-memory functionals for different fluctuators. At the optimal point instead, $\Omega_z = 0$, the first order term is quadratic. Thus the effect of the fluctuator is reduced with respect to the pure dephasing regime. The effects of different fluctuators in this case do not simply add up independently and no analytic solution is available. This simple observation suggests an important physical insight into the combined effect of various fluctuators at different working points. When the first order effect on the splitting is quadratic, even if the different fluctuators in themselves are independent, their effect on the qubit will be influenced by the position of all others. At pure dephasing, since effects sum up independently, all slow fluctuators are ineffective at times $\gamma t \ll 1$. This is no longer true when the leading term is quadratic, as they play a role in determining the effect of faster fluctuators. In fact even if they do not have time to switch during the experiment, they contribute to the average effective operating point the qubit is working as seen by the faster fluctuators. Thus very slow fluctuators may be of great importance at the optimal point. For example, Fig. 36 illustrates the point that even a single, strongly coupled fluctuator, out of the many fluctuators forming the $1/f$ spectrum, determines a dephasing more than twice the prediction of the weak coupling theory T_2^*, even when the fluctuator is not visible in the spectrum. Further slowing down of the fluctuator produces a saturation of dephasing, as expected based on the above considerations. In this regime effects related to the initial preparation of the fluctuator, or equivalently effects of the measurement protocol, are visible as illustrated in Fig. 37.

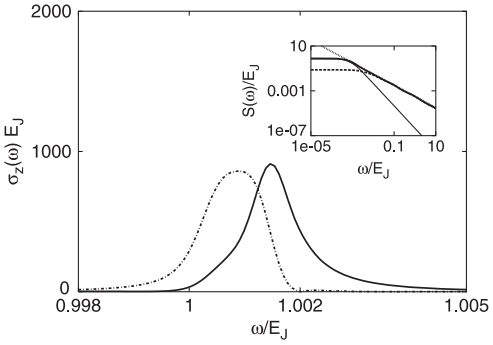

FIG. 37. The Fourier transform $\langle\sigma_z\rangle_\omega$ for a set of weakly coupled fluctuators plus a strongly coupled fluctuator ($2b/\gamma = 61.25$) prepared in the ground (dotted line) or in the excited state (thick line). Inset: corresponding power spectra (the thin line corresponds to the extra fluctuator alone). Adapted from Paladino *et al.*, 2002.

The presence of selected strongly coupled fluctuators in the ensemble leading to the $1/f$ spectrum may give rise to striking effects like beatings between the two frequencies $\Omega_\pm$ (see Fig. 40 and the discussion in Sec. III.B.1.b). Relevant effects of $1/f$ noise at a general working point, especially for protocols requiring repeated measurements, are captured by approximate approaches based on the adiabatic approximation which we discuss in Sec. III.B.

B. Approximate approaches for decoherence due to $1/f$ noise

In the context of quantum computation, the effects of stochastic processes with long-time correlations, like those characterized by a $1/f$ spectral density, depend on the quantum operation performed and/or on the measurement protocol. Here we present approximate approaches proposed to predict dephasing due to $1/f$ noise and its interplay with quantum noise. An approach based on the adiabatic approximation (Falci *et al.*, 2005; Ithier *et al.*, 2005) allows simple explanations of peculiar nonexponential decay reported in different experiments with various setups. In some protocols a Gaussian approximation captures the main effects at least on a short time scale (Makhlin and Shnirman, 2004; Rabenstein, Sverdlov, and Averin, 2004; Falci *et al.*, 2005). Some other protocols, instead, reveal the non-Gaussian nature of the noise. The adiabatic approximation suggests a route to identify operating conditions where leading order effects of $1/f$ noise are eliminated also for complex architectures.

1. Approaches based on the adiabatic approximation

Our staring point is the phenomenological Hamiltonian equation (43), where we separated the effect of quantum noise due to (high-frequency) modes exchanging energy with the system and low-frequency fluctuations $\delta q(t)$ of the bias parameter q. Environments with long-time memory, i.e., correlated on a time scale much longer than the inverse of the natural system frequencies, belong to the class of adiabatic noise. Stochastic processes can be treated in the adiabatic approximation provided their contribution to spontaneous decay is negligible, a necessary condition being $t \ll T_1 \propto S(\Omega)^{-1}$. This condition is satisfied for $1/f$ noise at

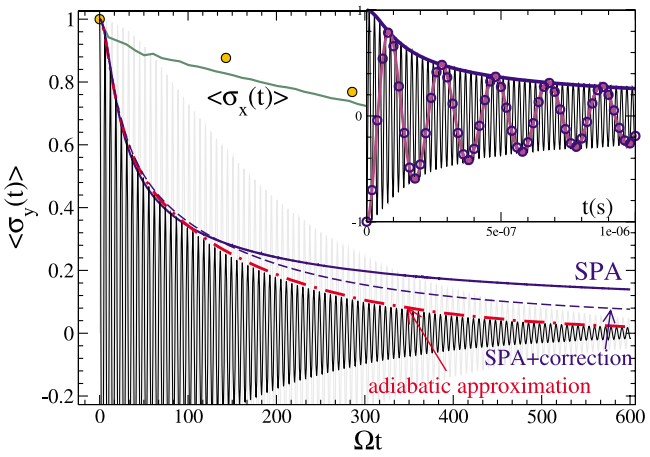

FIG. 38 (color online). Simulations of an adiabatic fluctuators $1/f$ environment at $\theta = \pi/2$. Relaxation studied via $\langle\sigma_x\rangle$ is well approximated by the weak coupling theory T_2(dots). Dephasing in repeated measurement damps the oscillations (thin black line). Part of the signal is recovered if the environment is recalibrated (thin gray line). Noise is produced by $n_d = 250$ fluctuators per decade, with $1/t_m = 10^5$ rad/s $\le \gamma_i \le \gamma_M = 10^9$ rad/s $< \Omega = 10^{10}$ rad/s. The coupling $\bar{v} = 0.02\ \Omega$ is appropriate to charge devices and corresponds to $S = 16\pi A E_C^2/\omega$ with $A = 10^{-6}$ (Zorin *et al.*, 1996). The adiabatic approximation, Eq. (91), fully accounts for dephasing (dot-dashed line). The static-path approximation (SPA), Eq. (95) (solid line) and the first correction (dashed line) account for the initial suppression, and it is valid also for times $t \gg 1/\gamma_M$. Inset: Ramsey fringes with parameters appropriate to the experiment (Vion *et al.*, 2002) (thin black lines). The SPA (solid line), Eq. (95), is in excellent agreement with observations and also predicts the correct phase shift of the Ramsey signal (dots, compared with simulations for small detuning $\delta = 5$ MHz, line), which tends to $\approx\pi/4$ for large times. Adapted from Falci *et al.*, 2005.

short enough times, considering that $S(\omega) \propto 1/\omega$ is substantially different from zero only at frequencies $\omega \ll \Omega$. For pure dephasing $\theta = 0$, relaxation processes are forbidden and the adiabatic approximation is exact for any $S(\omega)$. In the adiabatic approximation the instantaneous Hamiltonian of a qubit, manipulated only with dc pulses, reads

$$\hat{H}_{\rm tot} = \frac{\hbar\Omega(q)}{2}(\cos\theta_q\sigma_z + \sin\theta_q\sigma_x) + \frac{\hbar E(t)}{2}\sigma_z \equiv \frac{\hbar}{2}\Omega[q,\delta q(t)]\sigma_{\tilde{z}}, \tag{81}$$

where $E(t) = 2\delta q(t)\partial\Omega_z/\partial q$, and the instantaneous splitting is

$$\Omega(q,\delta q(t)) = \sqrt{\Omega^2(q) + E^2(t) + 2E(t)\Omega(q)\cos\theta_q}. \tag{82}$$

The $\sigma_{\tilde{z}}$ axis forms a time-dependent angle $\tilde{\theta}_q(t) = \arctan(\Omega\sin\theta_q/[\Omega\cos\theta_q + E(t)])$, with σ_z. In the qubit eigenbasis ($E \equiv 0$) the adiabatic Hamiltonian (81) reads

$$\hat{H} = \frac{\hbar\Omega(q,\delta q)}{2}(\cos[\tilde{\theta}_q(t)-\theta_q]\sigma_{z'} + \sin[\tilde{\theta}_q(t)-\theta_q]\sigma_{x'}). \tag{83}$$

The effect of an adiabatic stochastic field $E(t)$ is to produce fluctuations both of the qubit splitting $\Omega[q,\delta q(t)]$ and of the qubit eigenstates, or equivalently of the "direction" of the qubit Hamiltonian, expressed by the angle $\tilde{\theta}_q(t)$. Since we are interested in situations where $|E(t)| \ll \Omega$, both $\Omega[q,\delta q(t)]$ and $\tilde{\theta}_q(t)$ can be expanded in a Taylor series about $\Omega(q,0)$ and θ_q, respectively,

$$\Omega(q,\delta q) \approx \Omega(q,0) + \frac{\partial\Omega}{\partial q}(\delta q) + \frac{1}{2}\frac{\partial^2\Omega}{\partial q^2}(\delta q)^2 + \cdots, \tag{84}$$

$$\tilde{\theta}_q \approx \theta_q + \frac{\partial\tilde{\theta}_q}{\partial q}(\delta q) + \frac{1}{2}\frac{\partial^2\tilde{\theta}_q}{\partial q^2}(\delta q)^2 + \cdots, \tag{85}$$

where $(\delta q) \equiv \delta q(t)$ and all derivatives are evaluated at $\delta q = 0$. The adiabatic Hamiltonian (81) therefore can be cast in the form

$$\hat{H} = \frac{\hbar}{2}[\Omega(q,0)\sigma_{z'} + \delta\Omega_{\parallel}(t)\sigma_{z'} + \delta\Omega_{\perp}(t)\sigma_{\perp}], \tag{86}$$

where, from Eq. (83), $\delta\Omega_{\parallel}$ includes the derivatives of $\Omega[q,\delta q(t)]\cos[\tilde{\theta}_q(t)-\theta_q]$ and $\delta\Omega_{\perp}$ the derivatives of $\Omega[q,\delta q(t)]\sin[\tilde{\theta}_q(t)-\theta_q]$. The Pauli matrix $\sigma_{\perp}$ in the case of Eq. (83) is $\sigma_{x'}$; in general it can be a combination of $\sigma_{x'}$ and $\sigma_{y'}$.

The effect on the qubit dynamics of adiabatic transverse fluctuations weakly depends on time; on the other hand, longitudinal components are responsible for phase errors, which accumulate in time. Thus adiabatic transverse noise has possibly some effect at very short times, but the phase damping channel eventually prevails. The relevance of these effects quantitatively depends on the amplitude of the noise at low frequencies. It was demonstrated by Falci *et al.* (2005) (see Fig. 38) that, for the typical noise figures of superconducting devices and at least for short time scales relevant for quantum computing, the leading effect of adiabatic noise is defocusing originated by the fluctuating splitting during the repetitions of the measurement runs. This effect is captured by neglecting the transverse terms in Eq. (85), i.e., making the *longitudinal approximation* of the Hamiltonian (81)

$$\hat{H} \approx \frac{\hbar\Omega(q,0)}{2}\sigma_{z'} + \frac{\hbar\delta\Omega_{\parallel}(t)}{2}\sigma_{z'}. \tag{87}$$

In addition, consistent with $\tilde{\theta}_q(t) \approx \theta_q$, the splitting fluctuations are further approximated as (Falci *et al.*, 2005; Ithier *et al.*, 2005)

$$\delta\Omega_{\parallel}(t) \approx \frac{\partial\Omega}{\partial q}(\delta q) + \frac{1}{2}\frac{\partial^2\Omega}{\partial q^2}(\delta q)^2 + \cdots. \tag{88}$$

Considering the explicit dependence on δq of $\Omega(q,\delta q)$, the first terms of the expansion read [cf. with Eq. (36)],

$$\Omega(q,\delta q(t)) \approx \Omega(q) + E(t)\cos\theta_q + \frac{1}{2}\frac{[E(t)\sin\theta_q]^2}{\Omega(q)}. \tag{89}$$

For longitudinal noise $\theta_q = 0$, we recover the exact linear dependence on the noise of the instantaneous splitting. For transverse noise instead $\theta_q = \pi/2$, the first nonvanishing term of the expansion is quadratic. It is common to refer to this regime as the "quadratic coupling" (Ithier *et al.*, 2005), or the "quadratic longitudinal coupling" condition (Makhlin and Shnirman, 2004).

We remark that Eq. (86) also applies when both components Ω_x and Ω_z fluctuate. For instance, this is the case of flux qubits where both flux and critical current fluctuate with $1/f$ spectrum and the physical fluctuating quantity δq is a function of the magnetic flux or the critical current. The partial derivatives can be expressed in terms of noise sensitivities as follows:

$$\frac{\partial\Omega}{\partial q} = \frac{\partial\Omega}{\partial\Omega_z}\frac{\partial\Omega_z}{\partial q} + \frac{\partial\Omega}{\partial\Omega_x}\frac{\partial\Omega_x}{\partial q} = \frac{\Omega_z}{\Omega}\frac{\partial\Omega_z}{\partial q} + \frac{\Omega_x}{\Omega}\frac{\partial\Omega_x}{\partial q}, \tag{90}$$

where the noise sensitivities $\partial\Omega_z/\partial q$, $\partial\Omega_x/\partial q$ can be inferred from spectroscopy measurements as in the experiment (Bylander *et al.*, 2011).

A formal expression for the qubit dynamics in the adiabatic approximation, introduced by Falci *et al.* (2005), has been discussed in detail and extended to more complex gates by Paladino *et al.* (2009). Here we report the results in the adiabatic and longitudinal approximations. In this regime populations of the qubit density matrix in the eigenbasis do not evolve, whereas the off-diagonal elements are obtained by averaging over all realizations of the stochastic process $E(t)$ expressed by the path integral

$$\frac{\rho_{mn}(t)}{\rho_{mn}(0)} = \int \mathcal{D}[E(s)]P[E(s)]e^{-i\int_0^t ds\Omega_{mn}(q,\delta q(s))}. \tag{91}$$

Here $P[E(s)]$ contains information both on the stochastic processes and on details of the specific protocol. It is convenient to split it as follows:

$$P[E(s)] = F[E(s)]p[E(s)],$$

where $p[E(s)]$ is the probability of the realization $E(s)$. The filter function $F[E(s)]$ describes the specific operation. For most of the present day experiments on solid-state qubits $F[E(s)] = 1$. For open-loop feedback protocol, which allows initial control of some collective variable of the environment, say $E_0 = 0$, we should put $F[E(s)] \propto \delta(E_0)$. The different decay of coherent oscillations in each protocol in the presence of adiabatic noise originates from the specific filter function which needs to be specified at this stage.

A critical issue is the identification of $p[E(s)]$ for the specific noise sources, as those displaying a $1/f$ power spectrum. If we sample the stochastic process at times $t_k = k\Delta t$, with $\Delta t = t/n$, we can identify

$$p[E(s)] = \lim_{n\to\infty} p_{n+1}(E_n,t;\ldots;E_1,t_1;E_0,0), \tag{92}$$

where $p_{n+1}(\cdots)$ is a $n+1$ joint probability. In general, this is a formidable task. However, a systematic method can be found to select only the relevant statistical information on the stochastic process out of the full characterization included in $p[E(s)]$ (Falci *et al.*, 2005; Paladino *et al.*, 2009).

The signal decay in FID is obtained by performing in Eq. (91) the static path approximation (SPA), which consists of neglecting the time dependence in the path $E(s)=E_0$ and taking $F[E]=1$. In the SPA the problem reduces to ordinary integrations with $p_1(E_0,0)\equiv p(E_0)$. The qubit coherences can be written as $\rho_{01}(t)=\rho_{01}(0)\exp[-i\Omega t-i\Phi(t)]$ with the average phase shift

$$\Phi(t)\approx i\ \ln\left(\int dE_0 p(E_0)e^{it\sqrt{\Omega^2+E_0^2+2\Omega E_0\ \cos\theta}}\right). \tag{93}$$

Clearly, Eq. (93) describes the effect of a distribution of stray energy shifts $\hbar[\Omega(q,\delta q)-\Omega(q,0)]$ and corresponds to the rigid lattice breadth contribution to inhomogeneous broadening. In experiments with solid-state devices this approximation describes the measurement procedure consisting of signal acquisition and averaging over a large number N of repetitions of the protocol, for an overall time t_m (minutes in actual experiments). Due to slow fluctuations of the environment calibration, the initial value $\Omega\cos\theta+E_0$ fluctuates during the repetitions blurring the average signal, independently of the measurement being single shot or not.

The probability $p(E_0)$ describes the distribution of the random variable obtained by sampling the stochastic process $E(t)$ at the initial time of each repetition, i.e., at times $t_k=kt_m/N$, $k=0,\ldots,N-1$. If E_0 results from many independent random variables of a multimode environment, the central limit theorem applies and $p(E_0)$ is a Gaussian distribution with standard deviation σ,

$$\sigma^2=\langle E^2\rangle=2\int_0^\infty d\omega S(\omega),$$

where integration limits are intended as $1/t_m$, and the high-frequency cutoff of the $1/f$ spectrum γ_M. In the SPA the distribution standard deviation σ is the only adiabatic noise characteristic parameter. If the equilibrium average of the stochastic process vanishes, Eq. (93) reduces to

$$\Phi(t)\approx i\ \ln\left[\int\frac{dE_0}{\sqrt{2\pi\sigma^2}}e^{-E_0^2/2\sigma^2}e^{it\sqrt{\Omega^2+E_0^2+2\Omega E_0\ \cos\theta}}\right]. \tag{94}$$

Expanding the square root in Eq. (94) we obtain (Falci *et al.*, 2005)

$$\Phi(t)=-\frac{i}{2}\left[\frac{\Omega(\cos\theta\sigma t)^2}{\Omega+i\sin^2\theta\sigma^2 t}+\ln\frac{\Omega+i\sin^2\theta\sigma^2 t}{\Omega}\right]. \tag{95}$$

The short-time decay of coherent oscillations qualitatively depends on the working point. In fact, the suppression of the signal $\exp[\mathrm{Im}\Phi(t)]$ turns from an exponential behavior $\propto e^{-(\cos\theta\sigma t)^2/2}$ at $\theta\approx 0$ to a power law $[1+(\sin\theta^2\sigma^2 t/\Omega)^2]^{-1/4}$ at $\theta\approx\pi/2$. In these limits Eq. (95) reproduces the results for Gaussian $1/f$ environments in the so-called "quasistatic case" reported by Ithier *et al.* (2005). In particular, at $\theta=0$ we obtain the short-time limit $t\ll 1/\gamma_M$ of the exact result of Palma, Suominen, and Ekert (1996), Eq. (11). In fact, for very short times we can approximate $\sin^2(\omega t/2)/(\omega t/2)^2\approx 1$ inside the integral Eq. (11), obtaining the exponential quadratic decay law at pure dephasing predicted by the Gaussian approximation. At $\theta=\pi/2$ the short and intermediate times result of Makhlin and Shnirman (2004) for a Gaussian noise and quadratic coupling is reproduced.

The fact that results of a diagrammatic approach with a quantum environment, as those of Makhlin and Shnirman (2004), can be reproduced and generalized already at the simple SPA level makes the semiclassical approach quite promising. It shows that, at least for not too long times (but surely longer than times of interest for quantum state processing), the quantum nature of the environment may not be relevant for the class of problems, which can be treated in the Born-Oppenheimer approximation. Notice also that the SPA itself has surely a wide validity since it does not require information about the *dynamics* of the noise sources, provided they are slow. For Gaussian wide-band $1/f$ noise and for times $\gamma_m\ll 1/t<\gamma_M$, the contribution of frequencies $\omega\ll 1/t$ can be approximated by Eq. (95), where the noise variance is evaluated integrating the power spectrum from γ_m to $1/t$, that is, $\sigma^2=\mathcal{A}\ \ln\ (1/\gamma_m t)$ (Cottet *et al.*, 2001; Nakamura *et al.*, 2002; Ithier *et al.*, 2005). The diagrammatic approach of Makhlin and Shnirman (2004) for Gaussian noise and quadratic coupling also predicts a crossover from algebraic behavior to exponential decay at long times $\mathcal{A}t\gg 1$ with rate $\mathcal{A}/2$. This behavior is, however, hardly detectable in experiments, where the long-time behavior is ruled by quantum noise (see the discussion in Sec. III.B.1.b).

Equation (91) can be systematically approximated by proper sampling $E(t')$ in $[0,t]$. In this way the dynamics of the noise sources during the runs can also be systematically included. For the first correction, $p[E(t')]$ can be approximated by the joint distribution $p[E_t t;E_0,0]$, where $E_t\equiv E(t)$. At $\theta=\pi/2$ for generic Gaussian noise we find

$$\Phi(t)=-\frac{i}{2}\ \ln\left[\left(\frac{\Omega+i\sigma^2 t[1-\Pi(t)]}{\Omega}\right)\left(\frac{3\Omega+i\sigma^2 t\Pi(t)}{3\Omega}\right)\right],$$

where $\Pi(t)\equiv\int_0^\infty(d\omega/\sigma^2)S(\omega)(1-e^{-i\omega t})$ is a transition probability, depending on the stochastic process. For Ornstein-Uhlenbeck processes it reduces to the result of Rabenstein, Sverdlov, and Averin (2004). The first correction suggests that the SPA, in principle valid for $t<1/\gamma_M$, may have a broader validity (see Fig. 38). For $1/f$ noise due to a set of bistable impurities it is valid also for $t\gg 1/\gamma_M$, if $\gamma_M\lesssim\Omega$. Of course, the adiabatic approximation is tenable if $t<T_1=2/S(\Omega)$.

As pointed out for the SF model, the signal decay during echo protocols is very sensitive to the dynamics of the noise sources within each pulse sequence. The SPA cannot capture these effects and would yield no decay for the echoes. On the other hand, predictions critically depend on the specific sampling of the stochastic process $E(t')$, making it difficult to obtain reliable estimates. The decay of the echo signal is

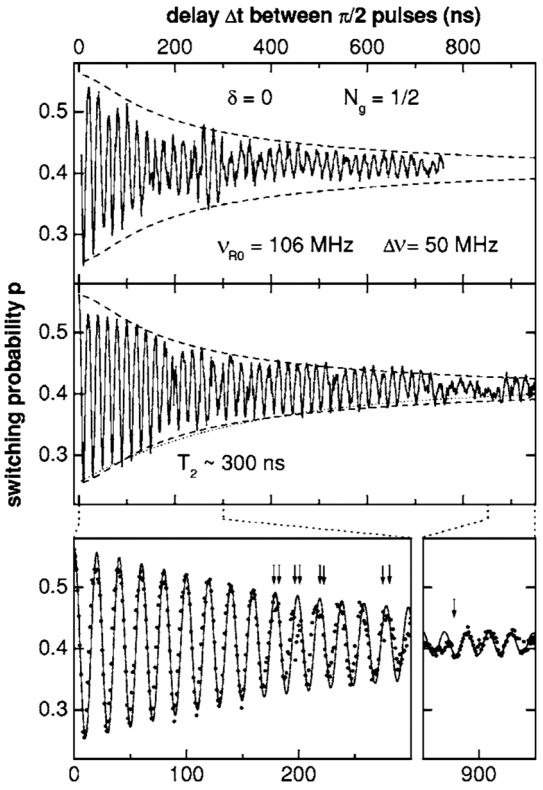

FIG. 39. Ramsey signals at the optimal point for $\omega_{R0}/2\pi = 106$ MHz and $\Delta\nu = 50$ MHz, as a function of the delay Δt between the two $\pi/2$ pulses. Top and middle panels: Solid lines are two successive records showing the partial reproducibility of the experiment. Dashed lines are a fit of the envelope of the oscillations in the middle panel leading to $T_2 = 300$ ns. The dotted line shows for comparison an exponential decay with the same T_2. Bottom panels: Zoom windows of the middle panel. The dots represent the experimental points, whereas the solid line is a fit of the whole oscillation with $\Delta\omega/2\pi = 50.8$ MHz. The arrows point out a few sudden jumps of the phase and amplitude of the oscillation, attributed to strongly coupled charged TLFs. Adapted from Ithier *et al.*, 2005.

often approximated assuming Gaussian quasistatic ($t < 1/\gamma_M$) noise (Ithier *et al.*, 2005).

Several experiments confirmed that the effect of $1/f$ noise in repeated measurement protocols can be described by the above simple theory (Cottet *et al.*, 2001; Martinis *et al.*, 2003; Van Harlingen *et al.*, 2004; Ithier *et al.*, 2005; Chiarello *et al.*, 2012; Sank *et al.*, 2012; Yan *et al.*, 2012). Of course, the dominant $1/f$ noise sources are device and material dependent and the decay of the measured signal depends on the measurement procedure. An accurate estimate and comparison with Gaussian theory of defocusing has been done by Ithier *et al.* (2005) for the quantronium. Clear evidence of an algebraic decay at the optimal point due to quadratic $1/f$ charge noise was reported (see Fig. 39), in agreement with the prediction of Falci *et al.* (2005) (see Fig. 38).

Van Harlingen *et al.* (2004) numerically computed the effects of $1/f$ noise in the critical current in various superconducting qubits incorporating Josephson junctions, showing that the envelope of the coherent oscillations scales as $\exp[-t^2/(2\tau_\phi^2)]$, in qualitative agreement with the adiabatic and longitudinal approximations. Interestingly, the extrapolated decay time τ_ϕ depends both on the elapsed time of the experiment and on the sequence in which the measurements are taken. Two averaging methods were employed: a time-delay averaging (method A) which averages only high-frequency fluctuations at each time-delay point, and a time-sweep averaging (method B) which averages both high- and low-frequency components. Method A gives longer dephasing times than method B, since the number of decades of $1/f$ noise that affect the qubit dynamics in method A is smaller than the number of decades sampled in method B. For a large number of repetitions, τ_ϕ for method B approaches the prediction of Martinis *et al.* (2003) of the effect of critical current $1/f$ noise on a phase qubit in the Gaussian approximation, i.e., Eq. (11) with integration limits 0 and Ω. The dephasing time τ_ϕ is found to scale as $I_0 \equiv \Omega\Lambda S_{I_0}^{1/2}(1\text{ Hz})$, where $S_{I_0}(1\text{ Hz})$ is the spectral density of the critical-current noise at 1 Hz, and $\Lambda = I_0 d\Omega/\Omega dI_0$ is computed for given parameters for each type of qubit that specifies the sensitivity of the level splitting to critical-current fluctuations (Van Harlingen *et al.*, 2004).

Of course, any setup also suffers from noise sources active at frequencies around GHz, which cannot be treated in the adiabatic approximation. In Sec. III.B.1.b we discuss a convenient procedure to deal with the interplay of noise sources responsible for spectral fluctuations in different frequency ranges.

a. $1/f$ noise during ac-driven evolution: Decay of Rabi oscillations

The manipulation of superconducting qubits is often achieved by varying the control parameters in a resonant way at a microwave angular frequency close to the qubit transition frequency Ω. Rabi oscillations are routinely measured in different laboratories (Nakamura, Pashkin, and Tsai, 2001; Martinis *et al.*, 2002; Vion *et al.*, 2002; Yu *et al.*, 2002; Chiorescu *et al.*, 2003). The decohering effect of $1/f$ noise during driven evolution is actually weaker than in the undriven case. The intuitive reason is that the ac field averages the effects of noise (Ithier *et al.*, 2005). This is explained treating the ac-driven noisy system in the adiabatic and longitudinal approximations (Falci *et al.*, 2012).

A qubit acted by an external ac field can be modeled by the Hamiltonian (43) where the control is operated via $\hat{H}_c(t) = \hbar\mathcal{B}\cos(\omega t)\hat{Q}$. The device is nominally biased at q and its low-frequency fluctuations $\delta q(t)$ can be treated in the SPA. The problem is solved in the rotating wave approximation which keeps only control entries "effective" in triggering transitions between different states. This effective part of the control also depends on the random variable δq. The populations in the rotating frame are readily found, e.g., the population of the first excited state is $P_1(t|\delta q) = (\Omega_R/2\Omega_{fl})[1-\cos(\Omega_{fl}t)]$, where the flopping frequency for Rabi oscillations is $\Omega_{fl}(q,\delta q) = \sqrt{\eta^2(q,\delta q) + \Omega_R^2(q,\delta q)}$. Here $\Omega_R(q,\delta q) = \mathcal{B}Q_{10}(q,\delta q)$ is the peak Rabi frequency, Q_{10} being the matrix element of $\hat{Q}$ in the instantaneous eigenbasis of $\hat{H}_0(q+\delta q)$ and the detuning is $\eta(q,\delta q) = \Omega(q,\delta q) - \omega$. Averages are evaluated by expanding Ω_{fl} to second order as in Eq. (84),

$$\Omega_{fl}(q,\delta q) \approx \Omega_{fl}(q,0) + \Omega'_{fl}(\delta q) + \frac{1}{2}\Omega''_{fl}(\delta q)^2 + \cdots, \quad (96)$$

where $\Omega'_{fl} = \partial\Omega_{fl}/\partial q$, $\Omega''_{fl} = \partial^2\Omega_{fl}/\partial q^2$. Assuming a Gaussian distribution of δq with variance σ_q one obtains

$$\langle e^{-i\Omega_{fl}(\delta q)t}\rangle = e^{-i\Omega_{fl}(0)t}e^{-i\Phi(t)},$$
$$e^{-i\Phi(t)} = \frac{1}{\sqrt{1+i\Omega''_{fl}\sigma_q^2 t}}\exp\left[-\frac{(\Omega'_{fl}\sigma_q t)^2}{2(1+i\Omega''_{fl}\sigma_q^2 t)}\right]. \quad (97)$$

Equation (97) describes different regimes for the decay of Rabi oscillations, namely, a Gaussian time decay $|e^{-i\Phi(t)}| \sim e^{-(\Omega'_{fl}\sigma_q t)^2/2}$ when the linear term in the expansion dominates, and power-law behavior $\sim 1/\sigma_q(\Omega''_{fl}t)^{1/2}$ when $\Omega'_{fl} \to 0$. In this regime Eq. (97) describes the initial suppression of the signal. The coefficients of the expansion depend on several parameters such as the amplitude of the control fields and the nominal detuning $\eta_0 = \Omega(q,0) - \omega$. Further information, such as the dependence on q of the energy spectrum and matrix elements $Q_{ij}(q)$, comes from the characterization of the device. The variance can be related to the integrated power spectrum, and can be extracted from FID or Ramsey experiments (Ithier *et al.*, 2005; Chiarello *et al.*, 2012). A similar power law decay of Rabi oscillations has been observed for an electron spin in a QD, due to the interaction with a static nuclear-spin bath in Koppens *et al.* (2007).

Notice that even if Eq. (97) describes the same regimes of the SPA in the undriven case, Eq. (95), here the situation is different. In particular, Eq. (97) quantitatively accounts for the fact that ac driving greatly reduces decoherence compared to undriven systems. In particular, at resonance $\eta_0 = 0$, nonvanishing linear fluctuations of the spectrum $\partial\Omega/\partial q \neq 0$ determine quadratic fluctuations of $\Omega_{fl}(q,\delta q)$ (neglecting fluctuations of Q_{ij}). Thus $\Omega'_{fl} = 0$ and Rabi oscillations undergo power-law decay, whereas in the absence of drive they determine the much stronger Gaussian decay $\sim e^{-(\partial\Omega/\partial q)^2\sigma^2 t^2/2}$ of coherent oscillations. In this regime measurements of Rabi oscillations (Bylander *et al.*, 2011) have been used to probe the environment of a flux qubit. At symmetry points $\partial\Omega/\partial q = 0$, coherent oscillations decay with a power law, whereas Rabi oscillations are almost unaffected by low-frequency noise. For nonvanishing detuning decay laws are equal being system driven or not.

This picture applies to many physical situations, since fluctuations of Q_{ij} are usually small, corresponding to a fraction of $\Omega_R \neq 0$, whereas $\eta(q,\delta q)$ fluctuates on the scale of the Bohr splitting $\Omega \gg \Omega_R$ and may be particularly relevant for $\eta_0 = 0$. The dependence $Q_{ij}(q)$ may have significant consequences in multilevel systems.

Recently, the influence of external driving on the noise spectra of bistable fluctuators was investigated by Constantin, Yu, and Martinis (2009). They proposed an idea that external driving may saturate the fluctuators thus decreasing their contribution to the dephasing. A calculation based on the Bloch-Redfield formalism showed that the saturation of some fluctuators does not lead to a significant decrease in decoherence. Brox, Bergli, and Galperin (2011) took into account the effect of driving on the dynamics of the fluctuators. The main result of this analysis is the prediction that additional low-frequency driving may shift the noise spectrum toward high frequencies. Since the dephasing is influenced mostly by the low-frequency tail of the noise spectrum, this shift decreases decoherence. However, the predicted effect is not very strong.

b. Broadband noise: Multistage approach

In the last part of this section, we warn the reader that when comparing the above predictions with experiments one has to keep in mind that in nanodevices noise is typically broadband and structured. In other words, the noise spectrum extends to several decades, it is nonmonotonic, and sometimes a few resonances are present. We mentioned that typical $1/f$ noise measurements extend from a few Hz to ~100 Hz (Zorin *et al.*, 1996). The intrinsic high-frequency cutoff of $1/f$ noise is hardly detectable. Recently, charge noise up to 10 MHz has been detected in a SET (Kafanov *et al.*, 2008). Flux and critical current noises with $1/f$ spectrum consistent with that in the 0.01–100 Hz range were measured at considerably higher frequencies (0.2–20 MHz) (Bylander *et al.*, 2011; Yan *et al.*, 2012). Incoherent energy exchanges between the system and environment, leading to relaxation and decoherence, occur at typical operating frequencies (about 10 GHz). Indirect measurements of noise spectrum in this frequency range often suggest a white or Ohmic behavior (Astafiev *et al.*, 2004; Ithier *et al.*, 2005). In addition, narrow resonances at selected frequencies (sometimes resonant with the nanodevice-relevant energy scales) have been observed (Cooper *et al.*, 2004; Simmonds *et al.*, 2004; Eroms *et al.*, 2006).

The various noise sources responsible for the above phenomenology have a qualitative different influence on the system evolution. This naturally leads to a classification of the noise sources according to the effects produced rather than to their specific nature. Environments with long-time memory belong to the class of adiabatic noise for which the Born-Oppenheimer approximation is applicable. This part of the noise spectrum can be classified as "adiabatic noise": $1/f$ noise falls in this noise class. High-frequency noise is essentially responsible for spontaneous decay and can be classified as "quantum noise." Finally, resonances in the spectrum unveil the presence of discrete noise sources which severely affect the system performances, in particular, reliability of devices. This is the case when classical impurities are slow enough to induce a visible bistable instability in the system intrinsic frequency. This part of the noise spectrum can be classified as "strongly coupled noise." Each noise class requires a specific approximation scheme, which is not appropriate for other classes. The overall effect results from the interplay of the three classes of noise. In order to deal with broadband and structured noise we resort to a multiscale theory which can be sketched as follows (Falci *et al.*, 2005; Taylor and Lukin, 2006; Paladino *et al.*, 2009).

Suppose we are interested in a reduced description of a n-qubit system, expressed by the reduced density matrix $\rho^n(t)$. It is formally obtained by tracing out environmental degrees of freedom from the total density matrix $W^{Q,A,SC}(t)$, which depends on quantum (Q), adiabatic (A), and strongly coupled (SC) variables. The elimination procedure can be conveniently

performed by separating in the interaction Hamiltonian, which we write analogously to Eq. (43), as $\sum_i \sigma_z^{(i)} \otimes \hat{E}_i$, various noise classes, e.g., by writing

$$\sigma_z^{(i)} \otimes \hat{E}_i = \sigma_z^{(i)} \otimes \hat{E}_i^Q + \sigma_z^{(i)} \otimes \hat{E}_i^A + \sigma_z^{(i)} \otimes \hat{E}_i^{SC}. \quad (98)$$

Adiabatic noise is typically correlated on a time scale much longer than the inverse of the natural frequencies Ω_i, and then application of the Born-Oppenheimer approximation is equivalent to replace $\hat{E}_i^A$ with a classical stochastic field $E_i^A(t)$. This approach is valid when the contribution of adiabatic noise to spontaneous decay is negligible, a necessary condition being $t \ll T_1^A \propto S^A(\Omega)^{-1}$. This condition is usually satisfied at short enough times since $S^A(\omega) \propto 1/\omega$.

This fact suggests a route to trace out different noise classes in the appropriate order. The total density matrix parametrically depends on the specific realization of the slow random drives $\vec{E}(t) \equiv \{E_i^A(t)\}$ and may be written as $W^{Q,A,SC}(t) = W^{Q,SC}[t|\vec{E}(t)]$. The first step is to trace out quantum noise. In the simplest cases this requires solving a master equation. In the second stage, the average over all realizations of the stochastic processes $\vec{E}(t)$ is performed. This leads to a reduced density matrix for the n-qubit system plus the strongly coupled degrees of freedom. These have to be traced out in a final stage by solving the Heisenberg equations of motion, or by approaches suitable to the specific microscopic Hamiltonian or interaction. In particular, this is the case discussed in the initial part of this section, of the spin-fluctuator model at pure dephasing. The ordered multistage elimination procedure can be written as

$$\rho^n(t) = \mathrm{Tr}_{SC}\left\{ \int \mathcal{D}[\vec{E}(t)] P[\vec{E}(t)] \mathrm{Tr}_Q [W^{Q,SC}(t|\vec{E}(t))] \right\}.$$

The multistage approach allows one to make predictions in realistic situations when the outcome of a measurement results from the effects of various noise classes. For instance, we can address the interplay of $1/f$ noise with RT noise produced by one fluctuator which is more strongly coupled with the qubit, having $\gamma_0 \ll 1/t \ll \Omega$, but $b_0 \leq \Omega$. Even if the fluctuator is not resonant with the qubit, it strongly affects the output signal. If $g_0 > 1$, it determines beats in the coherent oscillations and split peaks in spectroscopy, which are signatures of a discrete environment. Because of the mechanism discussed in Sec. III.A.2.a, the additional fluctuator makes the working point of the qubit bistable and amplifies defocusing due to $1/f$ noise. Even if the device is initially optimally polarized, during t_m the fluctuator may switch it to a different working point. The line shape of the signal shows two peaks, split by and differently broadened by the $1/f$ noise in the background. The corresponding time evolution shows damped beats, this phenomenology being entirely due to the non-Gaussian nature of the environment. Figure 40 shows results of a simulation at the optimal point, where $1/f$ noise is adiabatic and weaker than the typical noise level in charge qubits; this picture applies to smaller devices. The fact that even a single impurity on a $1/f$ background causes a substantial suppression of the signal poses the problem of reliability of charge based devices. We remark that the reported beatings do not arise from a resonant coupling between the qubit and the fluctuator. This situation is addressed later in this section.

Finally, we mention that a commonly used simplified version of the multistage approach consists of simply factorizing the effects of different noise classes, in particular, of adiabatic and quantum noise. For some measurement protocols, when the responsible noise classes act on sufficiently different time scales and the spectra are regular around the relevant frequency ranges, this approximation leads to a reasonable prediction of the signal decay (Martinis *et al.*, 2003; Ithier *et al.*, 2005).

2. $1/f$ noise in complex architectures

Realizing the promise of quantum computation requires implementing a universal set of quantum gates, as they provide the building blocks for encoding complex algorithms and operations. To this end, scalable qubit coupling and control schemes capable of realizing gate errors small enough to achieve fault tolerance are required. Fluctuations with $1/f$ spectrum represent a limiting factor also for the controlled generation of entangled states (two-qubit gates) and for the reliable preservation of two- (multi)qubit quantum correlations (entanglement memory). In addition to fluctuations experienced by each single qubit, solid-state coupled qubits,

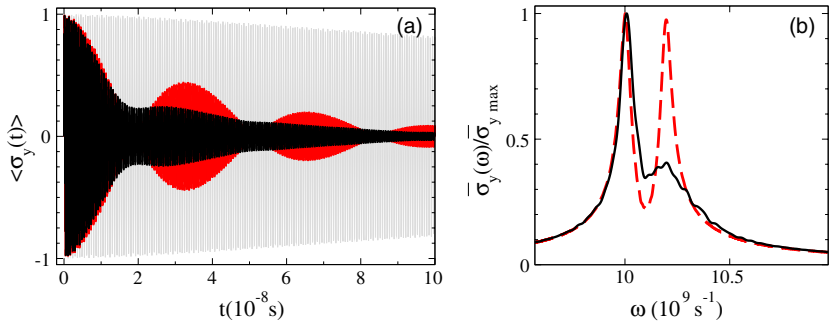

FIG. 40 (color online). (a) $\langle \sigma_y \rangle$ at $\theta = \pi/2$, $\Omega/(2\pi) = 10^{10}$ Hz. The effect of weak adiabatic $1/f$ noise (light gray line) ($\gamma \in 2\pi \times [10^5, 10^9]$ Hz, uniform $2b = 0.002\ \Omega$, $n_d = 250$) is strongly enhanced by adding a single slow ($\gamma/\Omega = 0.005$) more strongly coupled ($2b_0/\Omega = 0.2$) fluctuator (black line), which alone would give rise to beats (dark gray line). (b) When the bistable fluctuator is present the Fourier transform of the signal may show a split-peak structure. Even if peaks are symmetric for the single bistable fluctuator alone (dashed line), $1/f$ noise broadens them in a different way (solid line). Adapted from Falci *et al.*, 2005.

being usually built on chip, may suffer from correlated noise sources acing simultaneously on both subunits. Already in 1996, measurements on SET circuits revealed $1/f$ behavior of voltage power spectra on two transistors and the cross-spectrum power density (Zorin *et al.*, 1996).[6] In Josephson charge qubits, fluctuators in the insulating substrate can influence several qubits fabricated on the same chip, whereas fluctuating traps concentrated inside the oxide layer of the tunnel junctions are expected to act independently on the two qubits, due to screening by the junction electrodes. Background charge fluctuations could also lead to significant gate errors and/or decoherence in semiconductor-based electron *spin qubits* through interqubit exchange coupling (Hu and Das Sarma, 2006).

Recent investigations aimed at identifying operating conditions or control schemes allowing protection from $1/f$ fluctuations in complex architectures. On the one hand, passive protection strategies, such as "optimal tuning" of nanodevices extending the single-qubit optimal point concept (Paladino *et al.*, 2010, 2011; D'Arrigo and Paladino, 2012) and the identification of symmetry protected subspaces (Storcz *et al.*, 2005; Brox, Bergli, and Galperin, 2012), have been proposed. Alternatively, or in combination with passive protection, resonant rf pulses (Rigetti, Blais, and Devoret, 2005) and pulse sequences eventually incorporating spin echoes (Kerman and Oliver, 2008) have been considered as well.

In this section we focus on the first strategies; dynamical decoupling approaches are presented in Sec. III.D. In addition, we review the recent theoretical studies on the impact of $1/f$ noise correlations on the entanglement dynamics of coupled qubits. We refer to the strictly related experimental works, which also provided important indications on the microscopic origin of the observed noise. Rather extensive literature on decoherence of coupled qubits in the presence of correlated *quantum* noise will be omitted, as well as a variety of relevant experimental works demonstrating the feasibility of universal quantum gates and simple quantum algorithms based on superconductor and semiconductor technologies. It is worth mentioning that coupling schemes for superconductor-based qubits have been reviewed by Clarke and Wilhelm (2008); since the first demonstration of quantum oscillations in superconducting charge qubits (Pashkin *et al.*, 2003), several benchmarking results have been reached in different laboratories (Di Carlo *et al.*, 2010; Neeley *et al.*, 2010; Palacios-Laloy *et al.*, 2010; Fedorov *et al.*, 2011; Mariantoni *et al.*, 2011; Lucero *et al.*, 2012; Reed *et al.*, 2012).

The core element of an entangling two-qubit gate can be modeled as

$$\hat{H} = \sum_{\alpha=1,2} \hat{H}^{\alpha}_{\mathrm{tot}}[q_\alpha(t)] + \hat{H}_{\mathrm{coupling}}[\{q_\alpha(t)\}], \tag{99}$$

where for each qubit $\hat{H}^{\alpha}_{\mathrm{tot}}$ is given by Eq. (41), and we indicate that the interaction term $\hat{H}_{\mathrm{coupling}}$ may also depend on the control parameters $\{q_\alpha\}$. Following the same steps as leading to Eq. (42) and considering only classical bias fluctuations one can cast Eq. (99) as $\hat{H} + \delta\hat{H}$, where

$$\hat{H} = \frac{\hbar}{2}\sum_{\alpha} \vec{\Omega}_\alpha(q_\alpha)\cdot\vec{\sigma}^{\alpha} + \hbar\sum_{ij}\nu_{ij}(\{q_\alpha\})\sigma_i^1\sigma_j^2, \tag{100}$$

$$\delta\hat{H} = \hbar\sum_{i}\sum_{\alpha=1,2} E_i^{\alpha}(t)\sigma_i^{\alpha} + \hbar\sum_{i,j} E_{i,j}(t)\sigma_i^1\sigma_j^2, \tag{101}$$

$i,\ j \in \{x,y,z\}$. The stochastic processes $E_i^{\alpha}(t)$ include fluctuations affecting each unit and cross-talk effects due to the coupling element: $E_i^{\alpha}(t) = c_{\alpha i}\delta q_\alpha + d_{\alpha i}\delta q_\beta$ with $c_{\alpha i} \propto \partial\Omega_\alpha/\partial q_\alpha$ and $d_{\alpha i} \propto \nu_{ij}(\{q_\alpha\})$ $(\beta \neq \alpha)$. Fluctuations of the interaction energy $\hbar\nu_{ij}(\{q_\alpha\})$ are included in $E_{i,j}(t) = (\partial\nu_{ij}/\partial q_1)\delta q_1 + (\partial\nu_{ij}/\partial q_2)\delta q_2$. Charge fluctuations affecting the exchange splitting of two electrons in a gate-defined double dot (Hu and Das Sarma, 2006) or background charge-induced fluctuations of the coupling capacitance of charge qubits (Storcz *et al.*, 2005) can be modeled by a term of this form. The stochastic processes δq_α can originate from the same source, from different sources, or a combination. In the case of charge qubits, for instance, random arrangements of background charges in the substrate produce correlated gate-charge fluctuations to an extent depending on their precise location (see Fig. 41), whereas impurities within tunnel junction α are expected to induce only gate charge fluctuations δq_α (Zorin *et al.*, 1996). These correlations are quantified by the intrinsic correlation factor μ, which for stationary and zero average processes with the same variance follows from $\langle\delta q_\alpha(t)\delta q_\beta(t)\rangle = [\delta_{\alpha\beta} + \mu(1-\delta_{\alpha\beta})]\bar{\sigma}^2$. The overall degree of correlation between the processes $E_i^1(t)$ and $E_i^2(t)$ results both from intrinsic correlations and from cross-talk effects. It is expressed by the correlation coefficient μ_c defined, for two generic stochastic processes $X_\alpha(t)$, as

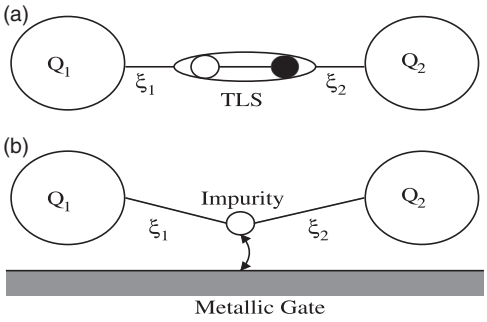

FIG. 41. (a) Two qubits Q_1 and Q_2 coupled to a fluctuator in the substrate between the two qubits, where the charge can tunnel between two sites. (b) The qubits are coupled to a charged impurity through its image charge on the metallic gate; the charge can tunnel between the gate and the impurity. The coupling strengths are given by ξ_1 and ξ_2. The configuration demonstrated in (a) gives origin to *anticorrelated* noise, while (b) gives origin to *correlated* noise. Adapted from Brox, Bergli, and Galperin, 2012.

[6]The cross spectrum of two stochastic processes $X_1(t)$ and $X_2(t)$ is defined as $S_{X_1X_2}(\omega) = (1/\pi)\int_0^\infty dt C_{X_1X_2}(t)\cos\omega t$, where $C_{X_1X_2}(t) = \langle X_1(t)X_2(0)\rangle - \bar{X}_1\bar{X}_2$ and $\bar{X}_\alpha = \langle X_\alpha(t)\rangle$.

$$\mu_c = \frac{\langle [X_1(t) - \bar{X}_1][X_2(t) - \bar{X}_2] \rangle}{\sqrt{\langle [X_1(t) - \bar{X}_1]^2 \rangle \langle [X_2(t) - \bar{X}_2]^2 \rangle}}, \tag{102}$$

where $\langle \cdots \rangle$ denotes the ensemble average and $\bar{X}_\alpha \equiv \langle X_\alpha(t) \rangle$.

The adiabatic approximation scheme introduced in Sec. III.B.1 can easily be extended to complex architectures to investigate the short-time behavior relevant for quantum computing purposes. In this approximation the effect of stochastic processes with $1/f$ spectrum and/or cross spectra on universal two-qubit gates has been studied by D'Arrigo *et al.* (2008), Paladino *et al.* (2009, 2010), Brox, Bergli, and Galperin (2012), and D'Arrigo and Paladino (2012) and entanglement memory element by Bellomo *et al.* (2010). In this case adiabatic noise does not induce the phenomenon of entanglement sudden death, but it may reduce the amount of entanglement initially stored faster than quantum noise for noise figures typical for charge-phase qubits. An extension of the multistage approach to complex architectures was reported by Paladino *et al.* (2011), where the characteristic time scales of entanglement decay in the presence of broadband noise have been derived. Analogously to single-qubit gates, low-frequency noise induces fluctuations of the device eigenenergies resulting in a defocused averaged signal. One way to reduce inhomogeneous broadening effects is to optimally tune multiqubit systems. Paladino *et al.* (2010) proposed a general route to reduce inhomogeneities due to $1/f$ noise by exploiting tunability of nanodevices. The basic idea is very simple: in the adiabatic and longitudinal approximations the system evolution is related to instantaneous eigenfrequencies $\omega_l[\mathbf{E}(t)]$, which depend on the noise realization $\mathbf{E}(t)$. For $\hat{H}$ given by Eq. (100), $\mathbf{E}(t) \equiv \{E_i^\alpha(t), E_{ij}(t)\}$. The leading effect of low-frequency fluctuations in repeated measurements is given within the SPA. The frequencies $\omega_{lm}(\mathbf{E})$ are random variables, with standard deviation $\Sigma_{lm} = \sqrt{\langle \delta\omega_{lm}^2 \rangle - \langle \delta\omega_{lm} \rangle^2}$, where $\delta\omega_{lm} = \omega_{lm}(\mathbf{E}) - \omega_{lm}$. Optimal tuning consists of fixing control parameters to values which minimize the variance Σ_{lm}^2 of the frequencies $\omega_{lm}(\mathbf{E})$. This naturally results in an enhancement of the decay time of the corresponding coherence due to inhomogeneous broadening. The short-time decay of the coherence in the SPA is given by

$$|\langle e^{-i\delta\omega_{lm}(\mathbf{E})t} \rangle| \approx \sqrt{1 - (\Sigma_{lm} t)^2}, \tag{103}$$

resulting in reduced defocusing for minimal variance Σ_{lm}. For a single-qubit gate, the optimal tuning recipe reduces to operating at the optimal point: if $\omega_{lm}(\mathbf{E})$ is monotonic, then $\Sigma_{lm}^2 \approx \sum_\alpha [\partial\omega_{lm}/\partial q_\alpha]^2 \sigma_{q_\alpha}^2$, and the variance attains a minimum for vanishing differential dispersion. When bands are nonmonotonic in the control parameters, minimization of defocusing necessarily requires their tuning to values depending on the noise variances. For a multiqubit gate, the optimal choice may be specific to the relevant coherence for the considered operation. By operating at an optimal coupling, considerable improvement of the efficiency of a $\sqrt{i-\mathrm{SWAP}}$ gate realized via a capacitive coupling of two quantronia has been proved, even in the presence of moderate amplitude charge noise (Paladino *et al.*, 2010, 2011). Optimization against $1/f$ flux and critical current noise of an entangling two-transmon gate has also been demonstrated (D'Arrigo, and Paladino, 2012). Other passive protection strategies are based on the use of a "coupler" element mediating a controllable interaction between qubits. In Kerman and Oliver (2008) a qubit mediates the controllable interaction between data qubits. By Monte Carlo simulation, the feasibility of a set of universal gate operations with $\mathcal{O}(10^{-5})$ error probabilities in the presence of experimentally measured levels of $1/f$ flux noise has been demonstrated.

The effect of correlated or partially correlated low-frequency noise acting on two qubit gates was studied by Storcz *et al.* (2005), Hu *et al.* (2007), D'Arrigo *et al.* (2008), Faoro and Hekking (2010), and Brox, Bergli, and Galperin (2012). Due to the complexity of the Hilbert space of coupled qubits, efforts primarily resulted in numerical surveying of various situations. The natural question to ask is whether correlations between noise sources increase or suppress dephasing of the coupled systems compared to uncorrelated noise. The answer depends on the symmetry of the system-environment interaction, i.e., the existence of decoherence-free subspaces (DFSs), possibly also one dimensional, and the initial system state. Brox, Bergli, and Galperin (2012), introducing a generalized Bloch-sphere method combined with the SPA, derived analytical expressions for the dephasing rates of the two-qubit system as a function of the degree of correlation μ_c. For resonant qubits with a $\sigma_z^1\sigma_z^2$ coupling in the presence of transverse noise, two one-dimensional DFSs are found $|00\rangle - |11\rangle$, which does not decay in the presence of correlated noise, but which is sensitive to anticorrelations (see Fig. 41), and $|00\rangle + |11\rangle$ showing the opposite behavior. In the absence of perfect symmetry (for instance, if qubits are not resonant), the above symmetric states are not eigenstates of the Hamiltonian and as a consequence are also less sensitive to noise correlations. In other words, it is both the symmetry of the initial state and how much this state overlaps with an eigenstate of the Hamiltonian in the absence of noise that determines the decoherence rate. This analysis suggests that, for each setup, the most convenient subspace for two-qubit encoding should be based on preliminary investigation of the nature of noise correlations. For instance, in the absence of correlations, the SWAP subspace generated by $(|01\rangle \pm |10\rangle)/\sqrt{2}$ is more resilient to transverse low-frequency fluctuations with respect to the orthogonal subspace, this fact being ultimately due to the dependence of the corresponding eigenvalues on the deviations δq_α as illustrated in Fig. 42. Note that the SWAP subspace is expected to be also more stable for the single qubit. An analogous conclusion was reached by De *et al.* (2011) for a pair of qubits coupled via the exchange interaction. Hu *et al.* (2007) and D'Arrigo *et al.* (2008) considered a phenomenological model for $1/f$ correlated noise affecting a two-qubit gate in a fixed coupling scheme. The effect of noise correlations on the entanglement generation in the SWAP subspace sensitively depends on the ratio σ/ν_{zz} between the amplitude of the low-frequency noise and the qubits coupling strength (D'Arrigo *et al.*, 2008). For small amplitude noise, correlations increase dephasing zat the relevant short times scales (smaller than the dephasing time). On the other hand, under strong amplitude noise, an

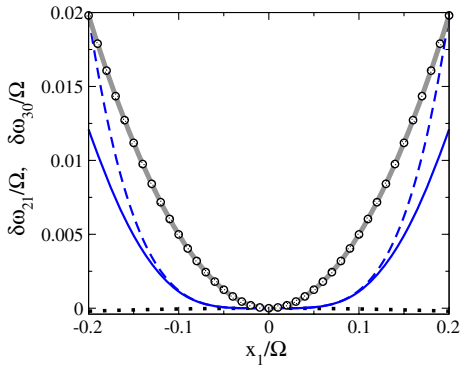

FIG. 42 (color online). Dispersion in the SWAP subspace $\delta\omega_{21}$ (thin continuous and dashed lines) and the orthogonal subspace $\delta\omega_{30}$ (thick gray) as a function of transverse fluctuations on qubit 1 $x_1 \equiv \delta q_1$ ($x_2 \equiv \delta q_2 = 0$) for resonant qubits with $\nu_{zz}/\Omega = 0.01$. The exact splitting (thin continuous) is compared with a second-order expansion (dotted) and the single qubit dispersion (circles). Adapted from Paladino *et al.*, 2010.

increasing degree of correlations between noise sources acting on the two qubits always leads to reduced dephasing. The reason for this behavior originates from the nonmonotonic dependence of the SWAP splitting variance on the correlation coefficient μ_c. A numerical analysis has shown that the above features hold true for adiabatic $1/f$ noise extending up to frequencies 10^9 s^{-1}, which are about 2 orders of magnitude smaller that the qubit Bohr frequencies. At longer times, the entanglement decay time (defined as the time where the signal is reduced by a factor e^{-1}) weakly increases with μ_c (Hu *et al.*, 2007).

Recent experiments on flux qubits quantified $1/f$ flux noise and flux-noise correlations providing relevant indications on its microscopic origin. Yoshihara, Nakamura, and Tsai (2010) studied flux-noise correlations in a system of coupled qubits sharing parts of their loops, whereas Gustavsson *et al.* (2011) used a single, two-loop qubit to investigate flux-noise correlations between different parts within a single qubit. In both experiments the qubit dephasing rate was measured at different bias points. Comparison of the data with the rate prediction in the Gaussian approximation, based on the assumption of $1/f$-type behavior of both spectra and cross spectrum, provided indications of the noise amplitudes and the sign of noise correlations. In the first experiment it was found that flux fluctuations originating from the shared branch lead to correlations in the noise of the two qubits. Gustavsson *et al.* (2011) found flux fluctuations in the two loops to be anticorrelated. Both experiments provided a strong indication that the dominant contribution to the noise comes from *local* fluctuations, in agreement with Martinis *et al.* (2002), Bialczak *et al.* (2007), Koch, DiVincenzo, and Clarke (2007), and Faoro and Ioffe (2008). In particular, in the setup of Gustavsson *et al.* (2011) a global fluctuating magnetic field would have given positive correlations, which were not observed. Results of both experiments are found to be consistent with a model, where flux noise is generated by local magnetic dipoles (randomly oriented unpaired spins) distributed on the metal surfaces. A similar conclusion on the local origin of flux noise was drawn by Lanting *et al.* (2010) from measurements of macroscopic resonant tunneling (MRT) between the lowest energy states of a pair of magnetically coupled rf-SQUID flux qubits. In this experiment, the MRT rate peak widths indicate that each qubit is coupled to a local environment whose fluctuations are uncorrelated with those of the other qubit. Indications of magnetic flux noise of local origin in two phase qubits separated by 500 μm on the same chip were recently reported by Sank *et al.* (2012).

Sendelbach *et al.* (2009) measured the cross spectrum of inductance and flux fluctuations in a dc SQUID. In this experiment, the imaginary part of the SQUID inductance and the quasistatic flux threading the SQUID loop were monitored simultaneously as a function of time. From the two time series, the normalized cross spectral density was computed. The inductance and flux fluctuations were found to be highly correlated at low temperature, indicating a common underlying physical mechanism. The high degree of correlation provided evidence for a small number of dominant fluctuators. The data were interpreted in terms of the reconfiguration of clusters of surface spins, with correlated fluctuations of effective magnetic moments and relaxation times. The observed specific correlation between low-frequency flux noise and inductance fluctuation suggests that the flux noise is related to the nonequilibrium dynamics of the spin system, possibly described by spin glass models (Chen and Yu, 2010) or fractal spin clusters, which appear naturally in a random system of spins with wide distribution of spin-spin interactions (Kechedzhi, Faoro, and Ioffe, 2011).

C. Quantum coherent impurities

The model of two-level tunneling systems formulated by Anderson, Halperin, and Varma (1972) and Phillips (1972), illustrated in Sec. II, has been extensively tested experimentally by ensemble measurements performed on samples having a large TLS density, such as structural glasses. Results reported in this section demonstrated that ensembles of TLSs, sparsely present in the disordered oxide barrier of Josephson junctions or in the insulating substrates, induce fluctuations with a $1/f$ spectrum which are a major source of decoherence in superconducting nanocircuits. However, the effects unambiguously proving quantum mechanical behavior of an individual fluctuator interacting with a qubit were not observed. Only recently highly sensitive superconducting circuits could be used as "microscopes" for probing spectral, spatial, and coupling properties of selected TLSs. Understanding the origin of these spurious TLSs, their coherent quantum behavior, and their connection to $1/f$ noise is important for any low-temperature application of Josephson junctions and it is a challenge, which is crucial to the future of superconducting quantum devices.

The first observations indicative of a considerable interaction of a superconducting circuit with a strongly anharmonic quantum system were reported on a large-area Josephson junction (≈ 10 μm^2) phase qubit at NIST Boulder Laboratories (Cooper *et al.*, 2004; Simmonds *et al.*, 2004). Microwave spectroscopy revealed the presence of small unintended avoided crossings in the transition spectrum suggestive of the interaction between the device and individual coherent TLSs resonantly coupled with the qubit. In these experiments, a

small number of spurious resonators with a distribution of splitting size, the largest being ∼25 MHz and an approximate density of one major TLS per ∼60 MHz, were observed. Magnitude and frequency of the TLS considerably changed after thermal cycling to room temperature, whereas cycling to 4 K produced no apparent effect. Moreover, different qubits in the same experimental setup displayed their own unique "fingerprint" of TLS frequencies and splitting strengths. Qubit Rabi oscillations driven resonantly with a TLS showed considerably reduced visibility with respect to off-resonant driving. It has been observed that similar spectroscopic observations may also result from macroscopic resonant tunneling in the extremely asymmetric double-well potential of phase qubits (Johnson *et al.*, 2005). The TLS and MRT mechanisms could be distinguished measuring the low-frequency voltage noise in a Josephson junction in the dissipative (running phase) regime (Martin, Bulaevskii, and Shnirman, 2005).

Since these first experiments, similar avoided crossings in spectroscopy have been observed in different superconducting circuits. In phase qubits they were reported by Martinis *et al.* (2005), Neeley *et al.* (2008), Hoskinson *et al.* (2009), Bushev *et al.* (2010), Lisenfeld *et al.* (2010a, 2010b), Palomaki *et al.* (2010), and Shalibo *et al.* (2010); in flux qubits by Plourde *et al.* (2005), Deppe *et al.* (2008), and Lupaşcu *et al.* (2009); in a Cooper-pair box (ultrasmall Josephson junction with nominal area 120×120 nm^2) by Kim *et al.* (2008); in the quantronium by Ithier *et al.* (2005), and in the transmon by Schreier *et al.* (2008).

The close analogies among these observations, despite the differences in the qubit setups, junction size, and materials, confirm that microscopic degrees of freedom located in the tunnel barrier of Josephson junctions, usually made of a 2- to 3-nm-thick layer of disordered oxide (usually AlO_x, $x \approx 1$), are at least one common cause of these effects. These microscopic degrees of freedom are strongly anharmonic systems and observations are fully consistent with coherent TLS behavior. Further confirmation comes from multiphoton spectroscopy in phase (Bushev *et al.*, 2010; Lisenfeld *et al.*, 2010b; Palomaki *et al.*, 2010; Sun *et al.*, 2010) and flux qubits (Lupaşcu *et al.*, 2009), where the hybridized states of the combined qubit-TLS systems have been probed under strong microwave driving. For instance, an additional spectroscopic line in the middle of the qubit-TLS anticrossing corresponding to a two-photon transition between the ground state and the two excitations state of the qubit-TLS system has been observed by Lupaşcu *et al.* (2009), Bushev *et al.* (2010), and Sun *et al.* (2010). Moreover, in some of these experiments, spontaneous changes of the resonator's frequency were observed. The instability was observed during many hours while the device was cold (Simmonds *et al.*, 2004), whereas Lupaşcu *et al.* (2009) observed the instability in some samples during a few tens of minutes data acquisition time. Other samples were instead stable over the few months duration of the experiment. The instability supports the idea that the coupled TLSs are of microscopic origin. The qualitative trend is that small-area qubits show fewer splittings than do large-area qubits, although larger splittings are observed in the smaller junctions (Martinis *et al.*, 2005).

Time-resolved experiments on phase qubits demonstrated that an individual TLS can be manipulated using the qubit as a tool to both fully control and read out its state. The trajectory (i.e., time record) of the switching current of a phase qubit revealed "quantum jumps" between macroscopic quantum states of the qubit coupled to a TLS in the Josephson tunnel junction, thus providing a way to detect the TLS state (Yu *et al.*, 2008). Through the effective, qubit mediated, coupling between the TLS and an externally applied resonant electromagnetic field "direct" control of the quantum state of individual TLSs was demonstrated by Lisenfeld *et al.* (2010a). In this experiment the qubit always remained detuned during TLS operations, merely acting as a detector to measure its resulting state. A characterization of the TLS coherence properties was possible via detection of TLS Rabi oscillations, relaxation dynamics, Ramsey fringes, and spin echo. Measurements at different temperatures showed stable TLS resonance frequencies and qubit's coupling strengths. The energy relaxation time is found to decrease quadratically with temperature, whereas the TLSs dephasing times had a different behavior, only one of the measured TLSs being close to $2T_1$. Shalibo *et al.* (2010) measured relaxation and dephasing times of a large ensemble of TLSs in a small-area ($\sim 1\ \mu$m^2) phase qubit (82 different TLSs obtained from 8 different cooling cycles of the same sample). Decay times ranged almost 3 orders of magnitude, from 12 to more than 6000 ns, whereas coherence times varied between 30 and 150 ns. The average T_1 followed a power-law dependence on the qubit-TLS coupling strength, whereas the average dephasing time was maximal for intermediate coupling. They suggested that both time scales naturally result from TLSs dipole phonon radiation and anticorrelated dependence of the TLS tunneling amplitude and bias energy on low-frequency environmental fluctuations. Nonmonotonous dependences of the qubit's decay time on the qubit-TLS coupling and temperature were also predicted by Paladino *et al.* (2008) for a qubit longitudinally coupled to a coherent TLS. In general, different experiments showed that some TLSs exhibit coherence times much longer than those of the superconducting qubits (Neeley *et al.*, 2008; Lisenfeld *et al.*, 2010a; Palomaki *et al.*, 2010).[7] This remarkable fact, together with the ability to directly control selected TLSs, shed new light on these microscopic systems. Indeed, it was proposed that TLSs in the barrier of a Josephson junction can themselves act as naturally formed qubits (Zagoskin *et al.*, 2006; Tian and Jacobs, 2009). Neeley *et al.* (2008) demonstrated the first quantum memory operation on a TLS in a phase qubit. An arbitrary quantum state was transferred to a TLS, stored there for some time and then retrieved. Sun *et al.* (2010) demonstrated creation and coherent manipulation of quantum states of a tripartite system formed by a phase qubit coupled to two TLSs. In this experiment, the avoided crossing due to the qubit-TLS interaction acted as a tunable quantum beam splitter of wave functions, which was

[7]TLSs' decay times following from Ramsey fringes are of the order of a few hundred nanoseconds, and maximal relaxation times are about 1 μs.

used to precisely control the quantum states of the system and demonstrate a Landau-Zener-Stückelberg interference. Although TLSs were suitable for these initial proof-of-principle demonstrations, their use in a quantum computer still seems unlikely because of their intrinsically random nature and limited coherence times. A relevant step further in this direction was done recently by Grabovskij *et al.* (2012) who reported an experiment in which the energy of coherent TLSs coupled resonantly to a phase qubit is tuned. When varying a static strain field *in situ* and performing microwave spectroscopy of the junction, they observed continuously changing energies of individual coherent TLSs. Moreover, results obtained over 41 individual TLS between 11 and 13.5 GHz are explained readily by the tunneling model and, therefore, provide firm evidence of the hypothesis that atomic TLSs are the cause of avoided level crossings in the spectra of Josephson junction qubits. Mechanical strain offers a handle to control the properties of coherent TLSs, which is crucial for gaining knowledge about their physical nature.

Alternative theoretical models of TLSs were proposed to explain the avoided level crossings observed in qubit spectroscopy data in phase and flux qubits. It was suggested that the state of the TLS modulates the transparency of the junction and therefore its critical current I_c (Simmonds *et al.*, 2004; Ku and Yu, 2005; Faoro and Ioffe, 2006; Constantin and Yu, 2007). In this case two-level defects could be formed by Andreev bound states (Faoro *et al.*, 2005; de Sousa *et al.*, 2009) or Kondo impurities (Faoro and Ioffe, 2007; Faoro, Kitaev, and Ioffe, 2008). Alternatively the TLS may couple to the electric field inside the junction, which is consistent with the TLS carrying a dipole moment located in the aluminum oxide tunnel barriers (Martin, Bulaevskii, and Shnirman, 2005; Martinis *et al.*, 2005). Recently Agarwal *et al.* (2013) analyzed the interaction with phonons of individual electrons tunneling between two local minima of the potential well structure due to the electron Coulomb interaction with the nearest atoms in the insulator. They concluded that the resulting strong polaronic effects dramatically change the TLS properties providing quantitative understanding of the TLS relaxation and dephasing observed in Josephson junctions. In particular, the strain effects observed by Grabovskij *et al.* (2012) are quantitatively interpreted.

Finally, a TLS may modulate the magnetic flux threading the superconducting loop (Sendelbach *et al.*, 2008; Bluhm *et al.*, 2009). Cole *et al.* (2010) performed a direct comparison between these models and high precision spectroscopy data on a phase qubit. Experimental data indicate a small or nonexistent longitudinal qubit-TLS coupling relative to the transverse term. In phase and flux qubits fluctuations of the critical current or magnetic flux generate both transverse and longitudinal components, whereas the coupling to the electric field within the junction is purely transverse. Although longitudinal coupling cannot be ruled out, no evident signatures of this coupling were observed in most of the experiments which have been consistently explained considering purely transverse dipolar interaction (Lupaşcu *et al.*, 2009; Bushev *et al.*, 2010; Lisenfeld *et al.*, 2010b). Other multilevel spectroscopy experiments did not uniquely pin down the coupling mechanism as well. Similar features observed in phase qubits and the flux qubit experiment (Lupaşcu *et al.*, 2009) suggested that strongly coupled TLS have the same origin in flux and phase qubits, even though the degrees of freedom manipulated are different. A charge coupling model is also supported by spectroscopic observations in a Cooper-pair box (Kim *et al.*, 2008). A distribution of avoided splitting sizes consistent with the qubit coupling to charged ions tunneling between random locations in the tunnel junction oxide and not directly interacting with each other was reported by Palomaki *et al.* (2010). Tian and Simmonds (2007) proposed a possible way to resolve the underlying coupling mechanism of TLSs to phase qubits through the use of a magnetic field applied along the plane of the tunnel barrier inside the junction. More generally, one or two noninteracting qubits can be conveniently used as a probe of a coherent environment (Paladino *et al.*, 2008; Oxtoby *et al.*, 2009; Jeske *et al.*, 2012).

The controllable interaction between a qubit and a microscopic coherent TLS also led to a number of interesting features in the qubit time evolution. One aspect is the reduced visibility of qubit Rabi oscillations driven resonantly with a TLS first observed by Simmonds *et al.* (2004). This problem was investigated using different approaches and under various driving conditions and TLS decoherence mechanisms by Galperin *et al.* (2005), Ku and Yu (2005), Meier and Loss (2005), Ashhab, Johansson, and Nori (2006), and Sun *et al.* (2010). The main conclusion of Meier and Loss (2005) was that fluctuators are the dominant source of visibility reduction at Rabi frequencies small compared to the qubit-TLS coupling strength, while leakage out of the qubit computational subspace becomes increasingly important for large Rabi frequencies of experiments with phase qubits. Galperin *et al.* (2005) investigated the quantum dynamics of the four-level system subject to an arbitrarily strong driving ac field, including both phase and energy relaxation of the TLS in a phenomenological way. It was demonstrated that if the fluctuator is close to resonance with the qubit, the Rabi oscillations of the qubit are suppressed at short times and demonstrate beatings when damping is weak enough. In addition, it was pointed out that if the readout signal depends on the state of the fluctuator, the visibility of the Rabi oscillations can be substantially reduced, a possible scenario in Simmonds *et al.* (2004). Depending on the relative strength of the resonant ac driving and the qubit-TLS coupling, additional features in the qubit dynamics have been predicted as anomalous Rabi oscillations and two-photon processes involving transitions between the four-level states of the coupled qubit TLS (Ashhab, Johansson, and Nori, 2006; Sun *et al.*, 2010). Some of these effects were observed in the experiments mentioned.

The role of coherent TLSs on qubit relaxation processes was investigated by Mueller, Shnirman, and Makhlin (2009). There a qubit is considered as interacting with coherent TLSs each subject to relaxation and pure dephasing processes (in the underdamped regime) and in resonance or close to resonance with the qubit. Depending on the distribution of the TLSs energies (uniform or with strong local fluctuations), the qubit T_1 can either be a regular function of the qubit splitting or display an irregular behavior. They suggested that this mechanism can explain the smooth T_1-versus-energy curve

in large-area junction phase qubits (Cooper *et al.*, 2004; Simmonds *et al.*, 2004; Neeley *et al.*, 2008) and the seemingly random dependence reported in smaller-area phase qubits and flux or charge qubits (Astafiev *et al.*, 2004; Ithier *et al.*, 2005). It is also speculated that the large splittings observed in spectroscopy of the same phase qubits may result from many weakly coupled spectrally dense TLSs.

A characterization of the effects of bistable coherent impurities in superconducting qubits was proposed by Paladino *et al.* (2008). Introducing an effective impurity description in terms of a tunable spin-boson environment, the qubit dynamics has been investigated for a longitudinal qubit-TLS interaction. The asymptotic time limit is ruled by a dominant rate which depends nonmonotonically on the qubit-TLS coupling strength and reflects the TLS dissipative processes and temperature. At intermediate times relevant for quantum computing, different rates and frequencies enter the qubit dynamics displaying clear signatures of non-Gaussian behavior of the quantum impurity.

Finally, the possibility of highlighting the coherent interaction between a superconducting circuit and a microscopic quantum TLS, in principle, allows one to investigate the important question of the applicability domain of the classical RTN model. Wold *et al.* (2012) investigated the decoherence of a qubit coupled to either a TLS again coupled to an environment or a classical fluctuator modeled by RTN. A model for the quantum TLS is introduced where the temperature of its environment and the decoherence rate can be adjusted independently. The model has a well-defined classical limit at any temperature and this corresponds to the appropriate asymmetric RT process. The difference in the qubit decoherence rates predicted by the two models is found to depend on the ratio between the qubit-TLS coupling and the decoherence rate in the pointer basis of the TLS. This is then the relevant parameter which determines whether the TLS has to be treated quantum mechanically or can be replaced by a classical RT process. This result also validates the application of the RT process model for the study of decoherence in qubits when the coupling between the qubit and the fluctuator is strong as long as the fluctuator couples even more strongly to its own environment.

D. Dynamical decoupling and $1/f$ noise spectroscopy

1. Noise protection and dynamical decoupling

In the last few years several strategies for coherence protection have been developed, both for quantum information processing and in the broader perspective of quantum control. An optimal bias point discussed earlier is a passive stabilization (or error avoiding) code very successful in solid-state nanodevices. Dynamical decoupling (DD) relying on repeated application of pulsed or switched control is an active stabilization (i.e., error correcting) scheme developed in the field of high-resolution NMR (Becker, 2000). DD has been proposed as a method to extend decoherence times in solid-state quantum hardware and has been recently applied to decouple spin baths in semiconductor-based qubits (Barthel *et al.*, 2010; de Lange *et al.*, 2010; Ryan, Hodges, and Cory, 2010; Bluhm *et al.*, 2011) and $1/f$ noise in superconducting nanocircuits (Bylander *et al.*, 2011; Gustavsson *et al.*, 2012).

Coherent averaging of unwanted couplings is at the heart of DD. The principle is illustrated by the spin echo which is operated by a single π pulse inducing a spin-flip transition. Shining a pulse X_π (evolution operator $U = \sigma_x$) at half of the evolution time t, say $\{t/2, X_\pi, t/2\}$, dynamically suppresses terms $\propto \sigma_y, \sigma_z$ in the qubit Hamiltonian. In NMR samples unwanted terms $H_1 \propto \delta B \sigma_z$ are due to static randomly distributed local fields. The Bloch vector dynamics for the ensemble of spins is defocused resulting in inhomogeneous broadening. The Hahn echo $\{X_{\pi/2}, t/2, X_\pi, t/2, X_{\pi/2}\}$ is routinely used to achieve efficient refocusing (Becker, 2000). Echoes also switch off "dynamically" two-qubit J couplings of the nuclear spin Hamiltonian in liquid NMR quantum computers (Vandersypen and Chuang, 2005).

2. Pulsed control

Coupling to a stochastic field $E(t)$ induces diffusion in the free spin precession and decoherence, which mitigates Hahn echoes. Carr and Purcell (1954) (CP) recognized that sequences of π pulses may suppress spin diffusion since they coherently average out $E(t)$ (see Fig. 43). Composite pulses are also used in NMR to stabilize a given quantum gate against errors in the control (Becker, 2000; Vandersypen and Chuang,

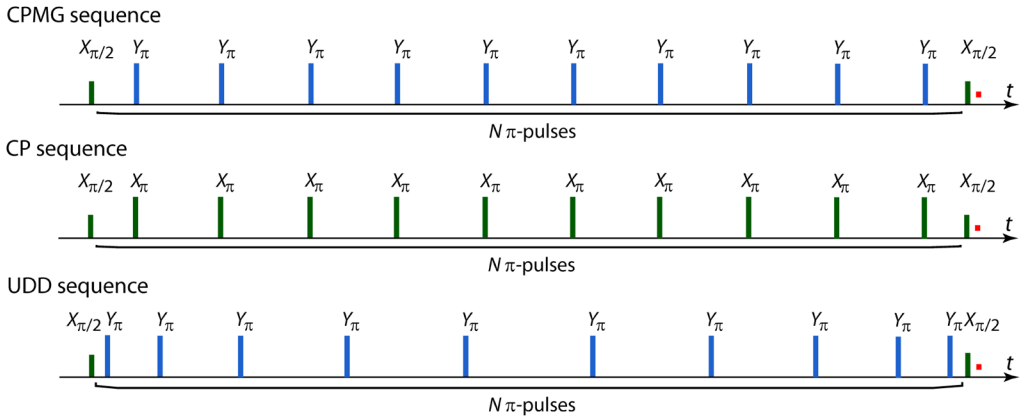

FIG. 43 (color online). Timing of the Carr-Purcell-Meilboom-Gill (CPMG), CP, and Uhrig DD (UDD) pulse sequences for $N = 10$. Adapted from Bylander *et al.*, 2011.

2005). NMR pulse sequences beyond Hahn echo have been employed in a superconducting qubit to demonstrate both gate stabilization (Collin *et al.*, 2004) and dynamical reduction of decoherence due to $1/f$ noise (Ithier *et al.*, 2005).

From echo to DD: DD may selectively remove a noisy environment with a finite correlation time τ_c. Control is operated via a time-dependent $\hat{H}_c(t)$ describing a sequence of π pulses. We consider hard X_π pulses, whose duration is very short $t_p \to 0$, at times t_j $(j = 1, \ldots, N)$. The time-evolution operator reads

$$U_N(t,0) = \sigma_x U(t, t_{N-1})\sigma_x \cdots U(t_2, t_1)\sigma_x U(t_1, 0), \quad (104)$$

where $U(t,t')$ describes the noisy free evolutions between pulses. Notice that pulses in $\sigma_x U(t_{n-1}, t_n)\sigma_x$ reverse the sign of operators $\sigma_{y,z}$ appearing in U. Therefore such "orthogonal" components flip in sequential steps of the protocol. It is convenient to use the language of average Hamiltonian theory (Vandersypen and Chuang, 2005) and introduce the effective Hamiltonian $H_N(t)$, defined as $e^{iH_N(t)t/\hbar} := U_N(t,0)$. Then a periodic train of pulses $t_{j+1} - t_j = \Delta t = t/N$, implementing a sequence named periodic DD (PDD), with elementary block $\{\Delta t, X_\pi, \Delta t, X_\pi\}$, tends to average out orthogonal spin components (provided N is even) (Viola, Knill, and Lloyd, 1999). This emerges from the perturbative (Magnus) expansion (Vandersypen and Chuang, 2005) of H_N, which washes these terms out in the limit of continuous flipping $\Delta t \to 0$. In the simple case of a qubit coupled to pure dephasing classical noise $H = (\hbar/2)[\Omega + E(t)]\sigma_z + \hat{H}_c(t)$, calculations can be carried out exactly (Biercuk, Doherty, and Uys, 2011). Coherences decay as

$$\rho_{01}(t) = \rho_{01}(0)\langle e^{-i\Phi_N(t)}\rangle = \rho_{01}(0)e^{-\Gamma_N(t) - i\Sigma_N(t)}, \quad (105)$$

where the phase $\Phi_N(t) = \int_0^t ds y_N(s)E(s)$ is obtained by sampling a realization of noise with the piecewise constant $y_N(t)$ whose discontinuities reflect the effect of pulses at t_i. The *decay function* $\Gamma_N(t)$ obtained by noise averaging depends on the pulse sequence. For Gaussian noise with power spectrum $S(\omega)$ the averaging yields

$$\Gamma_N(t) = \int \frac{d\omega}{\omega^2} S(\omega) F_N(\omega t), \quad (106)$$

where the *filter function* $F_N(\omega t) = |y_N(\omega t)|^2$ has been defined as (Uhrig, 2007)

$$F_N(\omega t) = \left| 1 + (-1)^{N+1} e^{i\omega t} + 2\sum_{j=1}^{N} (-1)^j e^{i\omega t_j} \right|^2.$$

In the absence of pulses the function $F_0(\omega) = 4\sin^2(\omega t/2)$ reproduces the decay in a FID protocol, whereas in the presence of pulses it yields diffraction patterns induced by interference in the time domain (Ajoy, Álvarez, and Suter, 2011) and, in particular, to coherent suppression of F_N at low frequencies. As a consequence, $\Gamma_N(t)$ decreases and the signal decay due to decoherence is effectively recovered.

Viola and Lloyd (1998) applied such techniques to selectively decouple a pure dephasing quantum environment, obtained by letting $\frac{1}{2}\sigma_z E(t) \to \frac{1}{2}\sigma_z \hat{E} + \hat{H}_R$, where $\hat{H}_R$ describes the environment alone. The structure of Eq. (105) is still valid, $\Gamma_N(t)$ depending only on the dynamics ruled by $\hat{H}_R$. In particular, Viola and Lloyd (1998) studied an environment of linearly coupled quantum oscillators $\hat{E} = \sum_\alpha g_\alpha (a_\alpha^\dagger + a_\alpha)$. They found that Eq. (106) holds true, $S(\omega)$ being related to the symmetrized correlation function of $\hat{E}$, uniquely expressed via the spectral density $J(\omega) = \sum_\alpha g_\alpha^2 \delta(\omega - \omega_\alpha)$, namely,

$$S(\omega) = \frac{1}{2}\langle \hat{E}(t)\hat{E}(0) + \hat{E}(0)\hat{E}(t)\rangle_\omega = \coth\left(\frac{\hbar\omega}{2k_B T}\right) J(\omega).$$

The ultraviolet (UV) cutoff ω_c of $J(\omega)$, sets the time scale of fastest response of the environment. As for classical noise, decoherence is washed out completely for $\Delta t \to 0$ and greatly suppressed for $\omega_c \Delta t \sim 1$.

In general, open loop schemes with a finite set of pulsed fields allow one to perform fault-tolerant control (Viola, Knill, and Lloyd, 1999), i.e., to design the dynamics of a quantum system to attain a given objective. The simplest goal is the effective decoupling of the environment. With respect to other active stabilization strategies, as quantum error correction or closed loop (quantum feedback) schemes, DD has the advantage that only unitary control of a small and well characterized system is needed and it does not require additional measurement resources. Relying on coherent averaging, DD can suppress errors regardless of their amplitude. In the last few years optimization of pulse sequences (Biercuk, Doherty, and Uys, 2011) has been an active subject of investigation allowing substantial improvement when dealing with real open quantum systems.

Optimized sequences and robust DD: Performances of sequences strongly depend on their details such as the parity of the number of pulses or their symmetrization. For instance, in odd-N PDD the noise during the final Δt remains uncompensated. Proper symmetrization of the sequences, such as CP sequence (see Fig. 43), may lead to higher order cancellations in $H_N(t)$. Meiboom and Gill (1958) proposed a refinement (CPMG sequence), which is usually very efficient against spin diffusion (Becker, 2000), since it also averages errors due to control field inhomogeneities. Indeed, if pulses are implemented by resonant ac fields, the component producing spin-flip fluctuates in amplitude due to the same noise responsible for the spin diffusion. For a given initial state of the Bloch vector, CP accumulates errors in X_π at second order, while in CPMG Y_π errors appear at fourth order (Borneman, Huerlimann, and Cory, 2010).

Recently Uhrig (2007) found that nonequidistant pulses improve performances in a pure-dephasing spin-boson environment. In the Uhrig DD (UDD) sequence $t_j/t = \sin^2[\pi j/(2N+2)]$ times are such that the first N derivatives of the filter function vanish, $[d^j F_N/dz^j]_{z=0} = 0$, $j \in \{1, 2, \ldots, N\}$. This ensures that pure dephasing is suppressed to $O(t^N)$ in the series expansion of $E(t)$. Lee, Witzel, and Das Sarma (2008) conjectured that UDD is universal for the generic pure dephasing model, and Yang and Liu (2008) proved that generalized UDD suppresses both pure dephasing

and relaxation to $O(t^N)$. In the spirit of UDD, several new pulse sequences were introduced in the last few years, achieving optimization for a given sequence duration (Biercuk *et al.*, 2009), or being nearly optimal for generic single-qubit decoherence (West, Fong, and Lidar, 2010) or for specific environments (Pasini and Uhrig, 2010).

Concatenated DD (CDD) proposed by Khodjasteh and Lidar (2005) is an alternative scheme based on the idea of recursively defined sequences, which guarantee to reduce decoherence below a pulse noise level. Within this framework high fidelity quantum gates have been demonstrated numerically (West *et al.*, 2010).

The quest for robust DD arises from the general problem of the tradeoff between the control resources involved and efficient suppression of decoherence. Ideal DD requires available couplings allowing the synthesis of controlled evolution (Viola, Knill, and Lloyd, 1999), large pulse repetition rate, and pulse hardness. Optimization can be used together with realistic bounded amplitude control or continuous always-on field schemes (Viola and Knill, 2003; Khodjasteh, Erdélyi, and Viola, 2011; Jones, Ladd, and Fong, 2012) to allow a flexible use of resources needed to attain a given decoupling error $\Gamma_N(t)$.

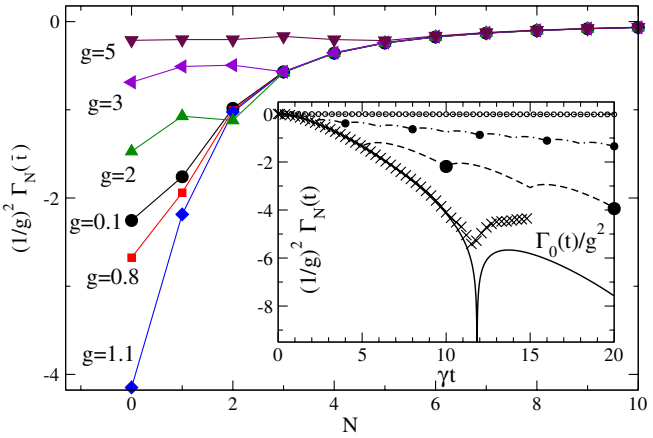

FIG. 44 (color online). Scaled decay rate of the qubit coherence $\Gamma_N(t)/g^2$ at fixed $t = 10\gamma^{-1}$ and DD (here N enumerates an echo pair of pulses). $N = 0$ corresponds to FID. A Gaussian environment with the same power spectrum would give, for arbitrary g, the curve labeled with $g = 0.1$, since $\Gamma_N(t) \propto g^2$. Inset: $\Gamma_N(t)$ for $g = 1.1$ for different intervals between pulses Δt (lines with dots, $\Delta t = 5, 2, 0.2$) are compared with the FID $\Gamma_0(t)$ (thick line) and with results obtained by numerical solution of the stochastic Schrödinger equation. Adapted from Falci *et al.*, 2004.

3. DD of $1/f$ noise

DD has a large potential impact in solid-state coherent nanosystems where noise has large low-frequency components. Indeed, DD of Gaussian $1/f$ noise does not always require ultrafast pulse rates (Shiokawa and Lidar, 2004). However, sources responsible for $1/f$ noise are often discrete producing non-Gaussian noise. For a proper treatment Eq. (106) must be generalized accordingly. Initially addressed for understanding charge noise in superconducting qubits (Falci *et al.*, 2004; Faoro and Viola, 2004), DD in non-Gaussian environments is important in other implementations since, independently of the microscopic origin, critical current noise and flux noise may also be described as due to a collection of discrete sources, and also resulting in a $1/f^\alpha$ spectrum. Recently this topic attracted large interest for solid-state quantum hardware based on electron and nuclear spins (Witzel and Das Sarma, 2007a; 2007b; Lee, Witzel, and Das Sarma, 2008). Besides determining the decay of coherences, non-Gaussian noises are responsible for additional structure (splitting of spectroscopic peaks and beats) observable in the qubit dynamics. This deteriorates the fidelity and must be washed out by stabilization.

a. RT noise and quantum impurities

The simplest physical non-Gaussian environment is a single impurity coupled to the qubit. Models of quantum impurities were studied by Falci *et al.* (2004), Lutchyn *et al.* (2008), and Rebentrost *et al.* (2009), whereas the classical counterpart was addressed by Faoro and Viola (2004), Gutmann *et al.* (2005), Bergli and Faoro (2007), and Cheng, Wang, and Joynt (2008). Falci *et al.* (2004) modeled the environment by an electron tunneling with switching rate γ from an impurity level to an electronic band (Paladino *et al.*, 2002). The parameter quantifying Gaussianity is $g = (\Omega_+ - \Omega_-)/\gamma$ (Sec. III.A.2). The problem is tackled by studying the reduced dynamics of the qubit-plus-impurity system (QI) for arbitrary qubit bias. The band acts as a Markovian environment for the QI reduced dynamics (Paladino, Faoro, D'Arrigo, and Falci, 2003) and can be treated exactly by a master equation. The key point is that DD has no effect on a Markovian environment. Thus the quantum map in the presence of a number N of pulses can be written as $\rho_{\rm QI}(t) = \mathcal{E}_N[\rho_{\rm QI}(0)] = \{\mathcal{P}\,\exp[\mathcal{L}\Delta t]\}^N\rho_{\rm QI}(0)$. Here the superoperators $\mathcal{L}$ and $\mathcal{P}$ describe, respectively, the QI reduced dynamics and X_π pulses on the qubit $\mathbb{1}_I \otimes \sigma_x$. The reduced qubit dynamics is obtained by tracing out the impurity $\rho_Q(t) = \mathrm{Tr}_I[\rho_{\rm QI}(t)]$ at the end of the whole protocol. In this way non-Gaussianity and non-Markovianity of the impurity are exactly accounted for. At pure dephasing ($\Omega_x = 0$) a simple analytic form can be found. The different physics due to a weakly ($g < 1$) or strongly coupled $g > 1$ impurity is discussed in Sec. III.A.1.a. This difference is washed out for large flipping rates ($N \gg \gamma t$), where the environment becomes effectively Gaussian with universal behavior $\Gamma_N(t) \sim g^2$ (see Fig. 44). On the other hand, for $N < \gamma t$ a crossover is clearly observed between different domains of g. Notice that in the intermediate regime $N \lesssim \gamma t$ DD is still able to cancel fast noise $g < 1$ and all features of the qubit dynamics appearing when $g \sim 1$. Qualitatively similar behavior is found also for $\Omega_x \neq 0$, where the solution requires the diagonalization of $\mathcal{E}_N$. The new feature in this regime is that DD of slow fluctuators $g > 1$ may be nonmonotonic with the flipping rate, yielding for $N < \gamma t$ decoherence acceleration which is reminiscent of the anti-Zeno effect.

Notice that this model reduces to a classical RT fluctuator if mutual QI backaction, described by frequency shifts, is dropped out. Numerical simulations in this limit by Gutmann *et al.* (2005) confirmed that decoherence is suppressed for large pulse rates $N \gg \gamma t$; Gutmann *et al.* (2004) addressed imperfect DD pulses and Bergli and Faoro (2007)

also found analytic solutions and showed that a train of Y_π pulses avoids decoherence acceleration. A quantum impurity modeled with a "rotating wave" spin-boson model was recently studied by Rebentrost *et al.* (2009) with the numerical gradient ascent pulse engineering (GRAPE) algorithm. They found decoherence acceleration at $t/N \approx \Omega/2\pi$ next to the optimal point, and optimal pulses allowing for relaxation-limited gates at larger pulse rates.

b. $1/f$ *noise*

An environment composed of a set of independent impurities can be treated along the same lines. At pure dephasing $\Gamma_N(t)$ is the sum of independent single impurity contributions, and the analytic solution can be found for an arbitrary distribution of parameters (Falci *et al.*, 2004). An analytic expression valid in the classical limit was also found by Faoro and Viola (2004) who pointed out that relatively slow DD control rates ($\Delta t \sim 1/\gamma_M$ which is only a soft cutoff of the environment) suffice for a drastic improvement. For figures of noise typical for experiments, pulse rates yielding recovery are insensitive to the average coupling strength of the impurities (Falci *et al.*, 2004). The situation changes when the distribution includes individual more strongly coupled impurities (Galperin, Altshuler, and Shantsev, 2003; Paladino, Faoro, and Falci, 2003). Time symmetric CP is found to perform better than PDD (Faoro and Viola, 2004). While no decoherence acceleration is found at pure dephasing, this may happen for low pulse rates ($\Omega\Delta t \sim 10$) when $\Omega_x \neq 0$ and noise acquires a transverse part (Faoro and Viola, 2004).

c. Robust DD

Suppression of $1/f$ pure dephasing longitudinal flux noise was demonstrated in a recent experiment (Bylander *et al.*, 2011) using a 200 pulses CPMG sequence yielding a 50-fold improved T_2 over the baseline value, whereas the performance of UDD sequences was slightly worse. Earlier work with few-pulse sequences demonstrated partial suppression of low-frequency transverse charge noise (Ithier *et al.*, 2005).

Referring to superconducting qubits, Cywinski *et al.* (2008) studied CMPG, UDD, and CDD for $1/f^\alpha$ ($0.5 \leq \alpha \leq 1.5$) Gaussian classical noise at pure dephasing with UV cutoff ω_c. For pulse rates larger than this cutoff, CPMG is the most effective sequences increasing T_2, UDD keeping however higher fidelity. Instead, CDD does not give relevant improvement even if it outperforms PDD for a wide range of parameters (Khodjasteh and Lidar, 2007). For pulse rates smaller than ω_c, CPMG slightly outperforms all other sequences. CPMG is also a better approach for strongly coupled RT noise, non-Gaussian features being suppressed in the large pulse rate limit. Similar conclusions were drawn by Lutchyn *et al.* (2008) for a quantum impurity environment of Andreev fluctuators. Pasini and Uhrig (2010) studied sequences optimized for specific power-law noise spectra and found that they approach CPMG for soft UV cutoff ($1/f$ noise), whereas for hard UV behavior (Ohmic) UDD is the limiting solution.

Bounded amplitude "dynamical control by modulation" was proposed by Gordon, Kurizki, and Lidar (2008) who studied optimization for Lorentzian and $1/f$ pure dephasing noise. A practical limitation of this optimal chirped modulation is the sensitivity to the low-frequency cutoff. The design of GRAPE-optimized quantum gates in the presence of $1/f$ noise and inhomogeneous dephasing was recently investigated by Gorman, Young, and Whaley (2012).

Note that in general solid-state nanodevices suffer from different noise sources with a multiaxis structure of couplings. In these cases CDD (Khodjasteh and Lidar, 2005) or concatenated UDD sequences (Uhrig, 2009; West, Fong, and Lidar, 2010) may give substantial advantages.

4. Spectroscopy

The possibility that DD could be used as a spectroscopic tool was raised in a number of early works (Falci *et al.*, 2004; Faoro and Viola, 2004) and has been formalized using the concept of filter function (Uhrig, 2007; Biercuk, Doherty, and Uys, 2011). The key observation is that for a Gaussian process the filter function in Eq. (106) can be interpreted, at a fixed time $\bar{t}$, as a linear filter (Biercuk, Doherty, and Uys, 2011), transforming the input phase noise $E(t)$ to the output phase $\Phi_N(\bar{t})$, yielding the decay function $\Gamma_N(\bar{t})$ after noise averaging. Each implementation of time-dependent control samples the noise in a distinctive way determining the form of the filter $F_N(\omega\bar{t})$. For suitable sequences, we define a filter frequency ω_{F1} such that $F(\omega_{F1}\bar{t}) \sim 1$, which roughly corresponds to the minimal interpulse Δt. DD is described by a filter with negative gain for $\omega < \omega_{F1}$, the steepness of the attenuation yielding a measure of the effectiveness of the given sequence. This analysis allows one to develop a filter-function-guided pulse design suited to a particular noise spectrum.

Application to spectroscopy emerges from the observation that, in addition to the decoupling regime, there exist spectral regions of positive gain about $\omega = \omega_F$, where the effect of the corresponding spectral components of noise is amplified. This is apparent from Fig. 45, where the modified filter function $F(\omega\bar{t})/\omega^2$ is plotted, indicating the dominant spectral contributions to decoherence. For CPMG and PDD there is a single dominant peak. The shift of the peak toward larger ω for increasing N indicates that effects of sub-Ohmic noise are reduced by DD. Cywinski *et al.* (2008) proposed that UDD spectroscopy may also give information on higher moments of noise via the additional structure of the filter function (see Fig. 45).

Yuge, Sasaki, and Hirayama (2011) proposed a method for obtaining the noise spectrum from experimental data. The method, valid for the case of pure dephasing, is based on the relationship between the spectrum and a generalized dephasing time, evaluated from the asymptotic exponential decay in the presence of a sufficiently large number of π pulses.

Recently Bylander *et al.* (2011) exploited the narrow-band filtering properties of CPMG to measure $1/f$ flux noise in a persistent current qubit, where flux noise is the main source of dephasing away from the optimal point $\Omega_z \neq 0$. Indeed, Eq. (106) is approximated as $\Gamma_N(\bar{t}) \propto \Delta\omega(\partial\Omega/\partial q)^2 S_q(\omega_F) \times F_N(\omega_F\bar{t})/\omega_F^2$, where $\omega_F = \pi/2\Delta t$ is the peak frequency, $\Delta\omega$ is the bandwidth of the filter, and S_q and $\partial\Omega/\partial q$ are related to

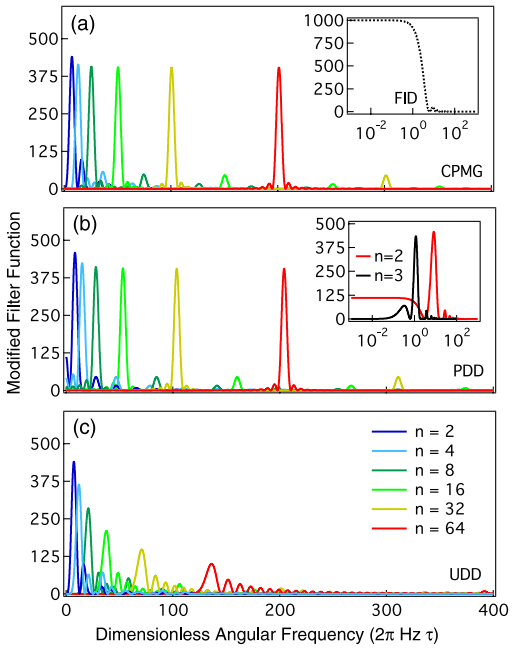

FIG. 45 (color online). (a)–(c) Modified filter function $F_N(\omega\bar{t})/\omega^2$, for the indicated pulse sequences and N values. Dominant spectral contributions to the measured $\Gamma_N(t)$ appear as peaks in the modified filter functions. (a) Modified filter function for FID showing a large weight for low-frequency noise on a semilog scale, with arbitrary units. (b) Demonstration of even-odd parity through the modified filter function of PDD on a semilog scale. Adapted from Biercuk, Doherty, and Uys, 2011.

the power spectrum of flux noise and the qubit sensitivity, depending on the flux bias, Eq. (90). This method has allowed one to access the unexplored spectral region 0.2–20 MHz where $1/f^{0.9}$ noise was detected. The decay of Rabi oscillations provides an alternative tool for environment spectroscopy in the same frequency range (Bylander *et al.*, 2011). As explained in Sec. III.B.1.a, quasistatic noise is efficiently averaged out and the observed decay of Rabi oscillations is essentially exponential with a contribution from frequency components around Ω_R behaving as $\Gamma_R \propto [\Omega_z(q)/\Omega]^2 S_q(\Omega_R)$ (Geva, Kosloff, and Skinner, 1995; Ithier *et al.*, 2005). Extracting this contribution yields independent information on the power spectrum at $\omega = \Omega_R \sim$ MHz. Remarkably, the very same power laws have been measured at much lower frequencies (0.01–100 Hz) by a direct method using the noise sensitivity of a free-induction Ramsey interference experiment (Yan *et al.*, 2012). The peculiarity of this technique is that it enables measurements of noise spectra up to frequencies limited only by achievable repetition rates of the measurements.

Two qubits: The extension of DD to entanglement protection from $1/f$ noise is a relevant issue, currently under investigation both theoretically and experimentally. The first experimental demonstration of DD protection of pseudo-two-qubit entangled states of an electron-nucleus ensemble in a solid-state environment was reported by Wang *et al.* (2011). DD control pulses operated on the electron spin suppressed inhomogeneous dephasing due to the static Overhauser field induced by the hyperfine interaction between electron spin and surrounding nuclear spins in a P:Si material. Recently, Gustavsson *et al.* (2012) extended single-qubit refocusing techniques to enhance the lifetime of an entangled state of a superconducting flux qubit coupled to a coherent TLS. Fluctuations of the qubit splitting due to $1/f$ flux noise induce low-frequency fluctuations of the qubit-TLS effective interaction. They demonstrated that by rapidly changing the qubit's transition frequency relative to TLS, a refocusing pulse on the qubit improved the coherence time of the entangled state. Further enhancement was demonstrated when applying multiple refocusing pulses. These results highlight the potential of DD techniques for improving two-qubit gate fidelities, an essential prerequisite for implementing fault-tolerant quantum computing. Quantum optimal control theory represents an alternative possibility to design high-fidelity quantum gates. Montangero, Calarco, and Fazio (2007), using the GRAPE numerical algorithm, demonstrated a stabilized two charge-qubit gate robust also to $1/f$ noise. For realistic noise figures, errors of 10^{-3}–10^{-4}, crossing the fault tolerance threshold, have been reached. A high-fidelity $\sqrt{\text{SWAP}}$ has been studied by Gorman, Young, and Whaley (2012) using GRAPE optimization in the presence of $1/f$ noise.

IV. CONCLUSIONS AND PERSPECTIVES

In this review we discussed the current state of theoretical work on $1/f$ noise in nanodevices with an emphasis on implications for solid-state quantum information processing. Our focus was on superconducting systems and we referred to implementations based on semiconductors only when physical analogies and/or formal similarities were envisaged. According to the existing literature, relevant mechanisms responsible for $1/f$ noise in superconducting nanocircuits have been largely identified. However, in many solid-state nanodevices this problem cannot be considered as totally settled and details of the interaction mechanisms remain controversial (see Sec. II). In some cases, available experiments do not allow drawing solid conclusions and further investigation is needed.

We discussed the role of low-frequency noises in decoherence of quantum bits and gates. Various methods to address this problem have been presented. A relevant issue in connection with quantum computation in the solid state is decoherence control and the achievement of the high fidelities needed for the succesful application of error correction codes. Various proposals have been put forward to limit the effects of $1/f$ noise. Since such noises in solid-state devices are created by material-inherent sources, an obvious way to improve performance of quantum devices is optimizing materials used for their fabrication. In particular, it is important to engineer the "dielectric" part of devices. Enormous effort in this direction based on identification of the noise sources and properties has resulted in significant optimizing of existing devices and suggesting novel ones. The main focus of the review is relating the device performance along different protocols to the properties of the noise sources. We hope that

understanding these relations may lead to improvement of the quantum devices.

The integration of control tools, like dynamical decoupling sequences appropriate to $1/f$ noise, with other functionalities, such as quantum gates, in a scalable architecture is a nontrivial open problem. Application of optimized pulse sequences to non-Markovian noise is the subject of future investigation. We reviewed the current status of the ongoing research along this direction, which represents an area for future development of the field.

Despite the tremendous progress in this field, there is still a long way to go until a practically important quantum computer will be realized. Many details have to be worked out, and at the present time it is actually not clear which physical implementation of quantum devices and even which architecture will be the most advantageous. However, it is fully clear that ongoing research on design and studies of devices for quantum information processing will significantly improve our understanding of the quantum world and interplay between classical and quantum physics. It will certainly lead to significant development of modern mesoscopic physics and, in particular, of quantum electronics.

LIST OF SYMBOLS AND ABBREVIATIONS

BCS	Bardeen, Cooper, Schrieffer
CDD	Concatenated dynamical decoupling
CP	Carr, Purcell
CPB	Cooper-pair box
CPMG	Carr, Purcell, Meilboom, Gill
CTRW	Continuous time random walk
CVD	Chemical vapor deposition
DD	Dynamical decoupling
DQD	Double quantum dot
FID	Free induction decay
GRAPE	Gradient ascent pulse engineering
LZ	Landau-Zener
MRT	Macroscopic resonant tunneling
NMR	Nuclear magnetic resonance
PDD	Periodic dynamical decoupling
QD	Quantum dot
QED	Quantum electrodynamics
QI	Qubit plus impurity
QPC	Quantum point contact
RKKY	Ruderman, Kittel, Kasuya, Iosida
RT	Random telegraph
RTN	Random telegraph noise
SEM	Scanning electron microscopy
SET	Single electron tunneling
SO	Spin orbit
SQUID	Superconducting quantum interference device
TLS	Two-level system
UDD	Uhrig dynamical decoupling
UV	Ultraviolet

ACKNOWLEDGMENTS

We thank Antonio D'Arrigo for carefully reading the manuscript and suggestions to improve the paper. We acknowledge fruitful discussions with J. Bergli, R. Fazio, A. Mastellone, M. Sassetti, G. Schön, D. Vion, U. Weiss, and A. Zorin. E. P. and G. F. acknowledge partial support from the Centro Siciliano di Fisica Nucleare e Struttura della Materia, Catania (I) and by the European Community through Grants No. ITN-2008-234970 NANOCTM and No. PON02-00355-339123 - ENERGETIC. E. P. and Y. M. G. contributed equally to the present work.

REFERENCES

Abel, B., and F. Marquardt, 2008, "Decoherence by quantum telegraph noise: A numerical evaluation," Phys. Rev. B **78**, 201302.

Agarwal, K., I. Martin, M. Lukin, and E. Demler, 2013, "Polaronic model for two level systems in amorphous solids," arXiv:1212.3299v2.

Ajoy, A., G. A. Álvarez, and D. Suter, 2011, "Optimal pulse spacing for dynamical decoupling in the presence of a purely dephasing spin bath," Phys. Rev. A **83**, 032303.

Anderson, P. W., B. I. Halperin, and C. M. Varma, 1972, "Anomalous low-temperature thermal properties of glasses and spin glasses," Philos. Mag. **25**, 1.

Anton, S. M., *et al.*, 2013, "Magnetic flux noise in dc SQUIDs: Temperature and Geometry Dependence," Phys. Rev. Lett. **110**, 147002.

Ashhab, S., J. R. Johansson, and F. Nori, 2006, "Rabi oscillations in a qubit coupled to a quantum two-level system," New J. Phys. **8**, 103.

Astafiev, O., Y. A. Pashkin, Y. Nakamura, T. Yamamoto, and J. S. Tsai, 2004, "Quantum noise in the Josephson charge qubit," Phys. Rev. Lett. **93**, 267007.

Astafiev, O., Y. A. Pashkin, Y. Nakamura, T. Yamamoto, and J. S. Tsai, 2006, "Temperature square dependence of the low frequency $1/f$ charge noise in the Josephson junction qubits," Phys. Rev. Lett. **96**, 137001.

Averin, D. V., and Yu. V. Nazarov, 1992, "Single-electron charging of a superconducting island," Phys. Rev. Lett. **69**, 1993.

Barends, R., *et al.*, 2013, "Coherent Josephson qubit suitable for scalable quantum integrated circuits," arXiv:1304.2322v1.

Barkai, E., Y. Jung, and R. Silbey, 2001, "Time-dependent fluctuations in single molecule spectroscopy: A generalized Wiener-Khintchine approach," Phys. Rev. Lett. **87**, 207403.

Barthel, C., J. Medford, C. M. Marcus, M. P. Hanson, and A. C. Gossard, 2010, "Interlaced dynamical decoupling and coherent operation of a singlet-triplet qubit," Phys. Rev. Lett. **105**, 266808.

Becker, Edwin D., 2000, *High Resolution NMR* (Academic Press, San Diego).

Bellomo, B., G. Compagno, A. D'Arrigo, G. Falci, R. Lo Franco, and E. Paladino, 2010, "Entanglement degradation in the solid state: Interplay of adiabatic and quantum noise," Phys. Rev. A **81**, 062309.

Bergli, J., and L. Faoro, 2007, "Exact solution for the dynamical decoupling of a qubit with telegraph noise," Phys. Rev. B **75**, 054515.

Bergli, J., Y. M. Galperin, and B. L. Altshuler, 2006, "Decoherence of a qubit by non-Gaussian noise at an arbitrary working point," Phys. Rev. B **74**, 024509.

Bergli, J., Y. M. Galperin, and B. L. Altshuler, 2009, "Decoherence in qubits due to low-frequency noise," New J. Phys. **11**, 025002.

Bertet, P., I. Chiorescu, G. Burkard, K. Semba, C. J. P. M. Harmans, D. P. DiVincenzo, and J. E. Mooij, 2005, "Relaxation and dephasing in a flux qubit," Phys. Rev. Lett. **95**, 257002.

Bialczak, R. C., *et al.*, 2007, "$1/f$ flux noise in Josephson phase qubits," Phys. Rev. Lett. **99**, 187006.

Biercuk, M. J., A. C. Doherty, and H. Uys, 2011, "Dynamical decoupling sequence construction as a filter-design problem," J. Phys. B **44**, 154002.

Biercuk, M. J., H. Uys, A. P. VanDevender, N. Shiga, W. M. Itano, and J. J. Bollinger, 2009, "Optimized dynamical decoupling in a model quantum memory," Nature (London) **458**, 996.

Black, J. L., 1978, "Relationship between the time-dependent specific heat and the ultrasonic properties of glasses at low temperatures," Phys. Rev. B **17**, 2740.

Black, J. L., 1981, in *Glassy Metals I*, edited by H.-J. Günterodt and H. Beck (Springer-Verlag, Berlin), p. 207.

Black, J. L., and B. L. Gyorffy, 1978, "Interaction of the conduction electrons with tunneling states in metallic glasses," Phys. Rev. Lett. **41**, 1595.

Black, J. L., and B. I. Halperin, 1977, "Spectral diffusion, phonon echoes, and saturation recovery in glasses at low temperatures," Phys. Rev. B **16**, 2879.

Blais, A., R.-S. Huang, A. Wallraff, S. M. Girvin, and R. J. Schoelkopf, 2004, "Cavity quantum electrodynamics for superconducting electrical circuits: An architecture for quantum computation," Phys. Rev. A **69**, 062320.

Bloch, F., 1957, "Generalized theory of relaxation," Phys. Rev. **105**, 1206.

Bloom, I., A. C. Marley, and M. B. Weissman, 1993, "Nonequilibrium dynamics of discrete fluctuators in charge-density waves in $NbSe_3$," Phys. Rev. Lett. **71**, 4385.

Bloom, I., A. C. Marley, and M. B. Weissman, 1994, "Discrete fluctuators and broadband noise in the charge-density wave in $NbSe_3$," Phys. Rev. B **50**, 5081.

Bluhm, H., J. A. Bert, N. C. Koshnick, M. E. Huber, and K. A. Moler, 2009, "Spinlike susceptibility of metallic and insulating thin films at low temperature," Phys. Rev. Lett. **103**, 026805.

Bluhm, H., S. Foletti, I. Neder, M. Rudner, D. Mahalu, V. Umansky, and A. Yacoby, 2010, "Dephasing time of GaAs electron-spin qubits coupled to a nuclear bath exceeding 200 μs," Nat. Phys. **7**, 109.

Borneman, T. W., M. D. Huerlimann, and D. G. Cory, 2010, "Application of optimal control to CPMG refocusing pulse design," J. Magn. Reson. **207**, 220.

Bouchiat, V., D. Vion, P. Joyez, D. Esteve, and M. H. Devoret, 1998, "Quantum coherence with a single Cooper pair," Phys. Scr. **T76**, 165.

Brandes, T., and B. Kramer, 1999, "Spontaneous emission of phonons of phonons by coupled quantum dots," Phys. Rev. Lett. **83**, 3021.

Brissaud, A., and U. Frisch, 1974, "Solving linear stochastic differential equations," J. Math. Phys. (N.Y.) **15**, 524.

Brox, H., J. Bergli, and Y. M. Galperin, 2011, "Effects of external driving on the coherence time of a Josephson junction qubit in a bath of two-level fluctuators," Phys. Rev. B **84**, 245416.

Brox, H., J. Bergli, and Y. M. Galperin, 2012, "Bloch-sphere approach to correlated noise in coupled qubits," J. Phys. A **45**, 455302.

Buckingham, M. J., 1989, *Noise in Electronic Devices and Systems* (Ellis Horwood Ltd., New York).

Buehler, T. M., D. J. Reilly, R. P. Starrett, V. C. Chan, A. R. Hamilton, A. S. Dzurak, and R. G. Clark, 2004, "Observing sub-microsecond telegraph noise with the radio frequency single electron transistor," J. Appl. Phys. **96**, 6827.

Buizert, C., F. H. L. Koppens, M. Pioro-Ladriére, H.-P. Tranitz, I. T. Vink, S. Tarucha, W. Wegscheider, and L. M. K. Vandersypen, 2008, "In situ reduction of charge noise in GaAs $-$ $Al_xGa_{1-x}As$ Schottky-gated devices," Phys. Rev. Lett. **101**, 226603.

Burin, A. L., B. I. Shklovskii, V. I. Kozub, Y. M. Galperin, and V. Vinokur, 2006, "Many electron theory of $1/f$ noise in hopping conductivity," Phys. Rev. B **74**, 075205.

Burkard, G., 2009, "Non-Markovian qubit dynamics in the presence of $1/f$ noise," Phys. Rev. B **79**, 125317.

Burkard, G., D. Loss, and D. P. DiVincenzo, 1999, "Coupled quantum dots as quantum gates," Phys. Rev. B **59**, 2070.

Bushev, P., C. Müller, J. Lisenfeld, J. H. Cole, A. Lukashenko, A. Shnirman, and A. V. Ustinov, 2010, "Multiphoton spectroscopy of a hybrid quantum system," Phys. Rev. B **82**, 134530.

Bylander, J., S. Gustavsson, F. Yan, F. Yoshihara, K. Harrabi, G. Fitch, D. G. Cory, Y. Nakamura, J. S. Tsai, and W. D. Oliver, 2011, "Noise spectroscopy through dynamical decoupling with a superconducting flux qubit," Nat. Phys. **7**, 565.

Carr, H. Y., and E. M. Purcell, 1954, "Effects of diffusion on free precession in nuclear magnetic resonance experiments," Phys. Rev. **94**, 630.

Catelani, G., J. Koch, L. Frunzio, R. J. Schoelkopf, M. H. Devoret, and L. I. Glazman, 2011, "Quasiparticle relaxation of superconducting qubits in the presence of flux," Phys. Rev. Lett. **106**, 077002.

Chandresekhar, S., 1943, "Stochastic problems in physics and astronomy," Rev. Mod. Phys. **15**, 1.

Chen, Z., and C. C. Yu, 2010, "Comparison of Ising spin glass noise to flux and inductance noise in SQUIDs," Phys. Rev. Lett. **104**, 247204.

Cheng, B., Q. H. Wang, and R. Joynt, 2008, "Transfer matrix solution of a model of qubit decoherence due to telegraph noise," Phys. Rev. A **78**, 022313.

Chiarello, F., E. Paladino, M. G. Castellano, C. Cosmelli, A. D'Arrigo, G. Torrioli, and G. Falci, 2012, "Superconducting qubit manipulated by fast pulses: experimental observation of distinct decoherence regimes," New J. Phys. **14**, 023031.

Chiorescu, I., P. Bertet, K. Semba, Y. Nakamura, C. J. P. M. Harmans, and J. E. Mooij, 2004, "Coherent dynamics of a flux qubit coupled to a harmonic oscillator," Nature (London) **431**, 159.

Chiorescu, I., Y. Nakamura, C. J. P. M. Harmans, and J. E. Mooij, 2003, "Coherent quantum dynamics of a superconducting flux qubit," Science **299**, 1869.

Chirolli, L., and G. Burkard, 2008, "Decoherence in solid-state qubits," Adv. Phys. **57**, 225.

Choi, S., D. H. Lee, S. G. Louie, and J. Clarke, 2009, "Localization of metal-induced gap states at the metal-insulator interface: Origin of flux Noise in SQUIDs and sperconducting qubits," Phys. Rev. Lett. **103**, 197001.

Chow, J. M., *et al.*, 2012, "Universal quantum gate set approaching fault-tolerant thresholds with superconducting qubits," Phys. Rev. Lett. **109**, 060501.

Clarke, J., and F. K. Wilhelm, 2008, "Superconducting quantum bits," Nature (London) **453**, 1031.

Cohen-Tannoudji, C., J. Dupont-Roc, and G. Grynberg, 1992, *Atom-Photon Interactions: Basic Processes and Applications* (Wiley, New York).

Coish, W. A., J. Fischer, and D. Loss, 2008, "Exponential decay in a spin bath," Phys. Rev. B **77**, 125329.

Cole, J. H., C. Mueller, P. Bushev, G. J. Grabovskij, J. Lisenfeld, A. Lukashenko, A. V. Ustinov, and A. Shnirman, 2010, "Quantitative evaluation of defect-models in superconducting phase qubits," Appl. Phys. Lett. **97**, 252501.

Collin, E., G. Ithier, A. Aassime, P. Joyez, D. Vion, and D. Esteve, 2004, "NMR-like control of a quantum bit superconducting circuit," Phys. Rev. Lett. **93**, 157005.

Constantin, M., C. C. Yu, and J. M. Martinis, 2009, "Saturation of two-level systems and charge noise in Josephson junction qubits," Phys. Rev. B **79**, 094520.

Constantin, M., and Clare C. Yu, 2007, "Microscopic model of critical current noise in Josephson junctions," Phys. Rev. Lett. **99**, 207001.

Cooper, K. B., M. Steffen, R. McDermott, R. W. Simmonds, O. Seongshik, D. A. Hite, D. P. Pappas, and John M. Martinis, 2004, "Observation of quantum oscillations between a Josephson phase qubit and a microscopic resonator using fast readout," Phys. Rev. Lett. **93**, 180401.

Cottet, A., A. Steinbach, P. Joyez, D. Vion, H. Pothier, D. Esteve, and M. E. Huber, 2001, in *Macroscopic Quantum Coherence and Quantum Computing*, edited by D. V. Averin, B. Ruggiero, and P. Silvestrini (Kluwer, New York), p. 111.

Cottet, A., D. Vion, A. Aassime, P. Joyez, D. Esteve, and M. H. Devoret, 2002, "Implementation of a combined charge-phase quantum bit in a superconducting circuit," Physica (Amsterdam) **367C**, 197.

Covington, M., M. W. Keller, R. L. Kautz, and J. M. Martinis, 2000, "Photon-assisted tunneling in electron pumps," Phys. Rev. Lett. **84**, 5192.

Culcer, D., X. Hu, and S. Das Sarma, 2009, "Dephasing of Si spin qubits due to charge noise," Appl. Phys. Lett. **95**, 073102.

Cywinski, L., R. M. Lutchyn, C. P. Nave, and S. Das Sarma, 2008, "How to enhance dephasing time in superconducting qubits," Phys. Rev. B **77**, 174509.

Dantsker, E., S. Tanaka, P.-A. Nilsson, R. Kleiner, and J. Clarke, 1996, "Reduction of $1/f$ noise in hightc dc superconducting quantum interference devices cooled in an ambient magnetic field," Appl. Phys. Lett. **69**, 4099.

D'Arrigo, A., A. Mastellone, E. Paladino, and G. Falci, 2008, "Effects of low frequency noise cross-correlations in coupled superconducting qubits," New J. Phys. **10**, 115006.

D'Arrigo, A., and E. Paladino, 2012, "Optimal operating conditions of an entangling two-transmon gate," New J. Phys. **14**, 053035.

De, A., A. Lang, D. Zhou, and R. Joynt, 2011, "Suppression of decoherence and disentanglement by the exchange interaction," Phys. Rev. A **83**, 042331.

de Lange, G., Z. H. Wang, D. Riste, V. V. Dobrovitski, and R. Hanson, 2010, "Universal dynamical decoupling of a single solid state spin from a spin bath," Science **330**, 60.

Deppe, F., *et al.*, 2008, "Two-photon probe of the jaynescummings model and controlled symmetry breaking in circuit QED," Nat. Phys. **4**, 686.

de Sousa, R., 2007, "Dangling-bond spin relaxation and magnetic $1/f$ noise from the amorphous-semiconductor/oxide interface: Theory," Phys. Rev. B **76**, 245306.

de Sousa, R., K. B. Whaley, T. Hecht, J. Von Delft, and F. K. Wilhelm, 2009, "Microscopic model of critical current noise in Josephson-junction qubits: Subgap resonances and Andreev bound states," Phys. Rev. B **80**, 094515.

de Sousa, R., K. B. Whaley, F. K. Wilhelm, and J. von Delft, 2005, "Ohmic and step noise from a single trapping center hybridized with a Fermi sea," Phys. Rev. Lett. **95**, 247006.

Di Carlo, L., M. D. Reed, L. Sun, B. R. Johnson, J. M. Chow, J. M. Gambetta, L. Frunzio, S. M. Girvin, M. H. Devoret, and R. J. Schoelkopf, 2010, "Preparation and measurement of three-qubit entanglement in a superconducting circuit," Nature (London) **467**, 574.

DiVincenzo, D. P., and D. Loss, 2005, "Rigorous Born approximation and beyond for the spin-boson model," Phys. Rev. B **71**, 035318.

Du, J., X. Rong, N. Zhao, Y. Wang, J. Yang, and R. B. Liu, 2009, "Preserving electron spin coherence in solids by optimal dynamical decoupling," Nature (London) **461**, 1265.

Dutta, P., and P. M. Horn, 1981, "Low-frequency fluctuations in solids: $1/f$ noise," Rev. Mod. Phys. **53**, 497.

Duty, T., D. Gunnarsson, K. Bladh, and P. Delsing, 2004, "Tunability of a 2e periodic single Cooper pair box," Phys. Rev. B **69**, 140504 (R).

Eiles, T. M., J. M. Martinis, and M. H. Devoret, 1993, "Even-odd asymmetry of a superconductor revealed by the Coulomb blockade of Andreev reflection," Phys. Rev. Lett. **70**, 1862.

Eroms, J., L. van Schaarenburg, E. Driessen, J. Plantenberg, K. Huizinga, R. Schouten, A. Verbruggen, C. Harmans, and J. Mooij, 2006, "Low-frequency fluctuations in solids: $1/f$ noise," Appl. Phys. Lett. **89**, 122516.

Eto, M., 2001, "Electronic states and transport phenomena in quantum dot systems," Jpn. J. Appl. Phys. **40**, 1929.

Falci, G., M. Berritta, A. Russo, A. D'Arrigo, and E. Paladino, 2012, "Effects of low-frequency noise in driven coherent nanodevices," Phys. Scr. **T151**, 014020.

Falci, G., A. D'Arrigo, A. Mastellone, and E. Paladino, 2004, "Dynamical suppression of telegraph and $1/f$ noise due to quantum bistable fluctuators," Phys. Rev. A **70**, 040101.

Falci, G., A. D'Arrigo, A. Mastellone, and E. Paladino, 2005, "Decoherence and $1/f$ noise in Josephson qubits," Phys. Rev. Lett. **94**, 167002.

Falci, G., E. Paladino, and R. Fazio, 2003, in *Quantum Phenomena in Mesoscopic Systems*, edited by B. L. Altshuler and V. Tognetti (IOS Press, Amsterdam), p. 173.

Faoro, L., J. Bergli, B. L. Altshuler, and Y. M. Galperin, 2005, "Models of environment and T_1 relaxation in Josephson charge qubits," Phys. Rev. Lett. **95**, 046805.

Faoro, L., and F. W. J. Hekking, 2010, "Cross-correlations between charge noise and critical-current noise in a four-level tunable Josephson system," Phys. Rev. B **81**, 052505.

Faoro, L., L. Ioffe, and A. Kitaev, 2012, "Dissipationless dynamics of randomly coupled spins at high temperatures," Phys. Rev. B **86**, 134414.

Faoro, L., and L. B. Ioffe, 2006, "Quantum two level systems and Kondo-like traps as possible sources of decoherence in superconducting qubits," Phys. Rev. Lett. **96**, 047001.

Faoro, L., and L. B. Ioffe, 2007, "Microscopic origin of critical current fluctuations in large, small, and ultra-small area Josephson junctions," Phys. Rev. B **75**, 132505.

Faoro, L., and L. B. Ioffe, 2008, "Microscopic origin of low-frequency flux noise in Josephson circuits," Phys. Rev. Lett. **100**, 227005.

Faoro, L., A. Kitaev, and L. B. Ioffe, 2008, "Quasiparticle poisoning and Josephson current fluctuations induced by Kondo impurities," Phys. Rev. Lett. **101**, 247002.

Faoro, L., and L. Viola, 2004, "Dynamical suppression of $1/f$ noise processes in qubit systems," Phys. Rev. Lett. **92**, 117905.

Fedorov, A., L. Steffen, M. Baur, M. P. da Silva, and A. Wallraff, 2011, "Implementation of a Toffoli gate with superconducting circuits," Nature (London) **481**, 170.

Feller, W., 1962, *An introduction to probability theory and its applications* (Wiley, New York).
Friedman, J. R., V. Patel, W. Chen, S. K. Tolpygo, and J. E. Lukens, 2000, "Quantum superposition of distinct macroscopic states," Nature (London) **406**, 43.
Fujisawa, T., T. Hayashi, H. D. Cheong, Y. H. Jeong, and Y. Hirayama, 2004, "Rotation and phase-shift operations for a charge qubit in a double quantum dot," Physica (Amsterdam) **21E**, 1046.
Fujisawa, T., T. Hayashi, and S. Sasaki, 2006, "Time-dependent single-electron transport through quantum dots," Rep. Prog. Phys. **69**, 759.
Fujisawa, T., T. H. Oosterkamp, W. G. van der Wiel, B. W. Broer, R. Aguado, S. Tarucha, and L. P. Kouwenhoven, 1998, "Spontaneous emission spectrum in double quantum dot devices," Science **282**, 932.
Galperin, Y. M., B. L. Altshuler, J. Bergli, and D. V. Shantsev, 2006, "Non-Gaussian low-frequency noise as a source of qubit decoherence," Phys. Rev. Lett. **96**, 097009.
Galperin, Y. M., B. L. Altshuler, J. Bergli, V. Shantsev, and V. Vinokur, 2007, "Non-Gaussian dephasing in flux qubits due to $1/f$ noise," Phys. Rev. B **76**, 064531.
Galperin, Y. M., B. L. Altshuler, and D. V. Shantsev, 2003, "Low-frequency noise as a source of dephasing of a qubit," arXiv:cond-mat/0312490v1.
Galperin, Y. M., B. L. Altshuler, and D. V. Shantsev, 2004, in *Fundamental Problems of Mesoscopic Physics*, edited by I. V. Lerner, B. L. Altshuler, and Y. Gefen (Kluwer, Dordrecht), p. 141.
Galperin, Y. M., and V. L. Gurevich, 1991, "Macroscopic tunneling in Josephson junctions with two-state fluctuators," Phys. Rev. B **43**, 12 900.
Galperin, Y. M., V. L. Gurevich, and V. I. Kozub, 1989, "Disorder-induced low-frequency noise in small systems - point and tunnel contacts in the normal and superconducting state," Europhys. Lett. **10**, 753.
Galperin, Y. M., D. V. Shantsev, J. Bergli, and B. L. Altshuler, 2005, "Rabi oscillations of a qubit coupled to a two-level system," Europhys. Lett. **71**, 21.
Galperin, Y. M., N. Zou, and K. A. Chao, 1994, "Resonant tunneling in the presence of a two-level fluctuator: Average transparency," Phys. Rev. B **49**, 13 728.
Geva, E., R. Kosloff, and J. Skinner, 1995, "On the relaxation of a 2-level system driven by a strong electromagnetic-field," J. Chem. Phys. **102**, 8541.
Geva, E., P. D. Reilly, and J. L. Skinner, 1996, "Spectral dynamics of individual molecules in glasses and crystals," Acc. Chem. Res. **29**, 579.
Glazman, L. I., F. W. J. Hekking, K. A. Matveev, and R. I. Shekhter, 1994, "Charge parity in Josephson tunneling through a superconducting grain," Physica (Amsterdam) **203B**, 316.
Gordon, G., G. Kurizki, and D. A. Lidar, 2008, "Optimal dynamical decoherence control of a qubit," Phys. Rev. Lett. **101**, 010403.
Gorman, D. J., K. C. Young, and K. B. Whaley, 2012, "Overcoming dephasing noise with robust optimal control," Phys. Rev. A **86**, 012317.
Grabert, H., and M. H. Devoret, 1991, Eds., in *Single Charge Tunneling, Coulomb Blockade Phenomena in Nanostuctures*, NATO ASI Series B, Vol. 294 (Plenum, New York).
Grabovskij, G. J., T. Peichl, J. Lisenfeld, G. Weiss, and A. V. Ustinov, 2012, "Strain tuning of individual atomic tunneling systems detected by a superconducting qubit," Science **338**, 232.
Grishin, A., I. V. Yurkevich, and I. V. Lerner, 2005, "Low temperature decoherence of qubit coupled to background charges," Phys. Rev. B **72**, 060509.
Gustafsson, M. V., A. Pourkabirian, G. Johansson, J. Clarke, and P. Delsing, 2012, "Activation mechanisms for charge noise," arXiv:1202.5350.
Gustavsson, S., J. Bylander, F. Yan, W. D. Oliver, F. Yoshihara, and Y. Nakamura, 2011, "Noise correlations in a flux qubit with tunable tunnel coupling," Phys. Rev. B **84**, 014525.
Gustavsson, S., F. Yan, J. Bylander, F. Yoshihara, Y. Nakamura, T. P. Orlando, and W. D. Oliver, 2012, "Dynamical decoupling and dephasing in interacting two-level systems," Phys. Rev. Lett. **109**.
Gutmann, H., F. K. Wilhelm, W. M. Kaminsky, and S. Lloyd, 2004, "Bang-bang refocusing of a qubit exposed to telegraph noise," Quantum Inf. Process. **3**, 247.
Gutmann, H., F. K. Wilhelm, W. M. Kaminsky, and S. Lloyd, 2005, "Compensation of decoherence from telegraph noise by means of an open-loop quantum-control technique," Phys. Rev. A **71**, 020302(R).
Halperin, B. I., 1976, "Can tunneling levels explain anomalous properties of glasses at very low-temperature," Ann. N.Y. Acad. Sci. **279**, 173.
Hanson, R., L. P. Kouwenhoven, J. R. Petta, S. Tarucha, and L. M. K. Vandersypen, 2007, "Spins in few-electron quantum dots," Rev. Mod. Phys. **79**, 1217.
Harris, R., *et al.*, 2008, "Probing noise in flux qubits via macroscopic resonant tunneling," Phys. Rev. Lett. **101**, 117003.
Hassler, F., A. R. Akhmerov, and C. W. J. Beenakker, 2011, "The top-transmon: a hybrid superconducting qubit for parity-protected quantum computation," New J. Phys. **13**, 095004.
Haus, J. W., and K. W Kehr, 1987, "Diffusion in regular and disordered lattices," Phys. Rep. **150**, 263.
Hayashi, T., T. Fujisawa, H. D. Cheong, Y. H. Jeong, and Y. Hirayama, 2003, "Coherent manipulation of electronic states in a double quantum dot," Phys. Rev. Lett. **91**, 226804.
Heinzel, T., 2007, *Mesoscopic Electronics in SolidState Nanostructures* (Wiley-VCH Verlag GmbH & Co. KGaA, Weinheim).
Hekking, F. W. J., L. I. Glazman, K. Matveev, and R. I. Shekhter, 1993, "Coulomb blockade of two-electron tunneling," Phys. Rev. Lett. **70**, 4138.
Hergenrother, J. M., M. T. Tuominen, and M. Tinkham, 1994, "Charge transport by Andreev reflection through a mesoscopic superconducting island," Phys. Rev. Lett. **72**, 1742.
Hessling, J. P., and Y. M. Galperin, 1995, "Flicker noise induced by dynamic impurities in a quantum point contact," Phys. Rev. B **52**, 5082.
Hoskinson, E., F. Lecocq, N. Didier, A. Fay, F. W. J. Hekking, W. Guichard, O. Buisson, R. Dolata, B. Mackrodt, and A. B. Zorin, 2009, "Quantum dynamics in a camelback potential of a dc SQUID," Phys. Rev. Lett. **102**, 097004.
Houck, A. A., *et al.*, 2007, "Generating single microwave photons in a circuit," Nature (London) **449**, 328.
Hu, P., and L. Walker, 1977, "Spectral diffusion in glasses at low temperatures," Solid State Commun. **24**, 813.
Hu, X., and S. Das Sarma, 2006, "Charge-fluctuation-induced dephasing of exchange-coupled spin qubits," Phys. Rev. Lett. **96**, 100501.
Hu, Y., Z. W. Zhou, J. M. Cai, and G. C. Guo, 2007, "Decoherence of coupled Josephson charge qubits due to partially correlated low-frequency noise," Phys. Rev. A **75**, 052327.
Hunklinger, S., and M. von Schickfus, 1981, in *Amorphous Solids: Low Temperature Properties*, edited by W. A. Phillips (Springer-Verlag, Berlin), p. 81.
Itakura, T., and Y. Tokura, 2003, "Dephasing due to background charge fluctuations," Phys. Rev. B **67**, 195320.

Ithier, G., *et al.*, 2005, "Decoherence in a superconducting quantum bit circuit," Phys. Rev. B **72**, 134519.
Jäckle, J., 1972, "Ultrasonic attenuation in glasses at low-temperatures," Z. Phys. **257**, 212.
Jeske, J., J. H. Cole, C. Müller, M. Marthaler, and G. Schön, 2012, "Dual-probe decoherence microscopy: probing pockets of coherence in a decohering environment," New J. Phys. **14**, 023013.
Johnson, R. J., W. T. Parsons, W. Strauch, J. R. Anderson, A. J. Dragt, C. J. Lobb, and F. C. Wellstood, 2005, "Macroscopic tunnel splittings in superconducting phase qubits," Phys. Rev. Lett. **94**, 187004.
Jones, N. C., T. D. Ladd, and B. H. Fong, 2012, "Dynamical decoupling of a qubit with always-on control fields," New J. Phys. **14**, 093045.
Joyez, P., P. Lafarge, A. Filipe, D. Esteve, and M. H. Devoret, 1994, "Observation of parity-induced suppression of Josephson tunneling in the superconducting single electron transistor," Phys. Rev. Lett. **72**, 2458.
Jung, S. W., T. Fujisawa, Y. Hirayama, and Y. H. Jeong, 2004, "Background charge fluctuation in a GaAs quantum dot device," Appl. Phys. Lett. **85**, 768.
Kafanov, S., H. Brenning, T. Duty, and P. Delsing, 2008, "Charge noise in single-electron transistors and charge qubits may be caused by metallic grains," Phys. Rev. B **78**, 125411.
Kakuyanagi, K., T. Meno, S. Saito, H. Nakano, K. Semba, H. Takayanagi, F. Deppe, and A. Shnirman, 2007, "Dephasing of a superconducting flux qubit," Phys. Rev. Lett. **98**, 047004.
Kayanuma, Y., 1984, "Nonadiabatic transitions in level-crossing with energy fluctuation. 1. Analytical investigations," J. Phys. Soc. Jpn. **53**, 108.
Kayanuma, Y., 1985, "Stochastic-theory for nonadiabatic level-crossing with fluctuating off-diagonal coupling," J. Phys. Soc. Jpn. **54**, 2037.
Kechedzhi, K., L. Faoro, and L. B. Ioffe, 2011, "Fractal spin structures as origin of $1/f$ magnetic noise in superconducting circuits," arXiv:1102.3445.
Kerman, A. J., and W. D. Oliver, 2008, "High fidelity quantum operations on superconducting qubits in the presence of noise," Phys. Rev. Lett. **101**, 070501.
Khaetskii, A. V., and Y. V. Nazarov, 2000, "Spin relaxation in semiconductor quantum dots," Phys. Rev. B **61**, 12 639.
Khaetskii, A. V., and Y. V. Nazarov, 2001, "Spin-flip transitions between Zeeman sublevels in semiconductor quantum dots," Phys. Rev. B **64**, 125316.
Khodjasteh, K., T. Erdélyi, and L. Viola, 2011, "Limits on preserving quantum coherence using multipulse control," Phys. Rev. A **83**, 020305.
Khodjasteh, K., and D. A. Lidar, 2005, "Fault-tolerant quantum dynamical decoupling," Phys. Rev. Lett. **95**, 180501.
Khodjasteh, K., and D. A. Lidar, 2007, "Performance of deterministic dynamical decoupling schemes: Concatenated and periodic pulse sequences," Phys. Rev. A **75**, 062310.
Kim, Z., V. Zaretskey, Y. Yoon, J. F. Schneiderman, M. D. Shaw, P. M. Echternach, F. C. Wellstood, and B. S. Palmer, 2008, "Anomalous avoided level crossings in a Cooper-pair box spectrum," Phys. Rev. B **78**, 144506.
Kirton, M. J., M. J. Uren, 1989, "Noise in solid-state microstructures: A new perspective on individual defects, interface states and low-frequency $(1/f)$ noise," Adv. Phys. **38**, 367.
Klauder, J. R., and P. W. Anderson, 1962, "Spectral diffusion decay in spin resonance experiments," Phys. Rev. **125**, 912.
Koch, H., David P. DiVincenzo, and John Clarke, 2007, "Model for $1/f$ flux noise in SQUIDs and qubits," Phys. Rev. Lett. **98**, 267003.
Koch, R. H. J., J. Clarke, W. M. Goubau, J. M. Martinis, C. M. Pegrum, and D. J. Van Harlingen, 1983, "Flicker $(1/f)$ noise in tunnel junction dc SQUIDs," J. Low Temp. Phys. **51**, 207.
Kogan, Sh. M., 1996, *Electronic Noise and Fluctuations in Solids* (Cambridge University Press, Cambridge, England).
Kogan, Sh. M., and K. E. Nagaev, 1984a, "Noise in tunnel junctions due to two-level systems in the dielectric layer," Pis'ma Zh. Tekh. Fiz. **10**, 313.
Kogan, Sh. M., and K. E. Nagaev, 1984b, "On the low-frequency current noise in metals," Solid State Commun. **49**, 387.
Kogan, Sh. M., and B. I. Shklovskii, 1981, "Excess low-frequency noise in hopping conduction," Fiz. Tekh. Poluprovodn. **15**, 1049 [Sov. Phys. Semicond. **15**, 605 (1981)].
Koppens, F. H. L., D. Klauser, W. A. Coish, K. C. Nowack, L. P. Kouwenhoven, D. Loss, and L. M. K. Vandersypen, 2007, "Universal phase shift and nonexponential decay of driven single-spin oscillations," Phys. Rev. Lett. **99**, 106803.
Kouwenhoven, L. P., C. M. Marcus, P. L. McEuen, S. Tarucha, R. M. Westervelt, and N. S. Wingreen, 1997, in *Mesoscopic Electron Transport*, edited by L. L. Sohn, L. P. Kouwenhoven, and G. Schön, NATO ASI, Ser. E, Vol. 345 (Kluwer, Dodrecht), p. 105.
Kozub, V. I., 1984, "Low-temperature properties of tunnel-junctions with an amorphous layer," Sov. Phys. JETP **59**, 1303 [http://www.jetp.ac.ru/cgi-bin/e/index/e/59/6/p1303?a=list].
Krupenin, V. A., D. E. Presnov, M. N. Savvateev, H. Scherer, A. B. Zorin, and J. Niemeyer, 1998, "Noise in al single electron transistors of stacked design," J. Appl. Phys. **84**, 3212.
Krupenin, V. A., A. B. Zorin, M. N. Savvateev, D. E. Presnov, and J. Niemeyer, 2001, "Single-electron transistor with metallic microstrips instead of tunnel junctions," J. Appl. Phys. **90**, 2411.
Ku, L. C., and C. C. Yu, 2005, "Decoherence of a Josephson qubit due to coupling to two-level systems," Phys. Rev. B **72**, 024526.
Ladd, T. D., F. Jelezko, R. Laflamme, Y. Nakamura, C. Monroe, and J. L. OBrien, 2010, "Quantum computers," Nature (London) **464**, 45.
Lafarge, P., P. Joyez, D. Esteve, C. Urbina, and M. H. Devoret, 1993, "Measurement of the even-odd free-energy difference of an isolated superconductor," Phys. Rev. Lett. **70**, 994.
Laikhtman, B. D., 1985, "General theory of spectral diffusion and echo decay in glasses," Phys. Rev. B **31**, 490.
Landau, L. D., 1932, "On the theory of transfer of energy at collisions II," Phys. Z. Sowjetunion **1**, 46.
Lanting, T., M. H. Amin, A. J. Berkley, C. Rich, S.-F. Chen, S. LaForest, and Rogerio de Sousa, 2013, "Flux noise in SQUIDs: Evidence for temperature dependent spin-diffusion," arXiv:1306.1512v1.
Lanting, T., *et al.*, 2009, "Geometrical dependence of the low-frequency noise in superconducting flux qubits," Phys. Rev. B **79**, 060509.
Lanting, T., *et al.*, 2010, "Cotunneling in pairs of coupled flux qubits," Phys. Rev. B **82**, 060512.
Lee, B., W. M. Witzel, and S. Das Sarma, 2008, "Universal pulse sequence to minimize spin dephasing in the central spin decoherence problem," Phys. Rev. Lett. **100**, 160505.
Lisenfeld, J., C. Müller, J. H. Cole, P. Bushev, A. Lukashenko, A. Shnirman, and A. V. Ustinov, 2010a, "Measuring the temperature dependence of individual two-level systems by direct coherent control," Phys. Rev. Lett. **105**, 230504.
Lisenfeld, J., C. Müller, J. H. Cole, P. Bushev, A. Lukashenko, A. Shnirman, and A. V. Ustinov, 2010b, "Rabi spectroscopy of a qubit-fluctuator system," Phys. Rev. B **81**, 100511.

Liu, R.-B., W. Yao, and L. J. Sham, 2010, "Quantum computing by optical control of electron spins," Adv. Phys. **59**, 703.
Loss, D., and D. P. DiVincenzo, 1998, "Quantum computation with quantum dots," Phys. Rev. A **57**, 120.
Louie, S. G., and M. L. Cohen, 1976, "Electronic structure of a metal-semiconductor interface," Phys. Rev. B **13**, 2461.
Lucero, E., *et al.*, 2012, "Computing prime factors with a Josephson phase qubit quantum processor," Nat. Phys. **8**, 719.
Ludviksson, A., R. Kree, and A. Schmid, 1984, "$1/f$ fluctuations of resistivity in disordered metals," Phys. Rev. Lett. **52**, 950.
Lundin, N. I., and Y. M. Galperin, 2001, "Impurity-induced dephasing of states," Phys. Rev. B **63**, 094505.
Lupaşcu, A., P. Bertet, E. F. C. Driessen, C. J. P. M. Harmans, and J. E. Mooij, 2009, "One- and two-photon spectroscopy of a flux qubit coupled to a microscopic defect," Phys. Rev. B **80**, 172506.
Lutchin, R., L. I. Glazman, and A. I. Larkin, 2005, "Quasiparticle decay rate of Josephson charge qubit oscillations," Phys. Rev. B **72**, 014517.
Lutchin, R., L. I. Glazman, and A. I. Larkin, 2006, "Kinetics of the superconducting charge qubit in the presence of a quasiparticle," Phys. Rev. B **74**, 064515.
Lutchyn, R. M., L. Cywiński, C. P. Nave, and S. Das Sarma, 2008, "Quantum decoherence of a charge qubit in a spin-fermion model," Phys. Rev. B **78**, 024508.
Makhlin, Y., G. Schön, and A. Shnirman, 2001, "Quantum-state engineering with Josephson-junction devices," Rev. Mod. Phys. **73**, 357.
Makhlin, Y., and A. Shnirman, 2004, "Dephasing of solid-state qubits at optimal points," Phys. Rev. Lett. **92**, 178301.
Manucharyan, V. E., J. Koch, L. I. Glazman, and M. H. Devoret, 2009, "Fluxonium: Single Cooper-pair circuit free of charge offsets," Science **326**, 113.
Mariantoni, M, *et al.*, 2011, "Implementing the quantum von Neumann architecture with superconducting circuits," Science **334**, 61.
Martin, I., L. Bulaevskii, and A. Shnirman, 2005, "Tunneling spectroscopy of two-level systems inside a Josephson junction," Phys. Rev. Lett. **95**, 127002.
Martin, I., and Y. M. Galperin, 2006, "Loss of quantum coherence due to nonstationary glass fluctuations," Phys. Rev. B **73**, 180201.
Martinis, J., *et al.*, 2005, "Decoherence in Josephson qubits from dielectric loss," Phys. Rev. Lett. **95**, 210503.
Martinis, J. M., S. Nam, J. Aumentado, K. M. Lang, and C. Urbina, 2003, "Decoherence of a superconducting qubit due to bias noise," Phys. Rev. B **67**, 094510.
Martinis, J. M., S. Nam, J. Aumentado, and C. Urbina, 2002, "Rabi oscillations in a large Josephson-junction qubit," Phys. Rev. Lett. **89**, 117901.
Matveev, K., M. Gisselfält, L. I. Glazman, M. Jonson, and R. I. Shekhter, 1993, "Parity-induced suppression of the Coulomb blockade of Josephson tunneling," Phys. Rev. Lett. **70**, 2940.
Matveev, K. A., L. I. Glazman, and R. I. Shekhter, 1994, "Effects of charge parity in tunneling through a superconducting grain," Mod. Phys. Lett. B **08**, 1007.
Maynard, R., R. Rammal, and R. Suchail, 1980, "Spectral diffusion decay of spontaneous echoes in disordered-systems," J. Phys. Lett. **41**, 291.
McWhorter, A. L., 1957, in *Semiconductor Surface Physics*, edited by R. H. Kingston (University of Philadelphia Press, Philadelphia, PA), p. 207.
Meiboom, S., and D. Gill, 1958, "Modified spin-echo method for measuring nuclear relaxation times," Rev. Sci. Instrum. **29**, 688.
Meier, F., and D. Loss, 2005, "Reduced visibility of Rabi oscillations in superconducting qubits," Phys. Rev. B **71**, 094519.
Mims, W. B., 1972, in *Electron Paramagnetic Resonance*, edited by S. Geschwind (Plenum, New York), p. 263.
Moerner, W. E., 1994, "Examining nanoenvironments in solids on the scale of a single, isolated impurity molecule," Science **265**, 46.
Moerner, W. E., and M. Orrit, 1999, "Illuminating single molecules in condensed matter," Science **283**, 1670.
Montangero, S., T. Calarco, and R. Fazio, 2007, "Robust optimal quantum gates for Josephson charge qubits," Phys. Rev. Lett. **99**, 170501.
Mooij, J. E., T. P. Orlando, L. Levitov, L. Tian, C. H. van der Wal, and S. Lloyd, 1999, "Josephson persistent-current qubit," Science **285**, 1036.
Mueller, C., A. Shnirman, and Y. Makhlin, 2009, "Relaxation of Josephson qubits due to strong coupling to two-level systems," Phys. Rev. B **80**, 134517.
Nakamura, Y., C. D. Chen, and J. S. Tsai, 1997, "Spectroscopy of energy-level splitting between two macroscopic quantum states of charge coherently superposed by Josephson coupling," Phys. Rev. Lett. **79**, 2328.
Nakamura, Y., Yu. A. Pashkin, and J. S. Tsai, 1999, "Coherent control of macroscopic quantum states in a single-Cooper-pair box," Nature (London) **398**, 786.
Nakamura, Y., Yu. A. Pashkin, and J. S. Tsai, 2001, "Rabi oscillations in a Josephson-junction charge two-level system," Phys. Rev. Lett. **87**, 246601.
Nakamura, Y., Yu. A. Pashkin, T. Yamamoto, and J. S. Tsai, 2002, "Charge echo in a Cooper-pair box," Phys. Rev. Lett. **88**, 047901.
Neeley, M., M. Ansmann, Radoslaw C. Bialczak, M. Hofheinz, N. Katz, E. Lucero, A. OConnell, H. Wang, A. N. Cleland, and J. M. Martinis, 2008, "Process tomography of quantum memory in a Josephson-phase qubit coupled to a two-level state," Nat. Phys. **4**, 523.
Neeley, M., *et al.*, 2010, "Generation of three-qubit entangled states using superconducting phase qubits," Nature (London) **467**, 570.
Nielsen, M., and I. Chuang, 1996, *Quantum Computation and Quantum Information* (Cambridge University Press, Cambridge, England).
Nishino, M., K. Saito, and S. Miyashita, 2001, "Noise effect on the nonadiabatic transition and correction to the tunneling energy gap estimated by the Landau-Zener-Stückelberg formula," Phys. Rev. B **65**, 014403.
Nugroho, D. D., V. Orlyanchik, and D. J. Van Harlingen, 2013, "Low frequency resistance and critical current fluctuations in al-based josephson junctions," Appl. Phys. Lett. **102**, 142602.
Oxtoby, N. P., A. Rivas, S. F. Huelga, and R. Fazio, 2009, "Probing a composite spin-boson environment," New J. Phys. **11**, 063028.
Palacios-Laloy, A., F. Mallet, F. Nguyen, P. Bertet, D. Vion, D Esteve, and A. N. Korotkov, 2010, "Experimental violation of a Bell's inequality in time with weak measurement," Nat. Phys. **6**, 442.
Paladino, E., A. D'Arrigo, A. Mastellone, and G. Falci, 2009, "Broadband noise decoherence in solid-state complex architectures," Phys. Scr. **T137**, 014017.
Paladino, E., A. D'Arrigo, A. Mastellone, and G. Falci, 2011, "Decoherence times of universal two-qubit gates due to structured noise," New J. Phys. **13**, 093037.
Paladino, E., L. Faoro, A. D'Arrigo, and G. Falci, 2003, "Decoherence and $1/f$ noise in Josephson qubits," Physica (Amsterdam) **18E**, 29.
Paladino, E., L. Faoro, and G. Falci, 2003, "Decoherence due to discrete noise in Josephson qubits," Adv. Solid State Phys. **43**, 747.

Paladino, E., L. Faoro, G. Falci, and R. Fazio, 2002, "Decoherence and $1/f$ noise in Josephson qubits," Phys. Rev. Lett. **88**, 228304.

Paladino, E., A. Mastellone, A. D'Arrigo, and G. Falci, 2010, "Optimal tuning of solid state quantum gates: A universal two-qubit gate," Phys. Rev. B **81**, 052502.

Paladino, E., M. Sassetti, G. Falci, and U. Weiss, 2008, "Characterization of coherent impurity effects in solid-state qubits," Phys. Rev. B **77**.

Palma, G. M., K. A. Suominen, and A. K. Ekert, 1996, "Quantum computers and dissipation," Proc. R. Soc. A **452**, 567.

Palomaki, T. A., *et al.*, 2010, "Multilevel spectroscopy of two-level systems coupled to a dc SQUID phase qubit," Phys. Rev. B **81**, 144503.

Parman, C. E., N. E. Israeloff, and Kakalios, J., 1991, "Random telegraph-switching noise in coplanar current measurements of amorphous silicon," Phys. Rev. B **44**, 8391.

Pashkin, Y. A., T. Yamamoto, O. Astafiev, Y. Nakamura, D. V. Averin, and J. S. Tsai, 2003, "Quantum oscillations in two coupled charge qubits," Nature (London) **421**, 823.

Pasini, S., and G. S. Uhrig, 2010, "Optimized dynamical decoupling for power-law noise spectra," Phys. Rev. A **81**.

Peters, M., J. Dijkhuis, and L. Molenkamp, 1999, "Random telegraph signals and $1/f$ noise in a silicon quantum dot," J. Appl. Phys. **86**, 1523.

Petersson, K. D., J. R. Petta, H. Lu, and A. C. Gossard, 2010, "Quantum coherence in a one-electron charge qubit," Phys. Rev. Lett. **105**, 246804.

Petta, J. R., H. Lu, and A. C. Gossard, 2010, "A coherent beam splitter for electronic spin states," Science **327**, 669.

Petta, J. R., J. M. Taylor, A. C. Johnson, A. Yacoby, M. D. Lukin, C. M. Marcus, M. P. Hanson, and A. C. Gossard, 2008, "Dynamic nuclear polarization with single electron spins," Phys. Rev. Lett. **100**, 067601.

Phillips, W. A., 1972, "Tunneling states in glasses," J. Low Temp. Phys. **7**, 351.

Phillips, W. A., 1987, "Two-level states in glasses," Rep. Prog. Phys. **50**, 1657.

Pioro-Ladrière, M., J. H. Davies, A. R. Long, A. S. Sachrajda, L. Gaudreau, P. Zawadzki, J. Lapointe, J. Gupta, Z. Wasilewski, and S. Studenikin, 2005, "Origin of switching noise in $GaAsAl_xGa_{1x}As$ lateral gated devices," Phys. Rev. B **72**, 115331.

Plourde, B. L. T., T. L. Robertson, P. A. Reichardt, T. Hime, S. Linzen, C.-E. Wu, and John Clarke, 2005, "Flux qubits and readout device with two independent flux lines," Phys. Rev. B **72**, 060506.

Pokrovsky, V. L., and N. A. Sinitsyn, 2003, "Fast quantum noise in the Landau-Zener transition," Phys. Rev. B **67**, 144303.

Pokrovsky, V. L., and D. Sun, 2007, "Fast quantum noise in the Landau-Zener transition," Phys. Rev. B **76**, 024310.

Pottorf, S., V. Patel, and J. E. Lukens, 2009, "Temperature dependence of critical current fluctuations in $Nb/AlO_x/Nb$ josephson junctions," Appl. Phys. Lett. **94**, 043501.

Rabenstein, K., V. A. Sverdlov, and D. V. Averin, 2004, "Qubit decoherence by Gaussian low-frequency noise," JETP Lett. **79**, 646.

Ralls, K. S., and R. A. Buhrman, 1991, "Microscopic study of $1/f$ noise in metal nanobridges," Phys. Rev. B **44**, 5800.

Ralls, K. S., W. J. Skocpol, L. D. Jackel, R. E. Howard, L. A. Fetter, R. W. Epworth, and D. M. Tennent, 1984, "Discrete resistance switching in submicrometer silicon inversion layers: Individual interface traps and low-frequency noise," Phys. Rev. Lett. **52**, 228.

Ramon, G., and X. Hu, 2010, "Decoherence of spin qubits due to a nearby charge fluctuator in gate-defined double dots," Phys. Rev. B **81**, 045304.

Rebentrost, P., I. Serban, T. Schulte-Herbrggen, and F. K. Wilhelm, 2009, "Optimal Control of a Qubit Coupled to a Non-Markovian Environment," Phys. Rev. Lett. **102**, 090401.

Redfield, A. G. F, 1957, "On the theory of relaxation processes," IBM J. Res. Dev. **1**, 19.

Reed, M. D., L. DiCarlo, S. E. Nigg, L. Sun, L. Frunzio, S. M. Girvin, and R. J. Schoelkopf, 2012, "Realization of three-qubit quantum error correction with superconducting circuits," Nature (London) **482**, 382.

Rigetti, C., A. Blais, and M. Devoret, 2005, "Protocol for universal gates in optimally biased superconducting qubits," Phys. Rev. Lett. **94**, 240502.

Rigetti, C., *et al.*, 2012, "Superconducting qubit in a waveguide cavity with a coherence time approaching 0.1 ms," Phys. Rev. B **86**, 100506(R).

Rogers, C. T., and R. A. Buhrman, 1984, "Composition of $1/f$ noise in metal-insulator-metal tunnel junctions," Phys. Rev. Lett. **53**, 1272.

Rogers, C. T., and R. A. Buhrman, 1985, "Nature of single-localized-electron states derived from tunneling measurements," Phys. Rev. Lett. **55**, 859.

Ryan, C. A., J. S. Hodges, and D. G. Cory, 2010, "Robust decoupling techniques to extend quantum coherence in diamond," Phys. Rev. Lett. **105**, 200402.

Saito, K., M. Wubs, S. Kohler, Y. Kayanuma, and P. Hänggi, 2007, "Dissipative Landau-Zener transitions of a qubit: Bath-specific and universal behavior," Phys. Rev. B **75**, 214308.

Sank, D., *et al.*, 2012, "Flux noise probed with real time tomography in a Josephson phase qubit," Phys. Rev. Lett. **109**, 067001.

Savo, B., F. C. Wellstood, and J. Clarke, 1987, "Low-frequency excess noise in $Nb-Al_2O_3-Nb$ Josephson tunnel-junctions," Appl. Phys. Lett. **50**, 1757.

Schlichter, C. P., 1992, *Principles of Magnetic Resonance 3ED (Springer Series in Solid-State Sciences)* (Springer-Verlag, Berlin).

Schreier, J. A., *et al.*, 2008, "Suppressing charge noise decoherence in superconducting charge qubits," Phys. Rev. B **77**, 180502.

Schriefl, J., M. Clusel, D. Carpentier, and P. Degiovanni, 2005a, "Dephasing by a nonstationary classical intermittent noise," Phys. Rev. B **72**, 035328.

Schriefl, J., M. Clusel, D. Carpentier, and P. Degiovanni, 2005b, "Nonostationary dephasing of two level systems," Europhys. Lett. **69**, 156.

Schriefl, J., Y. Makhlin, A. Shnirman, and G. Schön, 2006, "Decoherence from ensembles of two-level fluctuators," New J. Phys. **8**, 1.

Sendelbach, S., D. Hover, A. Kittel, M. Mück, J. M. Martinis, and R. McDermott, 2008, "Magnetism in SQUIDs at Millikelvin Temperatures," Phys. Rev. Lett. **100**, 227006.

Sendelbach, S., D. Hover, M. Mück, and R. McDermott, 2009, "Complex Inductance, Excess Noise, and Surface Magnetism in dc SQUIDs," Phys. Rev. Lett. **103**, 117001.

Shalibo, Y., Y. Rofe, D. Shwa, F. Zeides, M. Neeley, J. M. Martinis, and N. Katz, 2010, "Lifetime and coherence of two-level defects in a Josephson junction," Phys. Rev. Lett. **105**, 177001.

Shimshoni, E., and Y. Gefen, 1991, "Onset of dissipation in Zener dynamics: Relaxation versus dephasing," Ann. Phys. (N.Y.) **210**, 16.

Shimshoni, E., and A. Stern, 1993, "Dephasing of interference in Landau-Zener transitions," Phys. Rev. B **47**, 9523.

Shinkai, G., T. Tayashi, T. Ota, and T. Fujusawa, 2009, "Correlated coherent oscillations in coupled semiconductor charge qubits," Phys. Rev. Lett. **103**, 056802.

Shiokawa, K., and D. A. Lidar, 2004, "Dynamical decoupling using slow pulses: Efficient suppression of $1/f$ noise," Phys. Rev. A **69**, 030302.

Shklovskii, B. I., 1980, "Theory of$1/f$ noise for hopping conduction," Solid State Commun. **33**, 273.

Shnirman, A., G. Schoen, I. Martin, and Y. Makhlin, 2005, "Low- and high-frequency noise from coherent two-level systems," Phys. Rev. Lett. **94**, 127002.

Sillanpää, M., T. Lehtinen, A. Paila, Y. Makhlin, and P. Hakonen, 2006, "Continuous-time monitoring of Landau-Zener interference in a Cooper-pair box," Phys. Rev. Lett. **96**, 187002.

Simmonds, R. W., K. M. Lang, D. A. Hite, D. P. Pappas, and J. M. Martinis, 2004, "Decoherence in Josephson qubits from junction resonances," Phys. Rev. Lett. **93**, 077003.

Slichter, D. H., R. Vijay, S. J. Weber, S. Boutin, M. Boissonneault, J. M. Gambetta, A. Blais, and I. Siddiqi, 2012, "Measurement-induced qubit state mixing in circuit QED from up-converted dephasing noise," Phys. Rev. Lett. **109**, 153601.

Steffen, M., D. P. DiVincenzo, J. M. Chow, T. N. Theis, and M. B. Ketchen, 2011, "Quantum computing: An IBM perspective," IBM J. Res. Dev. **55**, 13:1.

Storcz, M. J, J. Vala, K. R. Brown, F. K Wilhelm, and K. B Whaley, 2005, "Full protection of superconducting qubit systems from coupling errors," Phys. Rev. B **72**, 064511.

Stueckelberg, E. C. G., 1932, "Theorie der unelastischen Stösse zwischen Atomen," Helv. Phys. Acta **5**, 369.

Sun, G., X. Wen, B. Mao, Z. Zhou, Y. Yu, P. Wu, and S. Han, 2010, "Quantum dynamics of a microwave driven superconducting phase qubit coupled to a two-level system," Phys. Rev. B **82**, 132501.

Surdin, M., 1939, J. Phys. Radium **10**, 188.

Takeda, K., T. Obata, Y. Fukuoka, W. M. Akhtar, J. Kamioka, T. Kodera, S. Oda, and S. Tarucha, 2013, "Characterization and suppression of low-frequency noise in Si/SiGe Quantum Point Contacts and Quantum Dots," Appl. Phys. Lett. **102**, 123113.

Taylor, J. M., and M. D. Lukin, 2006, "Dephasing of a quantum bits by a quasi-static mesoscopic environment," Quantum Inf. Process. **5**, 503.

Tian, L, and K. Jacobs, 2009, "A controllable interaction between two-level systems inside a Josephson junction," IEEE Trans. Appl. Supercond. **19**, 953.

Tian, L., and R. W. Simmonds, 2007, "Josephson junction microscope for low-frequency fluctuators," Phys. Rev. Lett. **99**, 137002.

Tuominen, M. T., J. M. Hergenrother, T. S. Tighe, and M. Tinkham, 1992, "Experimental evidence for parity-based $2e$ periodicity in a superconducting single-electron tunneling transistor," Phys. Rev. Lett. **69**, 1997.

Tuominen, M. T., J. M. Hergenrother, T. S. Tighe, and M. Tinkham, 1993, "Even-odd electron number effects in a small superconducting island: Magnetic-field dependence," Phys. Rev. B **47**, 11 599.

Uhrig, G. S., 2007, "Keeping a quantum bit alive by optimized π-pulse sequences," Phys. Rev. Lett. **98**, 100504.

Uhrig, G. S., 2009, "Concatenated control sequences based on optimized dynamical decoupling," Phys. Rev. Lett. **102**, 120502.

Vandersypen, L. M. K., and I. L. Chuang, 2005, "Nmr techniques for quantum control and computation," Rev. Mod. Phys. **76**, 1037.

Van der Wal, C. H., A. C. J. Ter Haar, F. K. Wihlelm, R. N. Schouten, C. J. P. M. Harmans, T. P. Orlando, S. Lloyd, and J. E. Mooij, 2000, "Quantum superposition of macroscopic persistent-current states," Science **290**, 773.

van der Wiel, W. G., S. De Franceschi, J. M. Elzerman, T. Fujisawa, S. Tarucha, and L. P. Kouwenhoven, 2002, "Electron transport through double quantum dots," Rev. Mod. Phys. **75**, 1.

van der Ziel, A., 1950, "On the noise spectra of semiconductor noise or of flicker effect," Physica (Amsterdam) **16**, 359.

Van Harlingen, D. J., T. L. Robertson, B. L. T. Plourde, P. A. Reichardt, T. A. Crane, and John Clarke, 2004, "Decoherence in Josephson-junction qubits due to critical-current fluctuations," Phys. Rev. B **70**, 064517.

Vestgården, J. I., J. Bergli, and Y. M. Galperin, 2008, "Nonlinearly driven Landau-Zener transition in a qubit with telegraph noise," Phys. Rev. B **77**, 014514.

Viola, L., and E. Knill, 2003, "Robust dynamical decoupling of quantum systems with bounded controls," Phys. Rev. Lett. **90**, 037901.

Viola, L., E. Knill, and S. Lloyd, 1999, "Dynamical decoupling of open quantum systems," Phys. Rev. Lett. **82**, 2417.

Viola, L., and S. Lloyd, 1998, "Dynamical suppression of decoherence in two-state quantum systems," Phys. Rev. A **58**, 2733.

Vion, D., A. Aassime, A. Cottet, P. Joyez, H. Pothier, C. Urbina, D. Esteve, and M. H. Devoret, 2002, " Manipulating the quantum state of an electrical circuit," Science **296**, 886.

von Schickfus, M., and S. Hunklinger, 1977, "Saturation of the dielectric absorption of vitreous silica at low temperatures," Phys. Lett. A **64**, 144.

Wakai, R. T., and D. J. Van Harlingen, 1986, "Low-frequency noise and discrete charge trapping in smallarea tunnel junction dc squids," Appl. Phys. Lett. **49**, 593.

Wakai, R. T., and D. J. Van Harlingen, 1987, "Direct lifetime measurements and interactions of charged defect states in submicron Josephson junctions," Phys. Rev. Lett. **58**, 1687.

Wang, Y., X. Rong, P. Feng, W. Xu, B. Chong, J. H. Su, J. Gong, and J. Du, 2011, "Preservation of bipartite pseudoentanglement in solids using dynamical decoupling," Phys. Rev. Lett. **106**, 040501.

Weiss, U, 2008, *Quantum Dissipative Systems* (World Scientific, Singapore), 3rd ed.

Weissman, M. B., 1988, "$1/f$ noise and other slow, nonexponential kinetics in condensed matter," Rev. Mod. Phys. **60**, 537.

Weissman, M. B, 1993, "What is a spin-glass? A glimpse via mesoscopic noise," Rev. Mod. Phys. **65**, 829.

Wellstood, F. C., C. Urbina, and J. Clarke, 1987a, "Excess noise in dc SQUIDs from 4.2 K to 0.022 K," IEEE Trans. Magn. **23**, 1662.

Wellstood, F. C., C. Urbina, and J. Clarke, 1987b, "Low-frequency noise in dc superconducting quantum interference devices below 1 K," Appl. Phys. Lett. **50**, 772.

Wellstood, F. C., C. Urbina, and J. Clarke, 2004, "Flicker $(1/f)$ noise in the critical current of Josephson junctions at 0.09–4.2 K," Appl. Phys. Lett. **85**, 5296.

West, J. R., B. H. Fong, and D. A. Lidar, 2010, "Near-optimal dynamical decoupling of a qubit," Phys. Rev. Lett. **104**, 130501.

West, J. R., D. A. Lidar, B. H. Fong, and M. F. Gyure, 2010, "High fidelity quantum gates via dynamical decoupling," Phys. Rev. Lett. **105**, 230503.

Witzel, W. M., and S. Das Sarma, 2007a, "Concatenated dynamical decoupling in a solid-state spin bath," Phys. Rev. B **76**, 241303.

Witzel, W. M., and S. Das Sarma, 2007b, "Multiple-pulse coherence enhancement of solid state spin qubits," Phys. Rev. Lett. **98**, 077601.

Wold, J., H. Brox, Y. M. Galperin, and J. Bergli, 2012, "Decoherence of a qubit due to a quantum fluctuator, or classical telegraph noise," Phys. Rev. B **86**, 205404.

Wolf, H., F. J. Ahlers, J. Niemeyer, H. Scherer, T. Weimann, A. B. Zorin, V. A. Krupenin, S. V. Lotkhov, and D. E. Presnov, 1997, "Investigation of the offset charge noise in single electron tunneling devices," IEEE Trans. Instrum. Meas. **46**, 303.

Wubs, M., K. Saito, S. Kohler, P. Hänggi, and Y. Kayanuma, 2006, "Gauging a quantum heat bath with dissipative Landau-Zener transitions," Phys. Rev. Lett. **97**.

Xiang, Z.-L., S. Ashhab, J. Q. You, and F. Nori, 2013, "Hybrid quantum circuits: Superconducting circuits interacting with other quantum systems," Rev. Mod. Phys. **85**, 623.

Yan, F., J. Bylander, S. Gustavsson, F. Yoshihara, K. Harrabi, D. G. Cory, T. P. Orlando, Y. Nakamura, J. S. Tsai, and W. D. Oliver, 2012, "Spectroscopy of transverse and longitudinal low-frequency noise and their temperature dependencies in a superconducting qubit," Phys. Rev. B **85**, 174521.

Yang, W., and R. B. Liu, 2008, "Universality of Uhrig dynamical decoupling for suppressing qubit pure dephasing and relaxation," Phys. Rev. Lett. **101**, 180403.

Yoshihara, F., K. Harrabi, A. O. Niskanen, Y. Nakamura, and J. S. Tsai, 2006, "Decoherence of flux qubits due to $1/f$ flux noise," Phys. Rev. Lett. **97**, 167001.

Yoshihara, F., Y. Nakamura, and J. S. Tsai, 2010, "Correlated flux noise and decoherence in two inductively coupled flux qubits," Phys. Rev. B **81**, 132502.

You, J. Q., X. Hu, S. Ashhab, and F. Nori, 2007, "Low-decoherence flux qubit," Phys. Rev. B **75**, 140515.

You, J. Q., and F. Nori, 2011, "Atomic physics and quantum optics using superconducting circuits," Nature (London) **474**, 589.

Yu, Y., S. Han, X. Chu, S.-I. Chu, and Z. Wang, 2002, "Coherent temporal oscillations of macroscopic quantum states in a Josephson junction," Science **296**, 889.

Yu, Y., L. L. Zhu, G. Sun, X. Wen, N. Dong, J. Chen, P. Wu, and S. Han, 2008, "Quantum jumps between macroscopic quantum states of a superconducting qubit coupled to a microscopic two-level system," Phys. Rev. Lett. **101**, 157001.

Yuge, T., S. Sasaki, and Y. Hirayama, 2011, "Measurement of the noise spectrum using a multiple-pulse sequence," Phys. Rev. Lett. **107**, 170504.

Yurkevich, I. V., J. Baldwin, I. V. Lerner, and B. L. Altshuler, 2010, "Decoherence of charge qubit coupled to interacting background charges," Phys. Rev. B **81**, 12305.

Zagoskin, A. M., S. Ashhab, J. R. Johansson, and F. Nori, 2006, "Quantum two-level systems as naturally formed qubits," Phys. Rev. Lett. **97**, 077001.

Zak, R. A., B. Röthlisberger, S. Chesi, and D. Loss, 2010, "Quantum computing with electron spins in quantum dots," Riv. Nuovo Cimento **033**, 345.

Zener, C., 1932, "Non-adiabatic crossing of energy levels," Proc. R. Soc. A **137**, 696.

Zhou, D., and R. Joynt, 2010, "Noise-induced looping on the Bloch sphere: Oscillatory effects in dephasing of qubits subject to broad-spectrum noise," Phys. Rev. A **81**, 010103(R).

Zimmerli, G., T. M. Eiles, R. L. Kautz, and J. M. Martinis, 1992, "Noise in the Coulomb blockade electrometer," Appl. Phys. Lett. **61**, 237.

Zorin, A. B., F. J. Ahlers, J. Niemeyer, T. Weimann, H. Wolf, V. A. Krupenin, and S. V. Lotkhov, 1996, "Background charge noise in metallic single-electron tunneling devices," Phys. Rev. B **53**, 13682.